Integrated Thermal and Energy Management of Plug-in Hybrid Electric Vehicles

By

Mojtaba Shams-Zahraei (M.Sc.)

Submitted in fulfilment of the requirements for the degree of

Doctor of Philosophy

Deakin University

August 2012

DEAKIN UNIVERSITY
ACCESS TO THESIS - A

I am the author of the thesis entitled *"Integrated Thermal and Energy Management of Plug-in Hybrid Electric Vehicles"*

submitted for the degree of Doctor of Philosophy

This thesis may be made available for consultation, loan and limited copying in accordance with the Copyright Act 1968.

'I certify that I am the student named below and that the information provided in the form is correct'

Mojtaba Shams-Zahraei

07/01/2013

DEAKIN UNIVERSITY

CANDIDATE DECLARATION

I certify that the thesis entitled *"Integrated Thermal and Energy Management of Plug-in Hybrid Electric Vehicles"* submitted for the degree of Doctor of Philosophy is the result of my own work and that where reference is made to the work of others, due acknowledgment is given.

I also certify that any material in the thesis which has been accepted for a degree or diploma by any other university or institution is identified in the text.

'I certify that I am the student named below and that the information provided in the form is correct'

Mojtaba Shams-Zahraei

24/08/2012

To my beautiful wife, Tina

ACKNOWLEDGMENTS

First and foremost, I would like to acknowledge respectfully, the help and support I have received from my supervisor, Assoc. Prof. Abbas Kouzani, who has been an enduring mentor, a great teacher, and a patient friend at all stages of my PhD candidature. I would also like to thank my co-supervisor Assoc. Prof. Hieu Trinh and of course all my friends and colleagues at Deakin University. The help and support I received from the lovely staff of School of Engineering and Higher Degree by Research is highly appreciated.

I would like express my gratitude to Prof. Bernard Baker for his support both financially and academically during my research stay at Institute of Automotive Technology Dresden/ Germany (IAD). I am grateful to all of my friends and colleagues at IAD for their help, discussion, and all the good times we shared. Especially I thank Steffen Kutter who facilitates the great research stay in Germany.

I would also like to thank my dear family, as their moral support has never ceased in my life and is always keeping me motivated and strong.

ABSTRACT

Plug-in hybrid electric vehicles (PHEVs) benefit from the features of both conventional hybrid electric vehicles (HEVs) and electric vehicles (EVs) by having a large battery which can be recharged when plugged into an electric power source. PHEVs are creating much interests due to their significant potential to improve fuel efficiency and reduce emissions particularly for daily commuters with short daily trips. PHEVs would be the next generation of vehicles in the market before full electrification of vehicles becomes mature. The aim of this research is to find the most efficient energy management strategy (EMS) to control the energy flow in the powertrain components of PHEVs. The simulations are conducted on a serial drivetrain model; however, the presented approach for EMS of PHEV in this thesis is equally applicable for other available hybrid architectures. The thesis also gives a review of control approaches that are exclusively applicable for the EMS of PHEVs.

The implementation of globally optimal energy management strategies is only feasible when an accurate prediction of driving scenario is available. There are many noise factors which affect both the drivetrain power demand and the vehicle performance even in identical drive-cycles. In this research, the effect of each noise factor is investigated by introducing the concept of power-cycle instead of

drive-cycle for a journey. A practical solution for developing a power-cycle library is introduced to improve the accuracy of power-cycle prediction.

PHEVs employ a rechargeable battery as an energy source alongside a fuel source. Consequently, in PHEVs the engine temperature declines due to the reduced engine load as well as the extended engine off period. It is proven that the engine efficiency and emissions depend on the engine temperature. Moreover, temperature, as one of the noise factors, has direct influence on the vehicle air-conditioner and the cabin heater loads. Particularly, while the engine is cold, the power demand of the cabin heater needs to be provided by the battery instead of the waste heat of the engine coolant. Existing studies on EMS of PHEVs mostly focus on the improvement of fuel efficiency based on the hot engine characteristics neglecting the effect of temperature on the engine performance and the vehicle power demand. This thesis presents two new EMSs which consider the temperature noise factor to maximise the performance and the efficiency of PHEVs for a predefined journey. First, a rule-based approach to find the best charge depleting regime of battery is introduced. The rule-based approach is a sub-optimal solution for the control problem but is easily implementable, as it requires limited computation effort. The second approach incorporates an engine thermal management method, which formulates the globally optimal battery charge depleting trajectories based on the Bellman's principle of optimality. A dynamic programming-based algorithm is developed and applied to enforce the charge depleting boundaries while optimizing a fuel consumption cost function by controlling the engine power as an input variable. The optimal control problem formulates the cost function based on two major state variables: battery charge

and internal temperature. The algorithm also considers a minimum duration for which the engine is allowed to switch from on to off modes preventing the concerns associated with the engine transient operation. It is demonstrated that the temperature and the cabin heater/air-conditioner power demand, even in an identical drive-cycle, can significantly influence the optimal solution for the EMS, and accordingly the fuel efficiency and the emissions of PHEVs.

List of Publications

M. Shams-Zahraei, A. Z. Kouzani, S. Kutter, and B. Bäker, "Integrated thermal and energy management of Plug-in hybrid electric vehicles," Journal of Power Sources, vol. 216, pp. 237-248, will be published in 15 October 2012.

M. Shams-Zahraei, A. Z. Kouzani, and B. Ganji, “Effect of noise factors in energy management of series plug-in hybrid electric vehicles," International Review of Electrical Engineering, vol. 6, pp. 1715-1726, 2011.

M. Shams-Zahraei and A. Z. Kouzani, “Effect of temperature noise factor in energy management of series plug-in hybrid electric vehicles” presented at Energy Efficient Vehicle Technology, Dresden, Germany, 2011.

M. Shams-Zahraei and A. Z. Kouzani, "Power-cycle-library-based control strategy for plug-in hybrid electric vehicles," presented at the IEEE Vehicle Power and Propulsion Conference Lille, France, 2010.

M. Shams-Zahraei and A. Kouzani, "A study on plug-in hybrid electric vehicles," presented at the TENCON IEEE Conference, Singapore, 2009.

B. Ganji, A. Kouzani, Kh.S. Yang, and M. Shams-Zahraei, "Adaptive cruise control of hybrid electric vehicle based on sliding mode control" under review.

Table of content

List of figures

List of tables

CHAPTER 1

INTRODUCTION

1.1 MOTIVATION

Living in the era of increasing environmental sensibility and rise in fuel price makes it necessary to develop new vehicles that are more fuel efficient and environmental friendly. The oil price has risen almost fourfold since 10 years ago and is likely to continue to increase in the future because of shrinking oil supplies and surge in demand. Increasing concerns about environmental issues, such as global warming and greenhouse gas emissions, boost the feasibility of new technologies of green vehicles. Implementation of fuel-economy regulations and

ever-tightening emission standards are major technology challenges that all automotive manufacturers currently face.

Electrification of vehicle drivetrains has been a major breakthrough to realise the reduction of fuel consumption and emission ambitions without sacrificing performance. An electric vehicle (EV) was once considered as a promising alternative for a conventional vehicle due to good overall efficiency, low audible noise, and zero on-board emissions. Nevertheless, technological and financial barriers regarding electrical storage devices such as batteries and super-capacitors delayed fully commercialization of electric vehicles. Still, available EVs in the market suffer from high cost and rang-anxiety issues. Hybrid electric vehicles as the second option (HEVs) have been available in the market since 1997, and their market share has improved since then. Plug-in hybrid electric vehicles (PHEVs) benefit from the features of both conventional HEVs and EVs. PHEVs have a large battery which can be recharged when plugged into an electric power source alongside an engine to replenish the battery for long journeys. The features of PHEVs are appealing for daily commuters since the larger battery could supply energy demand of short journeys and the combustion engine could realise the range extension. PHEVs could be a short-term solution before the technological barriers for full electrification of vehicles are overcome.

The highest level of powertrain control in HEVs or PHEVs is an energy management strategy (EMS) that interprets the driver power demand for drivetrain components. The EMS decides how to distribute the vehicle power demand between the electric power path and the conventional mechanical power path efficiently. The extra available energy source, the battery charge of PHEVs,

adds an extra dimension to the complexity of the EMS control problem compared to HEVs in which the engine is the sole source of energy. Therefore, to achieve full benefit out of having an extra energy source on-board, a charge management strategy should be incorporated into the EMS. The extra energy source also results in a decline in the engine temperature due to reduced engine load as well as extended engine off periods. It is well known that engine efficiency and emissions depend on the engine temperature. Moreover, temperature has direct influence on the vehicle air-conditioner and the cabin heater loads. Particularly, while the engine is cold, the power demand of the cabin heater needs to be provided by the battery instead of the waste heat of the engine coolant. This thesis addresses the sensitivity of PHEVs' drivetrain performance with regard to the temperature noise-factor. This research proposes methodologies based on a rule-based as well as an optimal control theory method to derive an optimal charge depleting trajectory for the PHEV battery. The significance of temperature on the optimal EMS of PHEVs is also demonstrated. The resulted charge management coincides with the optimal thermal management of the engine for minimum fuel consumption, while maximizing the use of the engine waste heat for the cabin warming in place of the battery electricity in cold weather.

1.2 HYBRID ELECTRIC VEHICLES

Hybrid vehicles benefit from an efficient combination of at least two power sources to propel the vehicle. Generally, one or more electric motors alongside an Internal Combustion Engine (ICE) or a fuel cell, as a primary energy source, operates the propulsion system of HEVs. A battery or a super-capacitor as a

bidirectional energy source provides power to the drivetrain, also recuperates part of the braking energy dissipated in conventional ICE vehicles. Usually the term HEV is used for a vehicle combining an engine with an electric motor. Hybrid-Inertia, Hybrid-Hydraulic, and fuel cell propulsion systems are also considered as members of the HEVs family.

The main advantages of the HEV drivetrain are as follows:

- ICE downsizing: Since the peak power demand could be provided by a combination of the ICE and the battery, the ICE could be sized for average power demand of the vehicle. This reduces the weight and improves the efficiency of the ICE when operating at the same load of a larger engine.
- Regenerative braking: The on-board battery or super-capacitor of HEV can be recharged while the electric motor operates in the generator mode providing braking force instead of friction brake.
- Engine on/off functionality: The engine can be turned off when the vehicle is at standstill or the vehicle power demand is low. This prevents unnecessary engine idling or its operation at low power which is generally inefficient.
- Control flexibility: The additional degree of freedom to provide the vehicle power demand from either of the power sources gives the flexibility to operate the powertrain components in a more efficient manner.

A more extensive introduction to HEVs and modern vehicle propulsion systems can be found in the literature [1-5].

1.3 PLUG-IN HYBRID ELECTRIC VEHICLES

Plug-in hybrid electric vehicles (PHEVs) benefit from the features of both conventional HEVs and electric vehicles (EVs) by having a large battery which can be recharged when plugged into an electric power source. A PHEV is a viable solution to replace some part of the energy used in vehicular transportation with electricity, before full electrification of vehicles becomes mature [6]. Moreover, PHEVs can eliminate concerns about EVs' recharging time and range anxiety. PHEVs have considerable influence on the shift from fossil fuels to electric energy sources for significant part of daily commutes. Hence, according to an investigation conducted by Toyota, the accumulative daily travel of around 75%, 80%, and 95% of vehicles in North America, Europe, and Japan are lower than 60 km, respectively [7]. The cumulative daily travel in Australian cities is depicted in Figure 1.1.

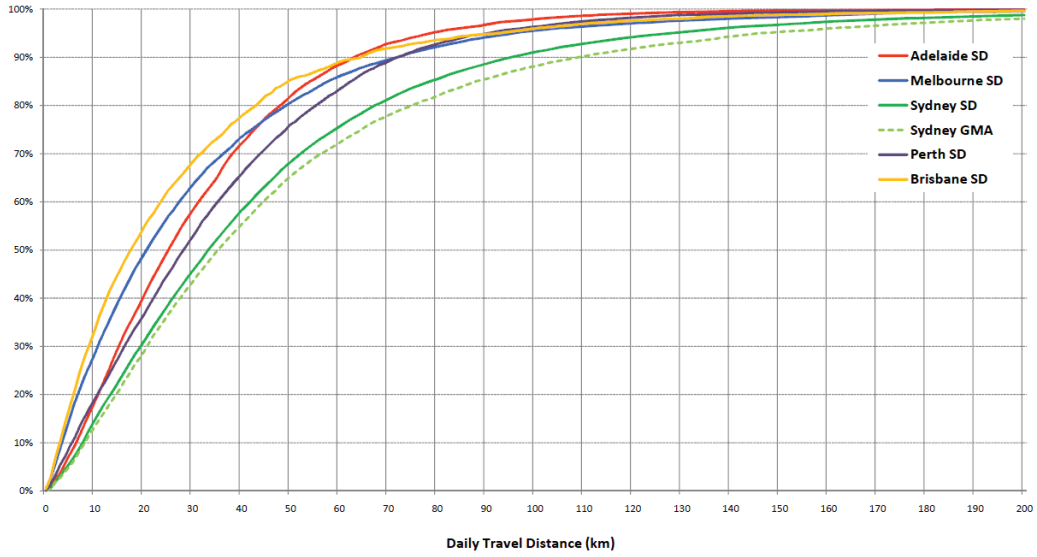

Figure 1.1.Cumulative distribution of daily driving distances in Australian cities, courtesy of R. Zito [8]

The benefits offered by the PHEVs drivetrain have both individual and national significance. Using the energy stored in the battery through the utility grid to displace part of fuel used for vehicular applications is the major feature of PHEVs. This means using a cleaner and between three to four times cheaper energy in comparison to petrol [9, 10]. The widespread use of PHEVs whose battery-generated energy is sufficient to meet average daily travel needs could reduce the petrol consumption between 40 to 50 percent [11-15]. From the national point of view, the full penetration of PHEV in society will result in an energy dependence shift from petroleum to the sources of electricity generation that are generally local industries. Greenhouse gas (GHG) and other air pollutant emissions will be shifted from high population urban area to electricity plants area. Also, there is an opportunity to produce the electricity from nuclear energy or sources of renewable energies [10]. Off-peak charging strategies or more sophisticated vehicle to grid technology can help load levelling in electricity generation industry which will consequently result in decreasing electricity cost

because of reduction in power plant start-up, operation, and maintenance costs [12]. However, the battery charging strategies significantly affect the electricity consumption from the power generation point of view [16].

1.3.1 Extended-Range Electric Vehicle

Extended-range electric vehicles (EREVs) are PHEVs that can operate on a pure electric vehicle (EV) mode. Both the battery and the tractive motor of PHEVs are capable of providing maximum tractive and auxiliary power demand for the powertrain. The maximum range that can be covered on the EV mode for a standard power-cycle is called all electric range (AER) for the specific cycle. The market of EREVs is focused on daily commuters who prefer the benefits of driving on the EV mode for daily routine travels while enjoying the driving without the range-anxiety for longer journeys.

1.3.2 Definition of operating modes for PHEVs and EREV

- Charge Depleting and EV mode

  Charge depleting (CD) refers to a PHEV operation mode in which the vehicle drains energy from the charged battery. However, sometimes because of the drivetrain restrictions, the engine operation is inevitable. The EV mode is a special case of the charge depleting. During the EV mode, the engine is turned off and the vehicle only relies on the battery energy to cover both the tractive and ancillary loads.

- Charge sustaining (CS) mode

Similar to HEVs, the battery charge is sustained around a predefined range. Generally, the CS mode happens when the battery is completely depleted to the minimum applicable threshold for the battery state of charge (SOC). That is, the PHEV operates like a conventional HEV when the SOC reaches the minimum applicable SOC defined for the battery.

- Blended mode

  In the blended mode, both the engine and the battery provide the required power demand for the vehicle. Generally, the control strategy of PHEV selects the ratio of the engine to the battery power in a more efficient fashion. That is, in comparison the simple CD, a blended mode possesses a more intelligent charge management strategy.

1.3.3 HEV and PHEV powertrain architecture

The combinations of connections between components of the propulsion system define the architecture of HEVs. Conventionally, HEVs are categorized into three basic drivetrain architectures: series, parallel, and series-parallel. A schematic representation of these three basic architectures is given in Figure 1.2. Detailed descriptions of the characteristics of each drivetrain can be found in the literature [1-4]. This introduction focuses on the characteristics that distinguish between these powertrain architectures for PHEV applications.

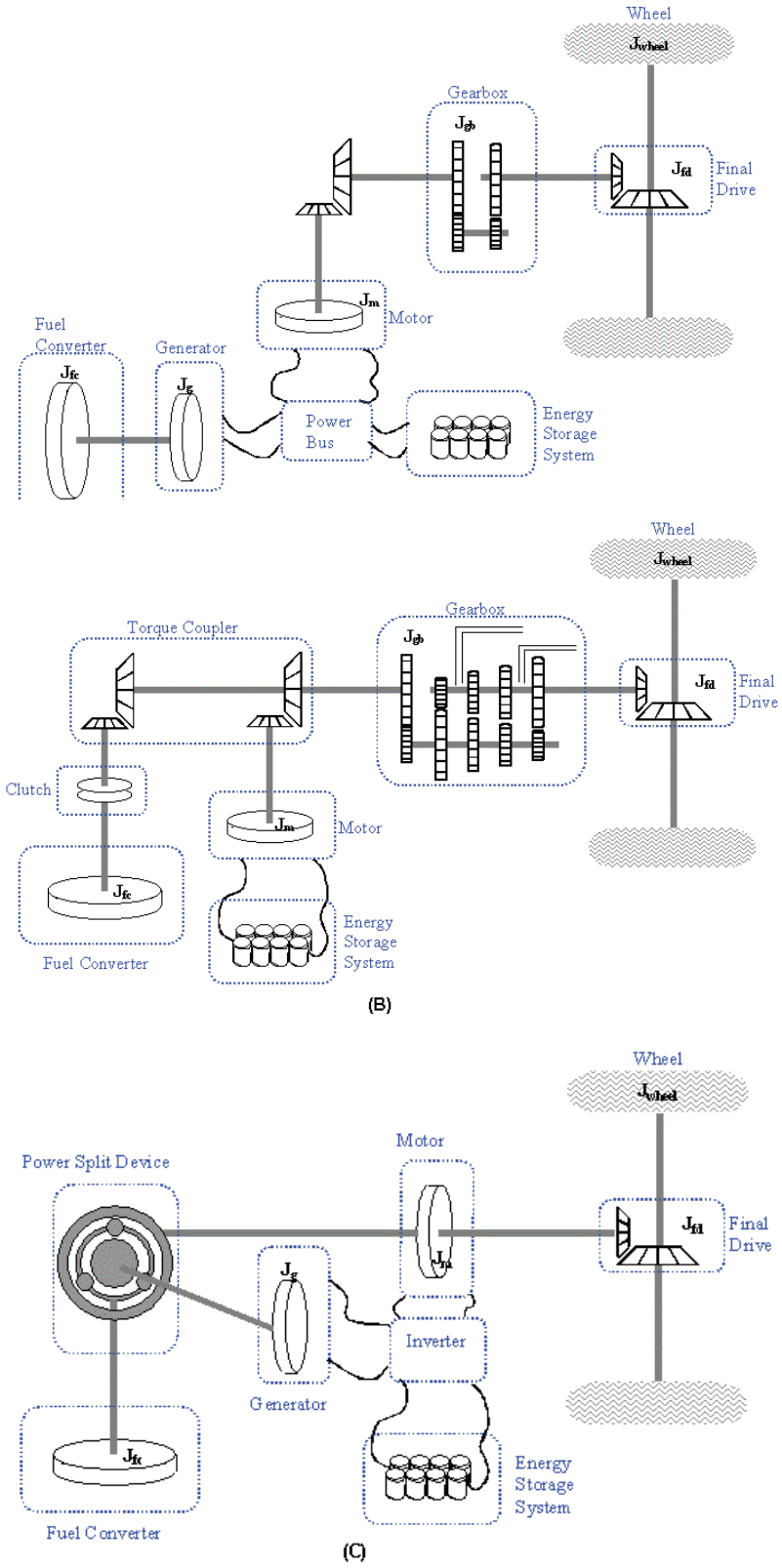

Figure 1.2. (A) Series drivetrain. (B) Parallel drivetrain. (C) Series-parallel drivetrain [ADVISOR help documentation]

The series configuration is commonly recognized as an electric vehicle that has an engine and a generator to recharge the battery so it is easier to upgrade it to a PHEV. The series architecture is a common drivetrain for diesel-electric locomotives and ships. The series architecture drivetrain has a sized electric motor to coupe the designed vehicle maximum traction power. The increase in power capacity of the battery enables the AER and the zero emission operation of the series architecture. Since there is no mechanical coupling between the wheels and the engine in this architecture, the engine can operate independently around its most efficient torque-speed region. However, the well-known drawback of the series drivetrain is the conversion of the engine mechanical power to electrical and then back to mechanical form in the electric motor. This efficiency chain reduces the overall efficiency of the drivetrain. For example, GM Volt is a 64 km EREV with a base platform of series drivetrain. Volt benefits from a mode changing architecture by employing a planetary-gear-set and two brakes. The mechanism enables the vehicle to shift from the series to the series-parallel architecture to solve the above-mentioned drawback. In this mode, the engine could mechanically transfer power to the final-drive in higher vehicle speeds and power demands. Also, it has two different EV modes in which the EV mode is shifted from one electric motor drive to two electric motor drives in order to reduce the losses associated with high speed operation of the electric motors, particularly during cruise operation [17]

In parallel drivetrain, both the engine and the electric motor can propel the wheels directly (see Figure 1.2 (B)). Properly sized electric motor and battery are necessary to upgrade a parallel drivetrain to an EREV. In the pre-transmission

parallel architecture similar to that of Honda Insight, Civic, and Accord HEVs, a small electric motor is located between the engine and the transmission replacing the flywheel [18]. It is also possible for a parallel HEV to use its engine to drive one of the vehicle axles, while its electric motor drives the other axle. Daimler Chrysler PHEV Sprinter has this powertrain configuration. A direct mechanical connection between the wheels and the engine eliminates the conversion losses from which the series architecture suffers. On the other hand, it reduces the degree of freedom of the engine speed control to the transmission ratio selection.

The series-parallel or power split architecture, the most commonly used drivetrain for HEVs, is illustrated in Figure 1.2 (C). Toyota Prius, the most sold HEV, Toyota Camry and Highlander hybrids, Lexus RX 400h, and Ford Escape and Mariner hybrids benefit from the features of this architecture. The series-parallel architecture first introduced by Toyota Hybrid System (THS) [19-23]. The series-parallel hybrid powertrain combines the series with the parallel hybrid architecture to achieve the maximum advantages of both systems. In this powertrain, the mechanical energy passes through the power split in two series and parallel paths. In the series path, the engine power output is converted to electrical energy by means of a generator. In the parallel path, on the other hand, there is no energy conversion and the mechanical energy of the engine is directly transferred to the final-drive through the power split, a planetary gear system [24]. Generally, similar to the parallel drivetrain, the series-parallel architecture does not have a sized electric motor for the maximum traction power demand of the vehicle. The pure EV mode is possible for the series-parallel drivetrain; however, in addition to the electric motor power capability, there is a mechanical

constraint which arises from the planetary gear set dynamics. There is no clutch to release the electric motor form the planetary gear-set in the series-parallel architecture. Therefore, during the EV mode, the generator speed increases sharply proportional to the motor speed with ring to sun gear teeth number ratio. One of the generator rolls in the series-parallel drivetrain is engine cranking. Therefore, both high speed and torque capability of the generator to start the engine is important for high speed EV driving. Toyota Prius PHEV can operate on the EV mode up to speed of 100 km/hr [24, 25].

Another design for the power split HEV is the Allison Hybrid System also known as AHSII [26]. This system is a dual mode system with two planetary gear set that is designed by GM and currently is employed for several mid-sized SUVs and pick-up trucks.

1.3.4 Drivetrain compatibility for PHEV applications

Each HEV architecture, as discussed in Section 1.3.3, has its own benefits and drawbacks. The characteristics of each powertrain should be reassessed when the battery capacity and the electric motor power are increased in PHEVs. Li et al. have compared the series and the parallel drivetrains of simulated mid-sized SUVs with completely same-sized components in ADVISOR [27]. Two simulations with two different battery capacities resulted in different outcomes in term of the overall powertrain efficiency. The first simulation with a 60 Ah Nickel-Metal Hydride battery resulted in 11.2% better overall drivetrain efficiency for a parallel architecture. This was caused by better efficiency of the electric motor operation in propelling and regenerative braking modes of the

parallel drivetrain. Another simulation with an upgraded battery to 80 Ah power showed that the series powertrain passed all the simulated power-cycle in the AER. While the upgraded overall efficiency of the parallel configuration did not improve with an upgraded battery, the series powertrain showed 30.5% better overall efficiency in comparison to the parallel drivetrain. The series powertrain had less pollutant operation while had sluggish acceleration performance due to the electric motor and the battery power limitations. The study concluded that with limited on-board electric energy, the parallel PHEV overall efficiency and the acceleration performance are more than the series drivetrain. However, by increasing the battery capacity the series drivetrain is completely preferable [27].

Jenkins et al. have investigated the correlation between the motor and the battery weight/power and the fuel economy of Prius series-parallel HEV in ADVISOR [28]. The aim of the investigation was to check the compatibility of the series-parallel drivetrain to be changed to a PHEV. Jenkins et al. simulations showed that there is a slight fuel economy improvement if the motor is upgraded to 75 kW, the motor mass is increased up to 60 kg, while the battery is remained unchanged. With an upgraded battery, fuel efficiency improved up to 80%. The improvement in the fuel economy of a Prius PHEV, which was recently released, is consistent with Jenkins et al. research result in [28].

Two retrofitted Hymotion Prius and EnergyCS Prius PHEVs were tested in the Advanced Powertrain Research Facilities (APRF) at Argonne National Laboratory (ANL) in Urban Dynamometer Driving Schedule (UDDS) and Highway Fuel Economy Test (HWFET) [29]. Hymotion Prius utilizes a Lithium polymer battery parallel to the Prius NiMH battery and EnergyCS replaces the Prius battery with a

higher capacity Li-ion battery. The engine in both tests is ignited in higher vehicle speeds and remained on less frequently compared with the conventional Prius. The operation of Prius PHEV is similar to OEM Prius when the battery is depleted. About two third and half of the fuel consumption is replaced by electricity in UDDS and HWFET, respectively. Due to the reduction of engine load, its efficiency for Prius PHEV were 20% and 24.5% for cold and hot starts, respectively. The engine efficiency were 30.8% and 34.1%, respectively for the conventional Prius in simulation over the same drive-cycle. The temperature of the engine has significant effect on its combustion efficiency and emission. In addition, the continual flow of combustion results gases from the exhaust system maintaining the catalyst at its operational temperature.

Freyermuth et al. have compared three PHEV configurations in PSAT [30]. The components of a midsize sedan sized to meet the following performance criteria:

- 0-60 mph < 9 s
- Gradeability 6% at 65 mph
- Maximum speed > 100 mph

Two different 16 km and 64 km AERs were assumed for sizing of the battery for all three architectures. Consequently, sizing of the components was different for each architecture to meet the above-mentioned performance criteria. In urban driving condition, the series-parallel showed the best fuel economy in comparison with the series and the parallel configurations. The parallel drivetrain had completely better efficiency for the vehicle with the battery sized for 16 km AER

in comparison with the series one, whereas for the vehicle with the battery sized for 64 km AER, the parallel and the series performances were almost similar. In a highway driving condition, the series-parallel and the parallel architectures showed better efficiency in comparison to the series architecture. This is caused by the power recirculation described as the drawback of the series architecture. On the other hand, the engine efficiency of the series PHEV was the highest, since the engine operation is independent of the wheels speed. The series-parallel had better engine efficiency in comparison with the parallel architecture. However, because of the power recirculation particularly in high vehicle speed, the series-parallel drivetrain presents similar overall efficiency to the parallel configuration.

In summary, to investigate the compatibility of different architectures for PHEVs, two parameters should be considered:

1. EV mode capability and range covered during AER

   Generally unlike the series architecture, the electric motor of the parallel and the series-parallel architectures is not capable of providing the maximum traction power demand for the vehicle. If an AER is defined for a PHEV, both the battery and the electric motor should be sized accordingly. That is, the maximum designated speed and gradeability should be achievable during AER with power only supplied with electric power path. Desirable AER has direct relation to the cumulative daily travel in the aimed market. Unused AER hinders the benefits of the PHEV drivetrain by imposing the extra cost and weight of the battery. On the other hand, the battery capable of short CD or AER, only adds extra

weight for a long CS mode operation of the vehicle during longer journeys.

2. Engine load and temperature reduction

During the blended mode or CD, the vehicle power demand is divided between two sources of energy, the battery and the electric motor. That is, the engine supplies a fraction of total energy demand of the vehicle. The engine efficiency is generally higher for medium to high power demand at high torque and medium speed range. Therefore, the engine operation at lower loads deteriorates its efficiency. In addition, the lower engine load reduces its temperature that leads to lower efficiency and higher emission particularly for cold weather operation.

Similar to what Li et al. asserted in [27], if the high capacity battery is available, the series drivetrain has more positive aspects to upgrade to a PHEV or an EREV. Volt GM with a considerable 64 km AER battery capability is selected a series drivetrain as a base of its drivetrain. However, to prevent the double energy transformation, Volt benefits from a mode shifting mechanism that switches the drivetrain to the series-parallel architecture [17]. The series-parallel with more complicated configuration has the most efficient CS mode when operates as a traditional HEV especially for drive-cycles simulating urban area driving. In addition, the planetary gear-set for the series-parallel configuration operates as a Continuous Variable Transmission (CVT). In spite of the fact that the AER cannot be defined for this drivetrain in high speed where the engine ignition is inevitable, still the series-parallel has a very efficient CD mode.

Therefore, it can be concluded that for PHEVs with a smaller battery similar to Prius PHEV, the series-parallel architecture is a suitable choice.

The overall performance of PHEVs dramatically depends on the driving style and conditions when compared to the conventional HEVs. This is due to the added weight of a large battery, when depleted during the AER or CD modes, is just an extra weight. Also, the reduced load of the engine leads to its lower efficiency when compared to conventional HEVs [25].

1.4 PATHWAY FOR BETTER FUEL ECONOMY

Improvements in: (i) well-to-tank, (ii) wheel-to-miles, and (iii) tank-to-wheel efficiencies are three possible approaches to reduce the fuel consumption of vehicles [1, 2].

Available techniques to improve the tank-to-wheel efficiency of vehicles are listed below:

1) Hybridization
2) Engine efficiency improvement
    - Turbocharging and supercharging
    - Direct injection
    - Low friction lubrication
    - Variable valve timing, variable compression ratio
    - Electric accessories (water pump, oil pump, air-condition compressor)
3) Transmission

- Manual transmission
- Continuous variable transmission (CVT)
- Electronic continuous variable transmission (ECVT)

4) Vehicle

- Aerodynamic improvement
- Low rolling resistance tires
- High strength/ low weight alloy and carbon fibre structure

The engine size has significant effect on the fuel economy of the vehicle. For the same power demand from the engine, the efficiency of smaller engines is generally higher. The reason is that the oversized engines are chosen for getting the maximum power demand of conventional vehicles. Drivability, acceleration, gradeability, and towing capacity design targets define the maximum power demand of vehicles. For HEVs or especially for PHEVs in which a powerful battery and an electric motor are available in the powertrain, depending to the architecture, the maximum power demand of the vehicle is supplied with an electric energy path in addition of the engine path. A downsized engine only provides the average power demand of the vehicle that is significantly lower than the designated maximum power capability of the drivetrain. The maximum power of the engine is sized equal to the power demand of the vehicle for cruising at designed maximum speed.

This research focuses on the improvement of the tank-to-wheel efficiency, assuming a predefined component selection for the propulsion system. The opportunities offered by a chosen drivetrain is realised by developing an appropriate EMS. In the following notes, the concept of the fuel consumption of

the vehicle is reviewed and the important parameters for the efficiency of PHEVs are highlighted.

1.4.1 Efficiency of PHEV components

The fuel economy and the maximum AER covered by a fully charged battery are dependent to the efficiency of each of the PHEV individual components. As mentioned before, it is assumed that the components of PHEVs are chosen and the aim of this research is to develop an appropriate EMS to maximise the total efficiency of the vehicle. This requires a comprehensive understanding of the components efficiency to avoid their low efficiency operation region by means of the degree of freedom that the hybrid system offers for selection of different energy paths.

Engine efficiency

The internal combustion (IC) engine is the most popular main source of power for vehicles. The term engine in this research mainly refers to the Spark Ignited (SI) engines. However, the developed methods in this research are similarly applicable to other types of engines like Compression Ignition (CI), two-stroke, Wankel rotary, and Stirling engines. Brake Specific Fuel Consumption (BSFC) is the term defined to show how efficiently an engine transforms fuel energy to the usable mechanical power at the crankshaft. BSFC is defined as the fuel flow rate per useful power output and generally is in $[gr/kWh]$ unit.

$$BSFC = \frac{\dot{m}_{feul}}{P_{eng}} \qquad \textit{Eq. 1-1}$$

$\dot{m}_{fuel}$ is the fuel flow rate and P_{eng} is the engine useful power output. The efficiency of the engine is defined as the ratio of the engine power to the amount of fuel energy supplied.

$$\eta_{eng} = \frac{P_{eng}}{\dot{m}_{fuel} . Q_{lhv}} \qquad \textit{Eq. 1-2}$$

where Q_{lhv} is the fuel lower heating value.

The efficiency of engine varies widely with its speed and torque. Among all applicable operation points of an engine, the most efficient region of engine operation is generally located at the middle range speed and high torque. BSFC and efficiency map of a typical engine is depicted in Figure 1.3. Avoiding low efficiency regions of the engine is almost part of all HEVs and PHEVs EMSs. The EV mode at low vehicle speed and power-boost with electric motor when high power required from the drivetrain are well-known approaches to avoid the low efficiency operation of the engine for HEVs.

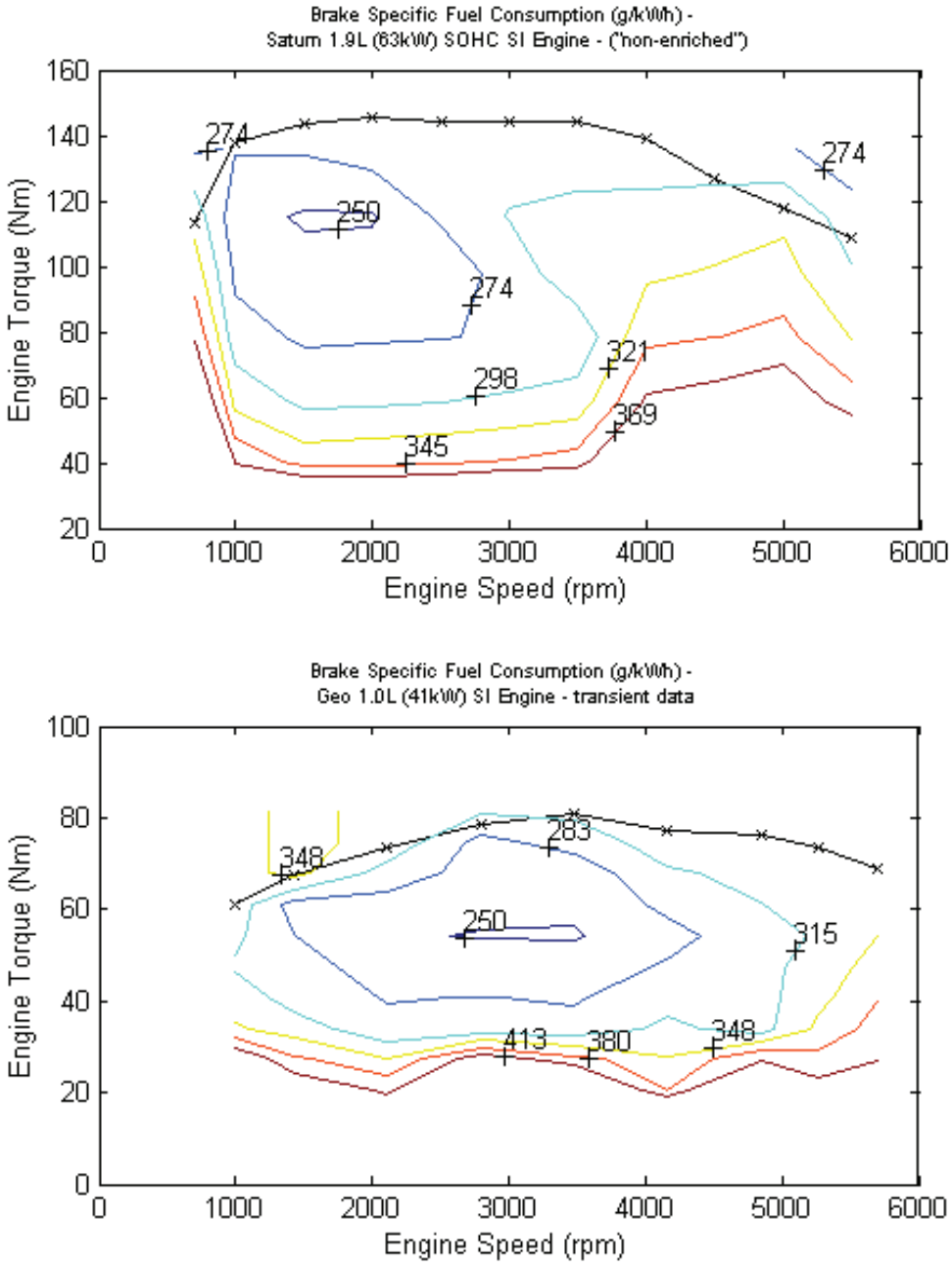

Figure 1.3. BSFC and efficiency map of two typical engines [ADVISOR database]

Electric motor/generators efficiency

Electric machines in all architectures of HEVs operate in both motor and generation modes. In addition to providing tractive force and assisting the engine to operate efficiently, one of the major roles of the traction motors is regenerative

braking. The efficiency map of the permanent magnet synchronous motor (PMSM) of Toyota Prius Gen.1 is depicted in Figure 1.4. The permanent magnet synchronous motors are completely dominant options for vehicular traction applications since they are well-known low maintenance and high power density electric motors.

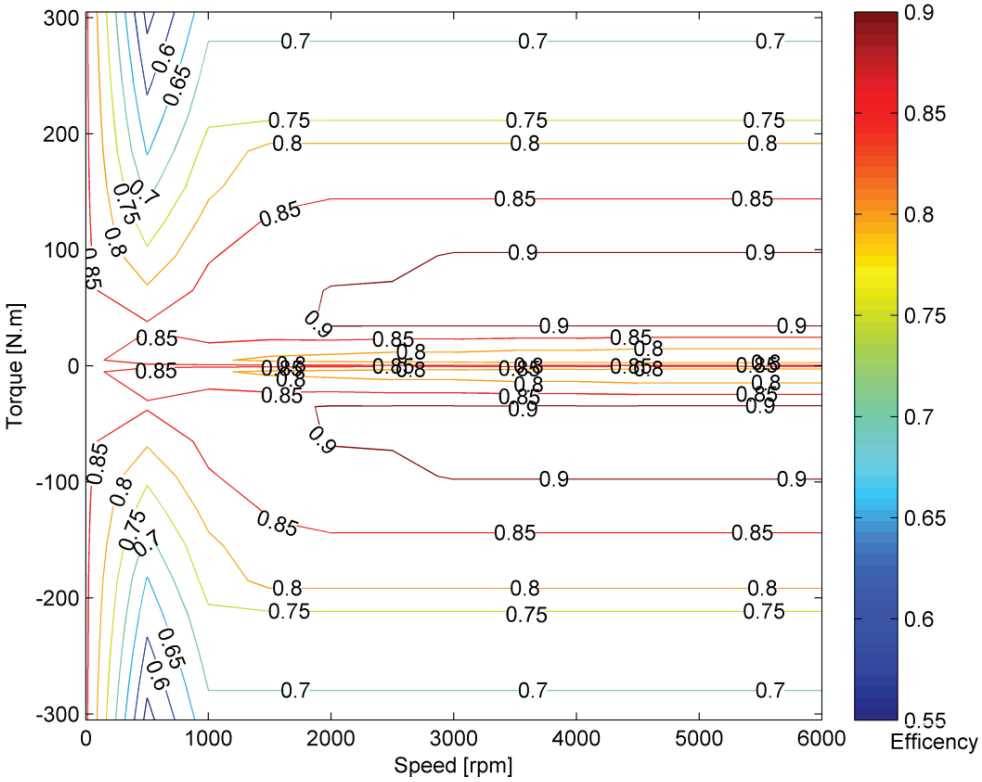

Figure 1.4. Toyota Prius Gen.1 traction motor efficiency map [ADVISOR database]

Battery efficiency

Chemical batteries, super capacitors, and ultrahigh-speed flywheels are different Energy Storage Systems (ESS) available for EV, HEV and PHEV applications. Recent advancements in the chemical battery technology enable marketability of PHEVs and EVs. The energy losses account for power recirculation from mechanical to electrical during recharging of the battery by the

engine should be considered in the EMS of HEVs and PHEVs. Internal resistance and columbic efficiency of the battery are major parameters in the battery operation efficiency. Here, battery is modelled as an equivalent circuit of a perfect open circuit voltage source in series with an internal resistance (see Figure 1.5). The characteristics of the charge reservoir and the internal resistance are a function of the remaining charge and the temperature of the battery cell. More information about the battery model can be found in Section 3.6.3.

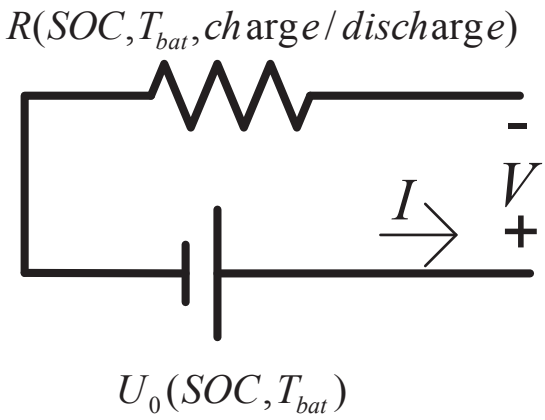

Figure 1.5. Equivalent circuit for a battery

Since the large PHEV ESS benefits from parallel modules, its internal resistance compared to the conventional HEVs is significantly lower. Therefore, the electrical waste in PHEV battery is reduced accordingly.

Transmission efficiency

Mechanical energy losses also occur in geared transmissions and especially in hydraulic torque couplers of automatic transmission. Continues Variable Transmissions (CVT) sometimes known as Electronically Controlled Continues

Variable Transmissions (ECVT) is dominant in power-split type hybrid systems. Most of the commercialized HEVs and PHEVs benefit from a planetary-gear-set power split system. Geared transmissions generally have very high efficiency. Gear ratio is the only controllable parameter affecting the vehicle performance by changing the engine or electric machines operation points. This can be controlled by part of EMS responsible for selection of the optimum engine to wheel speed ratio.

Power electronics efficiency

The efficiency of the power electronics has important role particularly for PHEVs in which a significant share of the required traction energy is provided electrically. In terms of the energy management strategy of PHEVs, there is no meaningful control over the power electronics efficiency. The detail of power electronics of PHEVs' converters and inverters is out of the scope of this research.

1.4.2 Auxiliary loads

Auxiliary loads have a significant role on energy consumption of vehicles. For instance, the air conditioning (AC) required power even outweighs the losses accounted for aerodynamic, rolling resistances, or driveline losses. The power required for the AC equals the amount of power required to run the vehicle at steady state speed of 56 km/hr [31]. Tests show that the AC contributes 37% of the emission of the vehicle over the US Supplemental Federal Test Procedure [32].

The effect of the auxiliary load is even higher for more fuel-efficient vehicles like HEVs and PHEVs. For instance, the Honda Insight fuel consumption is increased by 46% when the AC is used. The study by Johnson showed that the US uses 27 billion litres of gasoline every year for the AC in vehicles, equivalent to 6% of the domestic petrol consumption or 10% of US imported crude oil. [31].

Since it is completely likely for HEVs and PHEVs that the engine turns off for a long period, many auxiliary loads should be provided electrically by the battery. Therefore, the mechanical connection between the engine and the auxiliaries is replaced by electrically powered components. Electric water pump, oil pump, hydraulic steering fluid pump, brake booster vacuum pump, and AC compressor electric motor are some examples. There is a large difference between the HEVs and PHEVs auxiliary loads that arises from the very long engine-off mode or the AER capability of PHEVs. The engine in HEVs is the sole energy source assuring that hot water is always available for cabin heating for cold seasons. However, the electric cabin heaters must be employed to satisfy passengers comfort. This adds an extra auxiliary load which is conventionally supplied free of cost from the engine coolant.

1.4.3 Energy management strategy

An energy management strategy is a control rule that is pre-set in the vehicle controller and commands the operation of the drivetrain components. The vehicle controller receives the operation commands from the driver and the feedback from the drivetrain and all the components, and then makes decisions to use proper operation point for the drivetrain components. Obviously, the performance of the

drivetrain relies mainly on the control quality in which the energy management strategy plays a crucial role. This thesis focuses directly on the optimization of EMS of PHEVs. Therefore, a complete chapter is dedicated to describe the important concepts in the EMS of HEVs and PHEVs. The full literature review on the EMSs is outlined in Chapter 2.

1.5 RESEARCH AIM, OBJECTIVES AND CONTRIBUTIONS

The main aim of this research is to improve PHEVs' fuel consumption by developing an optimal energy management strategy (EMS) for the vehicles. Emissions reduction and saving the state of the health of the battery are also two secondary objectives of the research. It is assumed that the architecture and sizing of the vehicle components are already chosen. The EMS tries to harness the maximum benefit of the drivetrain potentials and specially the extra energy source that the grid-charged battery provides. Therefore, a charge management strategy is incorporated into the EMS.

As described in Section 1.4, the pathway for better fuel economy, a comprehensive knowledge of different environmental and vehicle internal characteristics is required to fulfil the aim of this study. The knowledge of future driving patterns for the journey is crucial to benefit optimally from the extra energy source available in the battery. The blended mode EMSs are only feasible when the driving pattern is known. The driving pattern consists of the drive-cycle and a comprehensive knowledge of the environmental impact on the power demand and the performance of the vehicle components. Particularly, PHEVs are more sensitive to the temperature noise-factor. Temperature alters the power

demand of the vehicle when the AC or the cabin heater operation is required. Besides, the performance of the vehicle components is influenced by temperature. Therefore, the integration of thermal management and the EMS of PHEVs is required to address the aim of the research.

The main contributions of this thesis are outlined as follows:

- The effects of noise factors on the drivetrain power demand and the performance are investigated by introducing the concept of the power-cycle in place of the drive-cycle for a journey.
- An applicable solution for developing a library of power-cycles inside the vehicle is introduced to potentially make the noise factors predictable. By considering the noise factors and the power-cycle library, the future power-cycle is predictable more accurately.
- The effect of temperature on the performance of PHEV components and its significance on optimal energy management strategies are identified and discussed.
- An easily implementable semi-optimised rule-based EMS for a known power-cycle is proposed. The effect of the temperature noise factor on the engine performance is also considered for the rule-based EMS.
- A globally optimised EMS based on the theory of dynamic programming (DP) is developed. It investigates the effect of temperature on the optimal charge depleting trajectory of PHEVs for a predefined journey. The optimal charge trajectory coincides with an engine temperature trajectory which guarantees the optimal engine operation and maximum availability

of engine hot water for cabin heating while satisfying the complete charge depleting constraint.

- A practical approach to employ the optimal charge trajectory for calibrating a real-time rule based EMS is proposed.

1.6 OUTLINE OF THE THESIS

This thesis is organized as follows:

Chapter 2 provides a comprehensive literature review on energy management strategies of HEVs and exclusively PHEVs.

Chapter 3 describes the modelling of the vehicle and presents a thermal model of the engine required for evaluation of PHEVs performance considering the temperature noise factor.

Chapter 4 introduces different noise factors which influence both the power demand of the vehicle and the operation performance of the powertrain components. Particularly, the temperature noise factor is highlighted since the PHEVs performance is more sensitive to temperature compared to the conventional HEVs. In addition, a library based prediction of the future power-cycle, necessary for optimal charge management of PHEV, is characterized.

Chapter 5 presents a new rule-based EMS for a known power-cycle. The EMS also considers the effect of the temperature noise factor on engine cold-factor penalty.

Chapter 6 describes the numerical optimization method used to implement the optimal EMS. A new EMS with the dynamic modelling approach based on the theory of dynamic programming (DP) is introduced.

Finally, Chapter 7 provides the concluding remarks and suggests the future works.

CHAPTER 2

REVIEW ON ENERGY MANAGEMENT STRATEGIES FOR HEVS AND PHEVS

2.1 INTRODUCTION

In all type of HEVs or PHEVs, an energy management strategy (EMS) must determine how to fulfil the power demand of the driver in an efficient manner from different energy paths available in the hybrid system. The main objective of the energy management strategies is generally the reduction of fuel/electricity consumption and emission while considering drivability requirement and components operation restrictions and characteristics. This chapter provides a

review on classification of energy management strategies employed for HEVs and PHEVs, with an emphasis on the recent literature on the EMS of PHEVs.

2.2 POWER, ENERGY, AND CHARGE MANAGEMENT STRATEGY

As described in Chapter 1, an EMS is a control rule that is pre-set in the vehicle controller, and that commands the operation of drivetrain components [1]. The terms "energy management strategy", "power management strategy", and "supervisory control strategy" are commonly used in similar context in HEV and PHEV literature. Nevertheless, in this thesis two terms "energy management strategy" and "power management strategy" are distinguished. In power management strategy of conventional HEVs, the controller goal is to maintain optimal operation of the powertrain for supplying a specific power demand as well as sustaining the battery state of charge (SOC) [33]. In PHEVs, however, the large battery has the role of both load levelling and energy source. Therefore, it is acceptable if the battery SOC reaches the minimum applicable range. The difference between the concepts of energy management and power management are more distinguished in PHEVs control strategies as both the engine and the battery are the sources of energy unlike HEVs in which the battery energy is also supplied by the engine [34]. The available charge in PHEVs' battery, generally a battery, adds more flexibility to the EMS of PHEVs in distributing load between the engine and the battery compared to conventional HEVs. A charge management strategy should be incorporated into the EMS of PHEVs. The charge management strategy in PHEVs defines how to share the available ESS energy during a journey to optimally utilize it for improving the performance of the

vehicle [35]. On the other hand, power management is generally concerned with how to split the drivetrain power demand between the two power sources to achieve the best performance in a real-time fashion.

2.2.1 PHEV operation modes

Brief description of PHEV operation modes is outlined in Section 1.3.2. The charge management of a PHEV is incorporated into the EMS of PHEV, and defines the vehicle operation mode. The simplest energy management of PHEVs is to run the vehicle on the CD or if possible on the EV mode until the battery depletes to a minimum applicable SOC. This stage is referred to as electric vehicle (EV) mode and the range covered is named all electric range (AER). Subsequently, the vehicle operates like a conventional HEV in the charge sustaining (CS) mode to stabilize the SOC. The advantage of the AER followed by the CS strategy is the maximum consumption of stored electric energy which is relatively cheaper before the vehicle reaches its destination with available recharging facilities.

Another energy management strategy, which is known as blended mode, uses both the battery and the engine simultaneously for vehicle propulsion to achieve higher efficiency as the available energy in the battery could help provide more efficient load levelling in the hybrid system. Different researchers have developed different blended mode EMS strategies, since they are considerably related to the architecture and the components sizing of a specific PHEV. Specially, in the parallel and the series-parallel architectures, the blended mode is inevitable because of the drivetrain mechanical restrictions and components sizing [13, 36-

39]. An appropriate powertrain load split between the battery and the engine energy sources is therefore an important issue in developing the blended mode strategies, as reaching the destination with surplus electric energy sacrifices the benefit of availability of large and expensive battery on-board of PHEVs. The schematic illustration of the PHEVs operation modes is depicted in Figure 2.1.

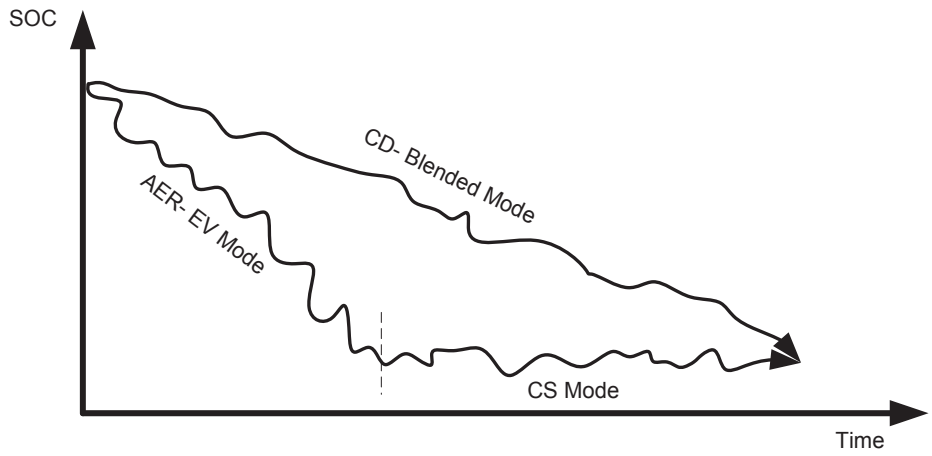

Figure 2.1. PHEV operation modes

2.3 CLASSIFICATION OF ENERGY MANAGEMENT STRATEGIES

The full classification of the control problem of the EMS for HEVs and PHEVs has been outlined in the literature [12, 33, 40-42]. The literature provides a number of approaches for the EMS of HEVs, many equally applicable to both plug-in and conventional (i.e., non plug-in) HEVs. The number of publications about the EMS of PHEVs is relatively lower than that of the HEVs. The control problem for the EMS of HEVs and PHEVs is generally grouped into two categories: (i) rule-based controllers and (ii) optimization-based controllers [41].

The classification of control problem formulation for the EMS of PHEVs is depicted in Figure 2.2.

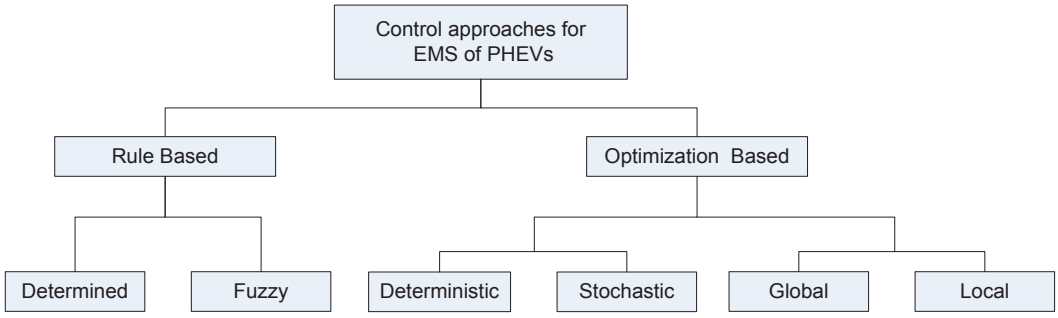

Figure 2.2. Control problem formulation tree for the EMS of PHEVs

2.3.1 Rule-based controllers

Rule-based controllers are the most common approaches implemented for the EMS of HEVs and PHEVs. State machine models reflected in flowcharts and lookup tables are implemented for deterministic rule-based controllers [43]. PHEV operation modes and drivetrain components operation points are selected based on a set of rules defined by input variables of the driver power demand and feedbacks from the components such as the battery SOC. Typical objectives defined by rules are:

- If there is a torque distribution in the hybrid system, it should result in high efficiency
- Engine low operation efficiency and transient engine operation should be avoided
- Electric energy should supply the low power demand of the vehicle
- Regenerative braking recuperates the depleted battery whenever possible

- Charge sustaining limits for HEVs and charge depleting limits for PHEVs are enforced with the controller

Fuzzy controllers are also another rule-based approach for designing the EMS, and are more efficient compared to deterministic rule-based controllers [44-46]. The main advantage of the rule-based controllers is that they are based on engineering intuition and physical tests and are generally easily implementable. Unfortunately, the behaviour of the rule-based controllers extremely depends on the selected thresholds for change of states or in case of the fuzzy controllers the definition of membership functions. The driving condition and the driver behaviour could substantially alter the optimal defined thresholds and membership functions. A blend of pattern recognition and fuzzy logic was proposed by Langari and Won for a HEV [47, 48].

2.3.2 Optimization based controllers

Optimization based controllers are identified based on the mathematical modelling approach selected to formulate the HEV or PHEV energy management control problem. Optimization based controllers can be classified into two branches: local vs. global optimization and deterministic vs. stochastic optimization (see Figure 2.2)

Local vs. global optimization

Performance and fuel economy of a PHEV depend on its efficiency in all segments of a journey. Local optimization approaches have a major drawback that

is they cannot find the global optimum solution resulting in non-optimal operation of HEVs or PHEVs for the whole journey [2, 25, 33-35, 41]. Particularly for the EMS of PHEVs, the optimal charge management requires insight about the driving pattern of the vehicle from the beginning to the end of journey. It is mathematically possible to find the optimal solution for the EMS of PHEVs if accurate information about the trip like drive-cycle and accessories power demand is available in advance to formulate the optimal control problem. Indeed, a correct formulation of the vehicle model is the perquisite to solve the optimal control problem. Using historic driving patterns, GPS, vehicle-to-vehicle, and vehicle-to-infrastructure communication facilitate more accurate prediction of driving scenario [34, 49-52]. In the absence of any information about the vehicle trip, the local optimization approaches are the only viable solutions.

- Global optimization based controller for EMS

Dynamic programming (DP) is one of the most well-known and powerful optimization tools to solve complex control problems. Dynamic programming is known as both a globally optimised and a deterministic energy management strategy. Dynamic programing is a globally optimal approach which can find the best charge depleting profile, also can act as the benchmark for other EMSs of PHEVs. It gives the best possible solution for the control problem with respect to the used discretization of time, state space, and inputs. Dynamic programming suffers from the curse of dimensionality, which means that the computational time increases exponentially with an increase in state variables. Its key disadvantage is the high computational effort which is opposed to its real-time implementation for online control of a vehicle [49, 53-60]. Since charge management is only

applicable when the whole journey is considered over optimization horizon, it is thus necessary to predict the driving pattern of the vehicle in advance to formulate the optimal control problem of the EMS of PHEVs.

- Local optimization based controller for EMS

Local optimization methods are somewhat similar to the rule-based controllers as only the current operation of the hybrid system is optimised. Since the EMS of PHEV should incorporate a charge management strategy alongside an online power management strategy, the local optimization based controllers are not appropriate to achieve the maximum benefit of having a large battery on board. A well-known locally optimised controller approach adopted for on-line control of HEVs is equivalent consumption minimization strategy (ECMS) [2, 61-64]. For the ECMS, the electricity consumption is converted to an equivalent amount of fuel consumption, and then the EMS tries to minimise the equivalent fuel consumption in an on-line fashion. The ECMS is a deterministic approach that can be derived based on Pontryagin's minimum principle introduced in [65]. The equivalence based control algorithms evaluate which combination of the traction sources is more appropriate for the current power demand. Generally, ECMS is developed for parallel hybrid architecture in the literature. The combined equivalent power is defined by Eq. 2-1.

$$P_{eq} = P_{Eng} + \beta . P_M + P_{Pen} \qquad \textit{Eq. 2-1}$$

where β is equivalence factor and P_{Pen} is a penalty defined to prevent frequent change of condition like gear shifting or rapid changes of engine velocity. If β

increases the cost of providing power demand of the vehicle from electric energy path rises proportionally compared to the engine energy path. The term equivalence factor , β , comes from the fact that in HEVs all energy comes ultimately from the fuel, the battery charge or discharge are translated respectively into equivalent fuel consumption or equivalent fuel savings. The knowledge of power-cycle is required to tune the equivalence factor, β, based on the past and future driving condition to satisfy the battery charge trajectory and boundary limitations [55, 66]. Another approach is to use a PI controller which changes β aiming for a given target battery charge. This adapting process of β is also known as A-ECMS [67]. The disadvantage of A-ECMS is its sub-optimality compared to the global optimal approaches. As the cost function based on the equivalent power, P_{Eq} is developed locally, consideration of the slow dynamic phenomena like temperature are not practically implementable for this approach.

Deterministic vs. stochastic optimization

Deterministic systems consistently provide a similar output to a set of input variables. As mentioned before, DP is a deterministic optimization approach to find a globally optimised EMS. Stochastic dynamic programming, however, deals with the optimization problems which involve some uncertainty and random elements. Stochastic dynamic programming (SDP) is appealing for optimization of EMSs over a probabilistic distribution of power-cycles, rather than a single cycle [68-74]. Unlike deterministic DP, the optimization process is performed on a class of trajectories from an underlying Markov chain power-cycle generator rather than a single predefined power-cycle. If this stochastic process is able to

well define the journey characteristics, the optimal EMS could be developed based on it. Since the process of Markov chain is time invariant, the assumption is that the vehicle will continue to drive forever which is not appealing for charge management of PHEVs. As described before, charge management has an important role in the EMS of long electric range PHEVs. Therefore, SDP suits better for HEVs or PHEVs in which the battery and motor are incapable of the AER or the EV mode.

2.4 EMSS EXCLUSIVELY DEVELOPED FOR PHEVS

In comparison to the literature of the HEVs' control strategies, there are a limited number of publications which investigate the EMS of PHEVs. In the following notes, some of the approaches that exclusively address the EMS of PHEVs are outlined.

Gao et al. suggested two different rule-based EV-CS and blended EMSs for a PHEV with the parallel architecture [13, 36]. They also suggested a manual shifting option between the EV and the CS for driver. In this rule-based strategy, the engine is constrained to operate around its efficient region defined by two minimum and maximum torque boundaries in the engine efficiency map. The engine is controlled as that no surplus energy remains to charge the battery to prevent charging and discharging power recirculation wastes. When the required torque is higher than the top torque boundary, the remaining power demand is supplied by the electric motor. The engine solely propels the wheel if the demanded torque from the engine is between the boundaries of the defined efficient region. The engine is turned off when the torque demand is below the

bottom torque boundary and the vehicle runs in purely in the EV mode. In this approach, it is assumed that there is no information available about the trip duration and length. Therefore, when vehicle operates in the blended mode, it is possible to reach destination with surplus in battery energy for short trips. Whereas, the EV-CS EMS uses relatively cheaper battery energy in place to petrol for the same trip. Therefore, this approach does not provide higher fuel economy for all situations.

Sharer et al. in [38] simulated and compared four different blended rule-based EMSs for a series-parallel PHEV with 16 km AER battery in PSAT for a vehicle with similar component sizing of the Freyermuth et al. model explained in reference [30]. The four EMSs are named as:

- Electric vehicle/charge sustaining (EV/CS)
- Differential engine power
- Full engine power
- Optimal engine power

In “EV/CS” EMS, the engine only turns on when the power demand is higher than the available power of the battery until the battery depletes to its minimum applicable SOC. “Differential engine power” EMS is similar to the EV/CS but the engine-turn-on threshold is defined lower than the maximum applicable power of the battery. In “full engine power” EMS, if the engine turns on it will supply all the power demand of the vehicle and no power will be drained from the battery. The aim of this strategy is to force the engine to operate at higher loads and consequently with higher efficiency. In “optimal engine power” EMS, the engine

is restricted to operate close to the peak efficiency point of the engine. For different predetermined journey distances, the engine-start threshold can be derived and calibrated by simulation. In other words, for longer journeys to continue further in the CD mode before entering the CS mode, the engine-turn-on threshold should be reduced. The concept behind this EMS is to force the engine to operate and ignite in higher average efficiencies during the journey as much as possible by saving electric energy for low power demand sections of drive-cycles. The simulation results prove that the "differential engine power" EMS has a similar overall efficiency with respect to "EV/CS" EMS since the engine operation in low loads deteriorates the vehicle overall fuel economy. "Full engine power" EMS resulted in the best fuel economy with about 9% improvement even more than the "optimal engine power" EMS. Although the engine operates more efficiently in the "optimal engine power" EMS, the overall efficiency is reduced due to the effect of power recirculation and efficiency chain. The interesting result was that the "optimum engine power" EMS produced no significant improvement and even sometimes deteriorated the efficiency for some trip distances compared to the EV/CS EMS [38].

The deterministic dynamic programming (DP) approach was employed by Gong et al. to force the battery to get fully depleted exactly at the end of journey. The global optimization by means of the DP algorithm offered significant efficiency improvement in comparison with the EV/CS EMS. As the DP is a deterministic approach, the trip information as a priori is required. Therefore, trip simulation with GPS and GIS information is introduced in this paper [49].

A stochastic optimal approach for the power management of PHEVs was suggested by Moura et al. to optimise a series-parallel drivetrain for a probabilistic distribution of many power-cycles, rather than a single one [69]. By using a discrete-time Markov chain, the model of power-cycle was predicted. Both fuel and electricity costs are considered in the defined cost function. Consequently, the benefits of controlled charge depleting were explored.

As mentioned before, the number of available published works in the field of EMS of PHEVs is quite limited. The effect of different noise factors on the EMS of PHEVs still has many aspects to explore (see Chapter 4).

2.5 CONCLUSION

Among all the existing EMS approaches described in this chapter, two different methods, (i) a rule-based/deterministic and (ii) an optimization-based /deterministic, are selected in this research. The deterministic approaches are selected because one of the major objectives of this research is the optimal charge management of PHEVs. Hence, the prediction of power demand pattern during the journey is a prerequisite for developing the deterministic methods. In addition, to explore the effect of slow dynamic phenomena like temperature on the performance of vehicle, deterministic methods are only feasible options. The rule-based approaches are easily implementable while the optimization-based/deterministic approaches provide the global optimal solution. The rule-based/deterministic approach is presented in Chapter 5 and the optimization-based/deterministic approach is introduced in Chapter 6.

CHAPTER 3

VEHICLE MODELLING

3.1 INTRODUCTION

In this thesis, vehicle modelling deals with mathematical representation of physical reality of longitudinal dynamics of the vehicle. This chapter discusses the modelling approach for the vehicle and its powertrain components. The level of acceptable approximation in modelling process defines the efficiency of the model. The more detailed is the mathematical modelling of the physical dynamics, the more complex and timely is the simulation process. The models in

this research are defined with the aim of solving the optimal control problem for the energy management strategy of PHEVs to improve fuel efficiency and reduce emissions. Therefore, the dynamic phenomena that are not related to the energy efficiency of the vehicle are neglected.

In order to evaluate the fuel economy of the vehicle, it is necessary to understand the energy flow in different powertrain components of the vehicle. In this chapter, first the basics of the longitudinal dynamics of the vehicle is introduced, then the characteristics of modelling and sizing of the powertrain components are outlined.

3.2 LONGITUDINAL DYNAMICS OF VEHICLES

The loads and parameters that affect the longitudinal dynamics of a vehicle and its load demand are depicted in Figure 3.1. The dynamic equation of the vehicle along the longitudinal direction is as follows:

$$F_t = M\frac{dV}{dt} + F_r + F_d + F_g \qquad \textit{Eq. 3-1}$$

where F_t is tractive effort, M is mass of vehicle, dV/dt is linear acceleration of vehicle along longitudinal direction, F_r, F_d, F_g are rolling, drag, and grading resistances, respectively. The required traction power, P_t, is derived from Eq. 3-1 as follows:

$$P_t = F_t V = \left(M\frac{dV}{dt} + F_r + F_d + F_g\right)V \qquad \textit{Eq. 3-2}$$

Detailed description of the resistive forces could be found in reference [1].

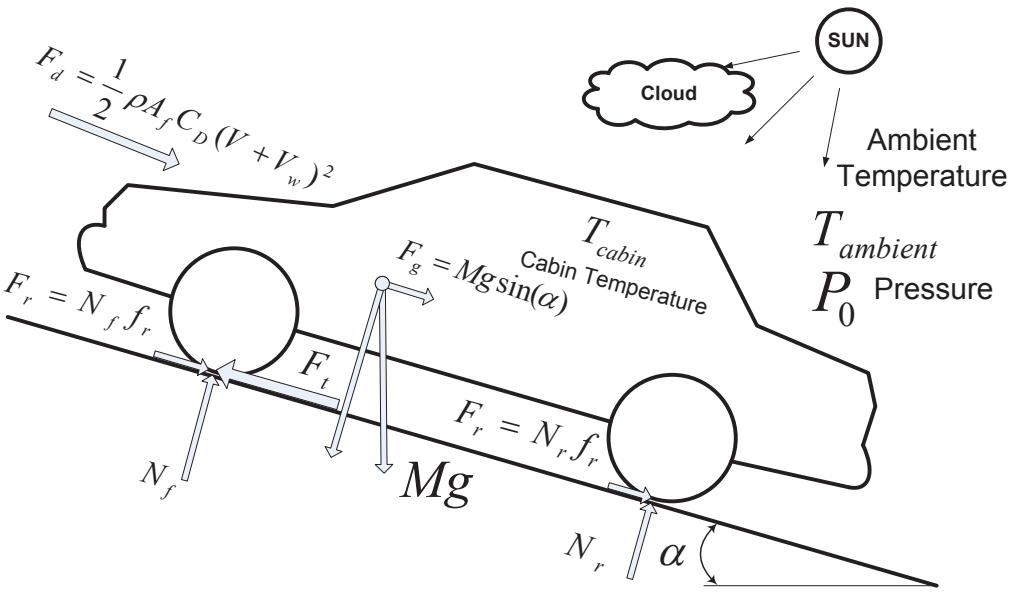

Figure 3.1. Vehicle loads and environmental parameters which affect the longitudinal dynamics of a vehicle.

3.3 METHODS OF MODELLING

There are three different methods to model the fuel consumption of vehicles. Each method has its characteristics, drawbacks, and level of accuracy [2].

3.3.1 The average operating point approach

This approach only gives a first approximation of fuel consumption of the vehicle. The key feature is that the engine operation and its fuel consumption are modelled by a lumped method. The engine efficiency is assumed constant and calibrated based on a datum drive-cycle. The efficiency of all drivetrain components, which transfer power in drivetrain, are also defined with a single efficiency coefficient. The simplicity of the average operating point approach

makes it suitable for preliminary steps of finding fuel consumption and performance investigation of vehicles. On the other hand, it has limited capability for developing EMS for complex drivetrains like PHEVs in which the efficiency of the components is significantly altered during different operation modes.

3.3.2 The quasi-static approach

In this approach, each simulation over a drive-cycle is divided into many time-steps during which it is assumed that the vehicle velocity, acceleration, and any other effective input variables remain constant. These time-steps should be short enough to satisfy the quasi-static assumption. In this approach, to find the efficiency of each component consisting of the engine, the electric motor/generators, the battery, and the transmission components, instead of a single efficiency coefficient an efficiency map is employed to reach more accurate physical modelling. That is, based on the amount and components of power (torque and angular velocity for mechanical parts or voltage and current for electrical parts) are transferred from each powertrain nodes, the efficiency of each component is derived from the efficiency maps for each time-step.

The quasi-static method is a powerful tool for development and analysis of the EMS for all vehicular drivetrains under different levels of complexity with limited numerical efforts. The main feature of the quasi-static modelling is its backward formulation which requires the knowledge of the driving scenario in advance. Therefore, this approach is not appropriate for feedback control or state events simulation. In Section 3.4, descriptive characteristics of the forward and the backward modelling approaches are explained.

3.3.3 Dynamic approach

This approach is based on the dynamic modelling of any physical phenomena by means of state space formulation or mixture of differential and algebraic equations. If modelling of the fast-dynamic physical phenomena like combustion or emission forming is needed, the dynamic approach is the only feasible solution. The dynamic approach is necessary for feedback control analysis like hardware-in-the-loop simulations. In addition to the complexity of this approach, the high computational cost of simulations is another drawback of the dynamic modelling approach.

3.4 FORWARD AND BACKWARD MODELLING APPROACHES

By rewriting Eq. 3-1 another form of the dynamic equilibrium equation can be rewrite as:

$$M\frac{dV}{dt} = \left(F_t - F_r - F_d - F_g\right) \qquad \textit{Eq. 3-3}$$

Eq. 3-1 and Eq. 3-3 are similar but each of them represents a different approach of modelling of vehicular longitudinal dynamics.

3.4.1 Backward approach

In this approach, it is assumed that vehicle follows a prescribed route. i.e. the drive-cycle is known in advance. Therefore, by using Eq. 3-1 and velocity profile, V, the tractive force, F_t, can be calculated. The calculated force is then interpreted

to torque and angular velocity over the electric motor and the engine considering the transmission ratios and wastes. As the calculation flows from force on the wheel to downstream components in each time-step, the method is named as backward approach. A combination of a quasi-static and backward approach is generally a powerful tool for fuel-consumption prediction and development of EMSs. Since the backward approach assures exact following of a prescribed route, it is useful when the performance of the vehicle over benchmark drive-cycles defined by authorities is the point of interest.

Since the backward quasi-static approaches are based on the static steady-state efficiency maps, the transient behaviour of the components is neglected in this approach.

3.4.2 Forward approach

In this approach, on the other hand, simulations start from a driver model. Generally, a PID controller as a driver compares the actual and the required vehicle speeds and provides the required control input commands. This input command is then interpreted by EMS for the powertrain components of the vehicle to minimise the error signal. The input commands transforms to torque output from the engine and the electric motor. Then, the model based on the dynamic Eq. 3-3 derives the real acceleration and velocity. The structure of the forward approach makes it suitable for dynamic simulations.

3.5 SIMULATION TOOLS

Fierce competition among automotive manufacturing entities puts significant pressure on the companies to introduce new vehicle models to the market as soon as possible. Almost all major automotive manufacturers have developed their own simulation tools which mostly are unavailable to the public [75]. Mathematical modelling has replaced many physical tests required for investigation of vehicle performance and fuel consumption. Particularly, when performance comparison and component sizing of newly developed HEVs and PHEVs is required, simulations based on the mathematical modelling approaches are desirable.

The Mathworks products, Matlab and Simulink are the most popular platforms for modelling of HEVs and PHEVs. Modelica also provides a causal modelling language based of which the commercialized Dynasim Dymola modelling platform has been developed. Some researches use it for their vehicular simulation and modelling [76-78].

Advance Vehicle Simulator (ADVISOR) developed in National Renewable Energy Laboratory, and Powertrain System Analysis Toolkit (PSAT) developed in Argonne National Laboratory are two dominant simulation tools specifically developed for advanced vehicles [79, 80]. Both ADVISOR and PSAT are developed in Matlab/Simulink. ADVISOR is an empirical map-based simulation tool that combines the vehicle dynamics model with the efficiency map of each component to predict the vehicle performance. ADVISOR is a unique combination of backward and forward simulation tool which calculates each component operation parameters for a known drive-cycle based on the quasi-static

assumption [79]. In contrast to ADVISOR, PSAT is a look-forward simulation tool that calculates the powertrain states based on the driver input.

In addition to the commercial simulation and modelling tools, many researchers have developed their own modelling tools to incorporate their suggested control strategy into the simulation platforms [24, 81-84]. The major reason is that the level of complexity of available commercial simulation tools like ADVISOR or PSAT makes it hard to incorporate new models or controller into them. Comprehensive understanding of the relationship between sub-models and significant number of parameters is essential if one needs to incorporate some new sub-models or controllers into the commercial simulation tools. In addition, the developers of the commercial tools might intentionally restrict access to the codes or sub-models. Nevertheless, this level of detailed modelling improves the accuracy of simulation as the models are generally verified with physical test conducted in well-equipped test facilities.

3.6 MODELLING APPROACH USED IN THIS WORK

Two different modelling approaches have been taken for this research. First, the vehicle components are sized and modelled in a backward quasi-static approach. As explained in the previous section, the backward quasi-static modelling approach has beneficial characteristics for investigation of EMSs and specially charge management to check the performance of the vehicle for a complete journey. To verify the simulations and modelling approach in this research, ADVISOR powertrain simulation tool is employed. ADVISOR developed by National Renewable Energy Laboratory (NREL) [79]. In 2003

(NREL) transferred a license to commercialize ADVISOR to AVL Powertrain Engineering, Inc. [85]. ADVISOR provides a trusted, verified, and detail model of the vehicle that assures accurate and close to reality simulation results.

The second modelling method that would be described in details in Chapter 6 is a dynamic approach based on the theory of dynamic programming. An inverse powertrain model analogous to the quasi-static model of a PHEV is formulated as an optimal control problem in dynamic programming to find the optimal charge depleting trajectory and the EMS of the PHEV.

3.6.1 Drivetrain architecture and sizing of the sub-models

A model of EREV is developed for the serial powertrain architecture. The basic characteristics of the considered vehicle are given in Table 3-1. The main components of the vehicle are illustrated schematically in Figure 3.2. We have tried to keep the sizing of the components similar to the published characteristics of GM Volt. GM Volt is a 64 km EREV benefiting from a mode changing architecture by means of a planetary gear set which can shift the vehicle architecture from serial to series-parallel. In this mode, the engine could mechanically transfer power to the final drive in higher speeds and power demands. Also, it has two different EV modes in which the EV mode is shifted from one electric motor drive to two electric motor drives in order to reduce the losses in higher speeds and cruise operation [17]. This mode shifting capability is not considered in the model of the vehicle used in this thesis, because the aim of this research is merely the investigation of the effect of temperature on charge

management of PHEVs which can be applied to all PHEVs regardless of their drivetrain architecture.

The reason that an EREV with the series drivetrain is selected for this research is that the influence of the temperature noise factor becomes more significant for PHEVs with a large battery than those with a small battery. A large battery can provide a larger portion of the total energy demand of the vehicle compared with a small battery. When more electric energy is used instead of fuel to support the wheel power demand, the engine would undesirably run cooler. Also, long EV modes are major characteristics of EREVs which leads to the long cool-down periods. Therefore, sensitivity of EREV to temperature noise factor is the worst case scenario affected by temperature noise factor if a blended mode EMS is operating the vehicle. Accordingly, this research focuses on the serial EREVs having a large battery.

Moreover, the operation of the power split hybrid vehicles is highly influenced by the dynamic of the planetary gear set. Therefore, this constraint leads to a lower degree of freedom for the engine operation associated with the wheel power demand. For instance, due to the dynamic restriction, the Prius PHEV cannot operate in the EV mode at speeds higher than 100 km/hr. Also, it is necessary to turn the engine on even at lower speeds if the maximum traction power, which is a combination of electric motor and engine power, is required.

Table 3-1 Powertrain model specifications

Vehicle	Type:	Small
	Weight:	1700
Engine	Type:	Petrol, 4 cylinder
	Displacement	1 lit
	Maximum Power	41 kW @ 5700 rpm
	Peak Torque	81 Nm @ 3477 rpm
Motor/Generator1	Type:	AC induction
	Maximum Power	124 kW
Motor/Generator2	Maximum Power	54 kW
Battery	Chemistry	Li-Ion
	Nominal Voltage of a Cell	10.67
	Nominal Capacity	6Ah
	Max Capacity @ 20 ˚C	7Ah
	Number of Cells in series	25
	Number of module in Parallel	10
	Energy Capacity	16 kWh

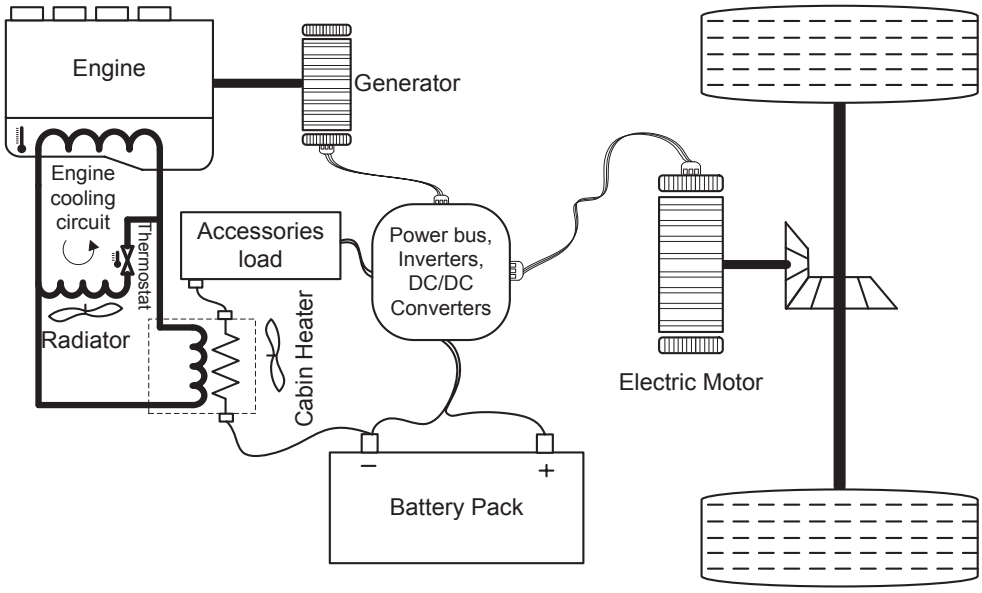

Figure 3.2. Schematic of the serial EREV components with a combined electric/engine-coolant cabin heater

Each subsystem in the model of the vehicle connects to others and transfers information and power components (torque and rotational speed mechanically or voltage and current electrically). The EMS controls the vehicle energy balance to satisfy drive-cycle power demand. A block diagram of the series HEV architecture is depicted in Figure 3.3.

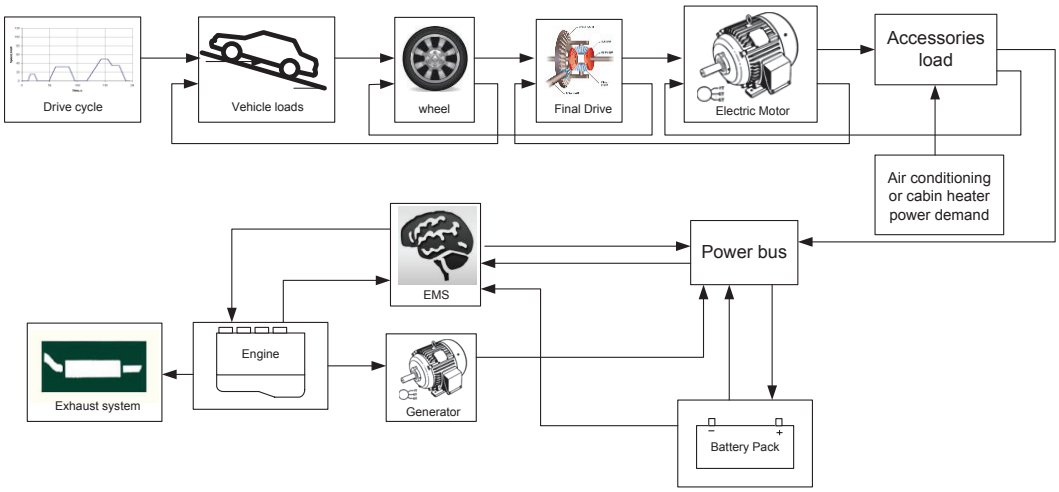

Figure 3.3. Block diagram of the series HEV architecture

3.6.2 Internal combustion engine

The engine model accepts inputs of torque and speed requested by the vehicle controller and upstream drivetrain components. The engine fuel consumption and emissions are calculated based on lookup tables derived from verified engine dynamometer tests. The engine dynamometer test generally runs on hot engines. That is, before the engine fuel consumption and emission data are collected for a predefined table of torques and speeds, the engine warms up to its coolant thermostat steady temperature. The efficiency map of the engine used in the EREV model is shown in Figure 3.4.

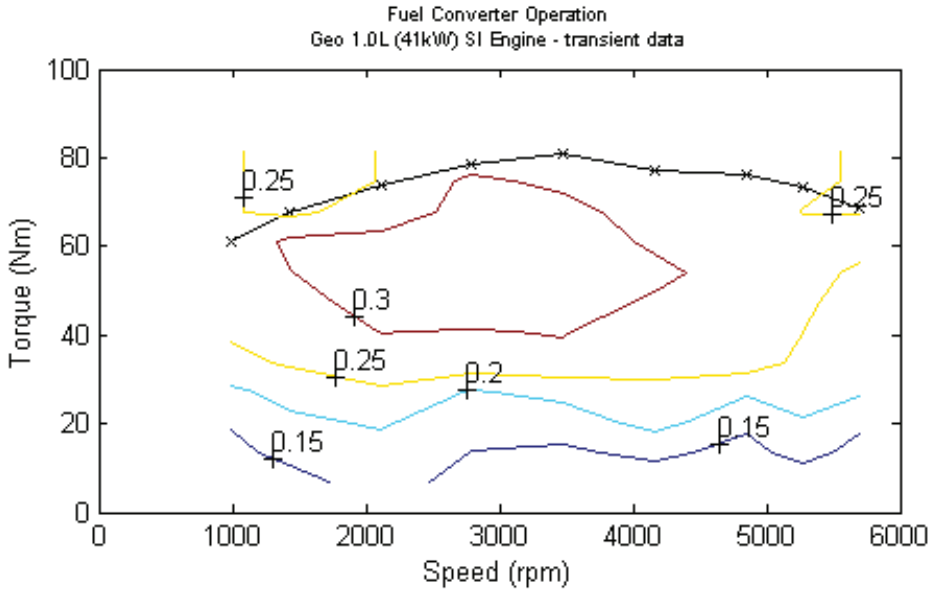

Figure 3.4. Engine efficiency map [ADVISOR database]

Eq. 3-4 defines the engine efficiency. The dynamometer tests are used to measure engine angular velocity, ω_{eng}, torque, τ_{eng}, and fuel mass flow rate, $\dot{m}_{fuel}$.

$$\eta_{eng} = \frac{\omega_{eng}.\tau_{eng}}{\dot{m}_{fuel}.Q_{lhv}} \qquad \textit{Eq. 3-4}$$

where Q_{lhv} is the lower heating value of fuel.

Effect of temperature on engine efficiency and emission

As discussed in Chapter 1, the performance and efficiency of PHEVs are more sensitive to temperature due to longer engine off periods and lower engine power load. Therefore, it is necessary to consider this physical phenomenon into the engine model. The effect of temperature accounted for change in the performance and efficiency of the engine could be considered by adding cold engine efficiency

maps to engine model or mathematically formulating the cold-factor efficiency penalty. The first option requires forced cold operation of the engine during dynamometer tests and repeating them for adequate range of operation temperatures. This option is more accurate as the engine efficiency is a dependent function of its temperature, torque, and speed. However, this requires repeating expensive tests to fully define the engine temperature correction factors.

In a mathematical modelling approach, the cold-to-hot engine fuel and emissions penalties for SI engines have been investigated by Murrell et al. [86]. The correction factor is incorporated based on normalised engine temperature factor, γ, which is related to the engine cooling system thermostat set point, $T_{Eng_{tstat}}$, and the coolant temperature, $T_{coolant}$:

$$\gamma = \frac{T_{Eng_{tstat}} - T_{coolant}}{T_{Eng_{tstat}} - 20} \qquad \textit{Eq. 3-5}$$

where temperature is in centigrade degrees. The fuel and emissions are then computed as follows based on, γ, and the engine performance in hot operation:

$$Cold\ Use = Hot\ Use * Cold\_factor$$

$$where$$

$$Cold\_factor = \begin{cases} (1+\gamma^{3.1}) & fuel \\ (1+7.4\gamma^{3.072}) & HC \\ (1+9.4\gamma^{3.21}) & CO \\ (1+0.6\gamma^{7.3}) & NOx \end{cases} \qquad \textit{Eq. 3-6}$$

In case the complete efficiency map of an engine is available for different operation temperatures, it is possible to use lookup tables instead of the abovementioned formulation. The only required temperature to define the cold-factor penalty is the engine coolant temperature which is assumed to be equal to the internal engine temperature, T_i. A multi node lumped-capacitance thermal network model, depicted in Figure 3.5, is defined for the engine thermal model based on ADVISOR model. The generated heat in the engine cylinder, considering the mechanical shaft output and the part removed via exhaust, is dissipated among the thermal model nodes based on the heat transfer equations as follows. The parameters definition are listed in Table 3-2.

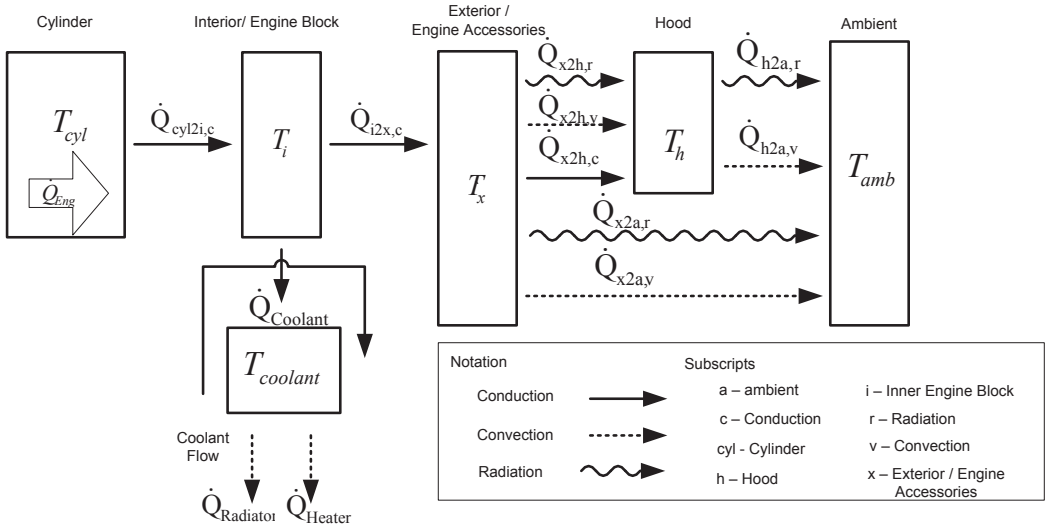

Figure 3.5. Schematic illustration of the engine thermal model [ADVISOR]

$$\dot{Q}_{Eng} = \dot{Q}_{fuel} - P_{traction} - \dot{Q}_{exh} \qquad \textit{Eq. 3-7}$$

$$= \dot{m}_{fuel}.Q_{lhv} - \tau_{eng}.\omega_{eng} - \dot{m}_{exh}C_{p,exh}(T_{exh} - T_{amb})$$

$$\dot{Q}_{cyl2i,c} = Eng_{cyl2i\_th\_c}.(T_{cyl} - T_i) \qquad \textit{Eq. 3-8}$$

$$\dot{Q}_{i2x,c} = Eng_{i2x\_th\_c}.(T_i - T_x) \qquad \textit{Eq. 3-9}$$

$$\dot{Q}_{Radiator} = \begin{cases} \dot{Q}_{c2i,c} - \dot{Q}_{i2x,c} - \dot{Q}_{Heater} & T_i > Eng_{tstat} \\ 0 & T_i \leq Eng_{tstat} \end{cases} \qquad \textit{Eq. 3-10}$$

$$\dot{Q}_{Htr} = \eta_{Htr}.Flw_{Htr}.C_{p,water}.(T_i - T_{amb}) \qquad \textit{Eq. 3-11}$$

$$\dot{Q}_{x2h,r} = \varepsilon\sigma.A.(T_x^4 - T_h^4) = Eng_{emisv}.5.67 * 10^{-8}.sarea_x.(T_x^4 - T_h^4) \qquad \textit{Eq. 3-12}$$

$$\dot{Q}_{x2h,v} = h_{air}.A.(T_x - T_h) = h_{air}.sarea_x.(T_x - T_h) \qquad \textit{Eq. 3-13}$$

$$\dot{Q}_{x2h,c} = Eng_{h2x\_th\_c}.(T_x - T_h) \qquad \textit{Eq. 3-14}$$

$$\dot{Q}_{x2a,r} = \varepsilon\sigma.A.(T_x^4 - T_{amb}^4) \qquad \textit{Eq. 3-15}$$

$$= Eng_{emisv} * 5.67E-8 * sarea_x.(T_x^4 - T_{amb}^4)$$

$$\dot{Q}_{x2a,v} = h_{air}.A.(T_x - T_{amb}) = h_{air}.sarea_x.(T_x - T_{amb}) \qquad \textit{Eq. 3-16}$$

$$\dot{Q}_{h2a,r} = \varepsilon\sigma.A.(T_h^4 - T_{amb}^4) \qquad \textit{Eq. 3-17}$$

$$= Eng_{emisv}.5.67E-8.sarea_h.(T_x^4 - T_{amb}^4)$$

$$\dot{Q}_{h2a,v} = h_{air}.A.(T_h - T_{amb}) = h_{air}.sarea_h.(T_h - T_{amb})$$ *Eq. 3-18*

$$h_{air} = 6 + 6(\Delta T/1000)^{0.25} + 60(V_{air}/30)^{0.63}$$ *Eq. 3-19*

$$T_c = \int_0^t \frac{\dot{Q}_{Eng} - \dot{Q}_{c2i,c}}{m_{Eng,c}.C_{p,Eng}} dt$$ *Eq. 3-20*

$$T_i = T_{Coolant} = \int_0^t \frac{\dot{Q}_{c2i,c} - \dot{Q}_{Radiator} - \dot{Q}_{Htr} - \dot{Q}_{i2x,c}}{m_{Eng,i}.C_{p,Eng}} dt$$ *Eq. 3-21*

$$T_x = \int_0^t \frac{\dot{Q}_{i2x,c} - \dot{Q}_{x2h,r} - \dot{Q}_{x2h,v} - \dot{Q}_{x2h,c} - \dot{Q}_{x2a,r} - \dot{Q}_{x2a,v}}{m_{Eng,x}.C_{p,Eng}} dt$$ *Eq. 3-22*

$$T_h = \int_0^t \frac{\dot{Q}_{x2h,r} + \dot{Q}_{x2h,v} + \dot{Q}_{x2h,c} - \dot{Q}_{h2a,r} - \dot{Q}_{h2a,v}}{m_{Eng,x}.C_{p,Eng}} dt$$ *Eq. 3-23*

The exhaust mass flow rate, $\dot{m}_{exh}$, and temperature, T_{exh}, are also derived from the lookup tables available from engine dynamometer tests. The exhaust temperature and mass flow rate, similar to the engine efficiency map, are tabulated for each engine speed, ω_{eng}, and torque, τ_{eng}. The accuracy of heat transfer modelling is quite dependent on how different constants are defined for a specific engine. Therefore, empirical approaches are employed to accurately fine tune these constants. In this thesis, the required coefficients are derived from ADVISOR database.

Heat transfer coefficient, h_{air}, defined by Eq. 3-19, is the most important parameter for simulation of convectional heat transfer equations: Eq. 3-13, Eq. 3-16, and Eq. 3-18. The heat transfer coefficient is computed by using known heat transfer coefficients for a given experimental conditions. For a given temperature difference, ΔT of 1000°C, h_{air} from natural convection is 6 [W/m^{2}K]. In addition, for airflow with speed of 48 km/hr, h_{air}, from forced convection is 60 [W/m^{2}K]. A minimum of h_{air} was set to a natural convection level at 6 W/m^{2}K. For natural convection over an arbitrary shape, the Nusselt number, Nu_l, is related to the Rayleigh number, Ra_l by the following equation [87]:

$$Nu_l = 0.52 Ra_l^{0.25} \qquad \textit{Eq. 3-24}$$

$$\frac{hL}{k} = 0.52\left(\frac{\beta.\Delta T.g.L^3}{v\alpha}\right)^{0.25} \qquad \textit{Eq. 3-25}$$

Therefore:

$$h \propto \Delta T^{0.25} \qquad \textit{Eq. 3-26}$$

For forced convection over a cylinder, the Nusselt number, Nu_l, is related to the Raynods, Re, and Prandtl, Pr, numbers by the following equation [87] :

$$Nu_l = 0.19 Re^{0.63} Pr^{0.36} \qquad \textit{Eq. 3-27}$$

$$\frac{hL}{k} = 0.19(\frac{VL}{\nu})^{0.63}(\frac{\nu}{\alpha})^{0.36} \qquad \textit{Eq. 3-28}$$

where, ν, is kinematic viscosity and α is thermal diffusion rate. Therefore:

$$h \propto V^{0.63} \qquad \textit{Eq. 3-29}$$

Thus, the equation for the heat transfer coefficient used in the model is given by Eq. 3-19. The same formulation is also used to define the heat transfer coefficient of electric motor.

Table 3-2. Definition of parameters used for engine thermal model

$\dot{Q}$	Heat flow rate $[W]$
T	Temperature [°C]
$C_{p,exh}$	Exhaust gases thermal heat capacity $[\frac{J}{kg.℃}]$
$Eng_{cyl2i\_th\_c}$	Cylinder to interior of engine thermal conductivity coefficient $[W/℃]$
$Eng_{i2x\_th\_c}$	Interior to exterior of engine thermal conductivity coefficient $[W/℃]$
η_{Htr}	Efficiency of the cabin heater heat exchanger
Flw_{Htr}	Hot water flow rate of the cabin heater $[m^3/s]$
$C_{p,water}$	Water thermal heat capacity $[\frac{J}{kg.℃}]$
ε	Emissivity factor
σ	Stefan–Boltzmann constant $[\mathrm{W \cdot m^{-2} \cdot K^{-4}}]$
A	Area $[m^2]$
$sarea$	Surface area $[m^2]$
Eng_{emisv}	Engine emissivity factor
h_{air}	Convectional heat transfer coefficient of air $[\mathrm{W \cdot m^{-2} \cdot K^{-1}}]$
m	Mass [kg]
V_{air}	Air velocity around engine assumed half of the vehicle speed $[\mathrm{m}.s^{-1}]$

3.6.3 Battery model

The battery model accepts a power request, usually from the power bus, and returns the available/actual power output of the battery, the battery voltage and current, and the battery State of Charge (SOC). The battery is modelled with an equivalent circuit with a perfect open circuit voltage in series with a resistor (see Figure 1.5). The battery open circuit voltage is a function of the SOC and the temperature of the battery. The battery resistance is a function of temperature, charge, and direction of current in charging/discharging modes. The dependency relationships could be devised empirically in battery test facilities. In this research, the data from a 6 Ah SAFT Li-ion battery is used from within the ADVISOR library (see Table 3-1).

The amount of charge that battery can store is considered to be constant, and the battery voltage exposure is subject to a minimum voltage limit. The coulombic efficiency of the battery, which is also a function of temperature, defines the amount of charge that is required to replenish the battery after discharge. Charging of the battery is limited by a maximum battery voltage limit. The characteristics of the battery which consists of 10 parallel modules of 25 serial SAFT battery cells are shown in Figure 3.6. The enormous instantaneous power capability of the battery shows the sizing of the battery is mainly affected by the energy capacity of the battery rather than its power capacity. The energy capacity of the battery is designed to let the vehicle cover 64 km of all electric range when depleting from 90% to 35% SOC (similar to the GM volt 65% SOC swing window) over the repeated UDDS drive-cycle. The number of parallel modules also significantly reduces the internal resistance of the battery which

increases the efficiency of the battery accordingly. As the maximum power of the electric motor is 124 kW, and the battery nominal voltage is 267 V, it is practically impossible to increase the battery current roughly over 500 A. Hence, the efficiency of the battery never goes lower than 90%.

As described above, the battery model calculates the battery SOC in response to the requirements of the power bus. The power loss is computed as RI^2losses plus losses due to Coulombic efficiency. The Coulombic efficiency of the battery is 96.8%, 99%, and 99.2% for 0˚C, 20˚C, and 41℃, respectively. The coulombic efficiency can be calculated for other temperatures by using interpolation.

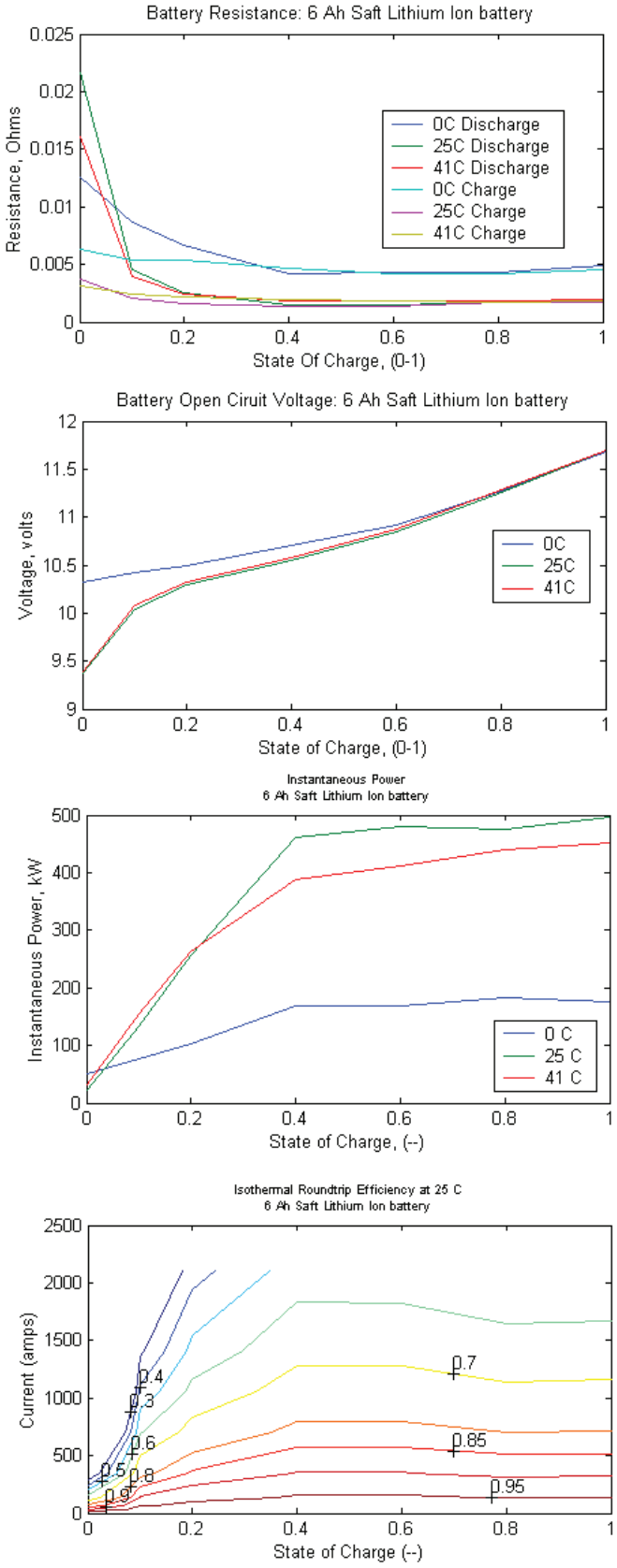

Figure 3.6. Battery characteristics (25 series, 10 parallel battery cells) [ADVISOR database]

Current calculation

Calculation of current is required for each power demand from the battery to update the charge of the battery in each simulation time-step. The output/input power of the battery are:

$$P_{bat} = V.I \qquad \textit{Eq. 3-30}$$

By using Kirchhoff's voltage law:

$$V = U_0 - R.I \qquad \textit{Eq. 3-31}$$

Using Eq. 3-30 and Eq. 3-31 :

$$\frac{P_{bat}}{I} = U_0 - R.I \qquad \textit{Eq. 3-32}$$

The power is assumed positive when the battery discharges power to the drivetrain. Rewriting Eq. 3-32, a quadratic equation is derived for the battery current based on known parameters:

$$RI^2 - U_0 I + P_{bat} = 0 \qquad \textit{Eq. 3-33}$$

There are two solutions to find the current for this equation, but the larger solution is not considered because it would require larger current, and thus a lower terminal voltage, to produce the same power.

$$I = \frac{U_0}{2R} - \sqrt{\left(\frac{U_0}{2R}\right)^2 - \frac{P_{bat}}{R}} \qquad \textit{Eq. 3-34}$$

Thermal model

A thermal model is required to predict the internal temperature of the battery while the vehicle is driven. The design of cooling system of the battery also affects the thermal model of the battery. Here, similar to ADVISOR model, an air cooled battery is assumed for the battery as the cells are cylindrical. In contrast, the battery cells of the GM Volt are flat and rectangular. The schematic of the thermal model around the battery cells is shown in Figure 3.7.

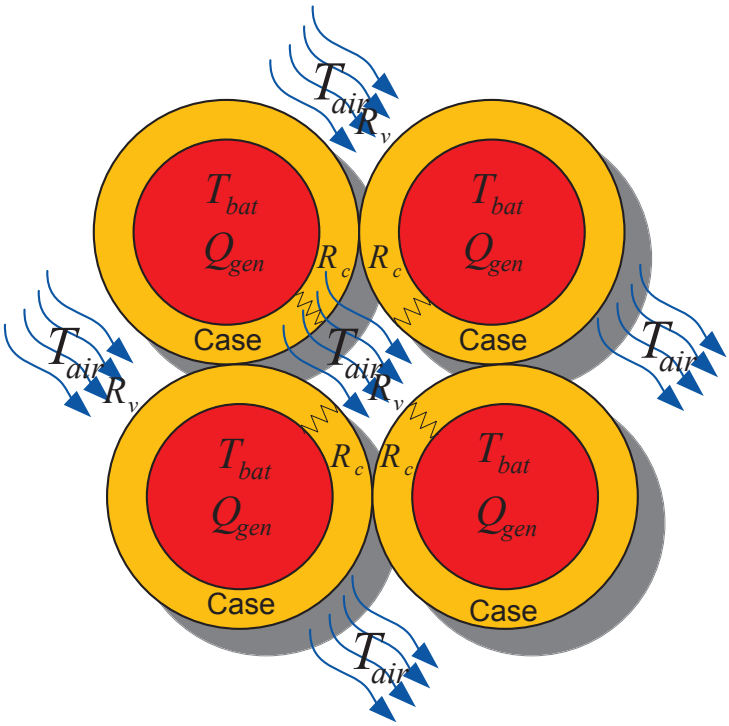

Figure 3.7. Schematic of the battery thermal model [ADVISOR]

The effective thermal resistance is calculated from two parts of conductive resistance, R_c, and convectional resistance, R_v.

$$R_{eff} = R_c + R_v \qquad \textit{Eq. 3-35}$$

$$R_{eff} = \frac{\Delta T}{KA} + \frac{1}{hA} \qquad \textit{Eq. 3-36}$$

where

$$h = \begin{cases} h_{forced} = 30 \times (\frac{\dot{m}/\rho A}{5})^{0.8} & T_{bat} > T_{fan\ forced} \\ h_{natural} = 4 & T_{bat} \leq T_{fan\ forced} \end{cases} \qquad \textit{Eq. 3-37}$$

Therefore, the heat flow rate to the case of the battery is:

$$\dot{Q}_{case} = (T_{bat} - T_{air})/R_{eff} \qquad \textit{Eq. 3-38}$$

Then the battery core temperature, which is necessary to define internal resistance, open circuit voltage, and columbic efficiency of the battery can be derived from Eq. 3-39:

$$T_{bat} = \int_0^t \frac{\dot{Q}_{bat,gen} - \dot{Q}_{case}}{m_{bat}.C_{p-bat}} dt \qquad \textit{Eq. 3-39}$$

The thermal model of the battery is also required to check the effect of EMS on its core temperature which accounts for battery aging.

3.6.4 Electric motor/generator

Electric motor/generator model translates a torque and speed requests from transmission to an electric power request from power bus. Since the motor operates in generator mode during regenerative braking, the name motor/generator is selected for this sub-system. This model considers losses, dynamics of motor inertia, and maximum torque capability of motor at each speed. The efficiency map of the motor/generator, similar to the engine, could be derived empirically with dynamometer tests (see Figure 3.8). The generator model, which directly transforms the engine mechanical power to electricity, is assumed to have 95% constant efficiency. If the efficiency map of the generator is available, the quantity of the map could be multiplied by the engine efficiency map as both the engine and the generator operate at similar torque and angular velocity. The result map is named genset efficiency map.

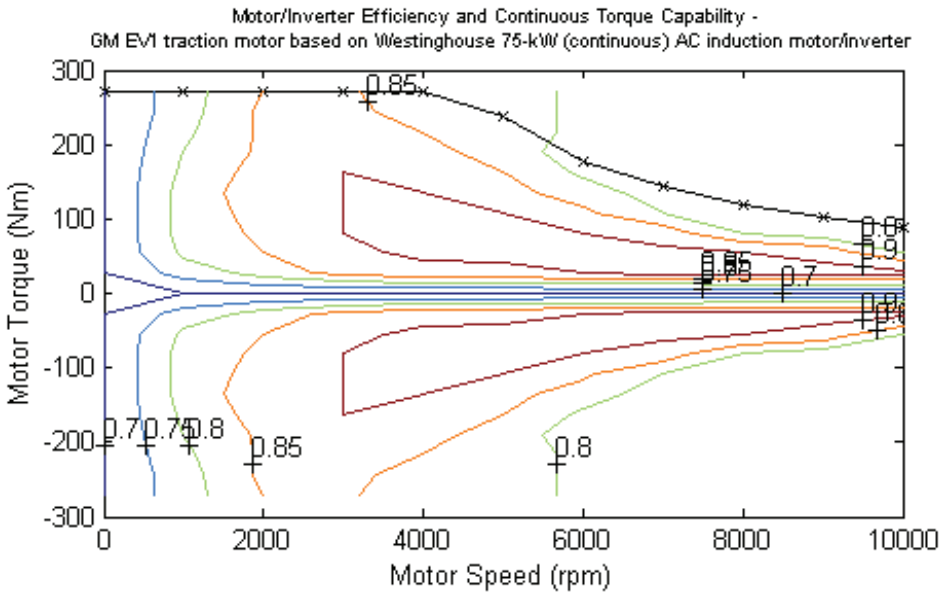

Figure 3.8. Electric motor efficiency map [ADVISOR database]

The electric motor power request from the power bus can be calculated with Eq. 3-40:

$$P_{M,mech} = \tau_M . \omega_M = \frac{P_{M,elec}}{\eta(\tau_M, . \omega_M)} \qquad Eq.\ 3\text{-}40$$

In a backward approach, the motor torque, τ_M, and speed, ω_M, are inputs of the model to define the required power from the power bus. In the power bus, the scalar summation of motor and accessories power demand and power available from the generator is requested from the battery model.

3.6.5 Transmission and final drive

Generally, the role of transmission is more important for conventional or parallel hybrid electric vehicles. For the series powertrain, a single ratio transmission is employed to transfer the electric motor torque to the final drive and wheels. The effects of inertia and gear surface losses could also be considered in the model. These effects are also modelled empirically via lookup tables that are mapped for each input torque and speed. In this model, gearbox ratio is 6.67 and the effect of losses is neglected.

3.6.6 Wheel and axel

The wheel and axel model transmits torque and angular velocity requested by the vehicle model to the final drive model. Friction wastes in the bearing and inertia of the wheel and axel are also considered in the model. Tyre slip model defined with lookup-tables based on maximum tractive force that tyres can

transform. The acceleration and deceleration rates defined in drive-cycle modelled in this research are limited. Therefore, slip never happens in our research simulations.

3.6.7 Vehicle model

The vehicle model calculates the resistive forces along the longitudinal direction, F_r, F_d, F_g rolling, drag, and grading resistances respectively. The tractive force is calculated using Eq. 3-1. The average speed of the beginning and the end of each time step is used for the calculations.

Rolling resistance

Rolling resistance is a function of rolling resistance coefficient, $f_{rolling}$, the normal load of the wheel, F_N, and the road slope, α .

$$F_R = f_{rolling}.F_N.cos(\alpha) \qquad \textit{Eq. 3-41}$$

The surface condition of the road also affects the rolling resistance coefficient. Here,

$$f_{rolling} = 0.009 \qquad \textit{Eq. 3-42}$$

Road grade

The road grade force is simply calculated with the following equation:

$$F_g = Mg.sin(\alpha)$$ *Eq. 3-43*

Aerodynamic load

The effect of both aerodynamic load components, shape drag and skin friction, is formulated into a single drag coefficient, C_d. The drag coefficient could be found empirically in wind tunnels for each vehicle. The drag force, F_d, is related to air density, ρ, and vehicle velocity, V:

$$F_d = \frac{1}{2}\rho A_f C_D V^2$$ *Eq. 3-44*

$$C_d = 0.33$$ *Eq. 3-45*

Acceleration load

The acceleration load is calculated from the following equation:

$$F_{acceleration} = M\frac{V_2 - V_1}{\Delta t}$$ *Eq. 3-46*

where, Δt, is the duration of time step and, V_2 and V_1, are speeds at the end and beginning of the time-step, respectively.

3.7 CONCLUSION

In this chapter, different modelling and simulation approaches available in the literature were introduced. The modelling method selected for this research was also outlined and different vehicle components model are discussed. Two different modelling approaches: (i) backward quasi-static and (ii) dynamic approach based on the theory of dynamic programming are selected to simulate the performance and efficiency of the vehicle. Specifically, the effect of temperature on the performance of the engine is modelled as a cold-factor penalty. This helps simulate the effect of temperature noise factor on the efficiency of PHEV. The second dynamic modelling approach would be discussed in details in Chapter 6. The vehicle components are sized to simulate an EREV with 64 km AER capability.

CHAPTER 4

NOISE-FACTORS AND POWER-CYCLE PREDICTION

4.1 INTRODUCTION

Since the knowledge of driving scenario as a priori has been proven essential for the globally optimal energy management approaches, drive-cycle simulations have been carried out in several existing works. Especially, for the PHEV blended mode energy management strategies, the knowledge of driving scenario helps the charge management of the battery during the journey. The knowledge of travel

distance or preferably drive-cycle would change the way the stored electric energy in the battery is allocated during the journey to optimise the fuel consumption. Gao et al. suggested a manual shifting mode between the EV and CS modes to somehow affect the knowledge of future driving pattern [13]. That is, the driver can shift to the EV mode for low speed in congested city driving and return back to the CS or a moderate CD modes for high speed in highway driving. Having the journey distance information, Sharer et al. calibrated engine-ignition power thresholds for different journey distances and concluded that the basic information on trip distance can decrease the fuel consumption [38]. Gong et al. suggested that it is possible to improve the control strategy of PHEV and implement a deterministic DP EMS, if the trip information is determined as a priori by means of recent advancements in intelligent transportation system (ITS) based on the use of global positioning system (GPS) and geographical information system (GIS) [49]. A model predictive control approach was used in test vehicles equipped with telemetric system [88, 89]. The controller of a HEV calibrates the ratio of the charge/discharge of the battery by means of the traffic information and road grade in a method suggested by Deguchi [90].

This chapter introduces an applicable solution to predict the driving scenario before the journey starts. Additionally, the noise factors affecting the power demand of the vehicle are categorised. A comprehensive knowledge of the noise factors guarantees accurate prediction of the driving pattern.

4.2 POWER-CYCLE AND NOISE FACTORS

As explained above, development of the optimal EMSs requires power-cycle information in advance, especially for the charge management of PHEVs in a blended mode operation. However, the drive-cycles are inadequate to predict the realistic power demand of the vehicle. The reason is that apart from the vehicle velocity profile, several other noise factors can affect the vehicle power demand. Therefore, a control strategy only based on the drive-cycle cannot provide a correct solution and might even deteriorate the performance of the vehicle. The benefit of having a large battery on-board could be sacrificed by reaching the destination with surplus electric energy. That is, a blended mode EMS could deteriorate the performance of a PHEV when compared with a simple AER-CS, if defined based on an inaccurate driving scenario prediction. Consequently, it is necessary to accurately define a power-cycle that can predict the vehicle required power consisting of both the traction and accessories power demand.

Noise factors affecting the power demand and performance of different components of a PHEV, as well as the velocity trajectory need to be taken into account to predict a realistic power trajectory. These noise factors consist of (i) traffic diversity and aggressive driving, (ii) road grade, (iii) wind, (iv) battery aging, and (v) ambient temperature. These noise factors can significantly alter the power demand even in identical journeys and drive-cycles. Besides, the performance of the vehicle components might be altered in different ambient temperatures and by aging. Especially with aging of the vehicle, the battery degradation reduces the available electric energy on-board of a PHEV. These noise factors are non-negligible parameters which have been completely neglected

in the current HEV and PHEV energy management strategy literature. To develop a robust blended mode EMS with an optimised charge management strategy, a comprehensive understanding of these noise factors is required.

4.2.1 Power-cycle library

The target market of PHEVs is daily commuters with short to medium range of driving. Since the majority of drivers use their vehicles on the same routes on a regular basis, each PHEV could calculate and store its own power-cycle in both time and spatial domains, and use it for implementing its energy management strategy. To develop a power-cycle library, each vehicle would log its own real power demands for routine commutes such as home-work, home-shopping centres, etc. Then, the energy management strategy is defined based on the power-cycle library. Figure 4.1 illustrates the required inputs for developing a power-cycle library in a series PHEV architecture. As the drive-by-wire control method is completely dominant in PHEVs, logging the required electric power by motor, battery, generator, and electric accessories is applicable. To develop a specific power-cycle library which is selected by the driver such as home-work, the data logger stores velocity, power to/from the electric motor, generator, battery, and different accessories specially AC in both time and spatial domain utilizing a GPS. Ambient, cabin, battery, and engine coolant temperatures are logged as well for future processes of noise factors affecting performance of vehicle and Air-conditioning/cabin heater load changes.

.

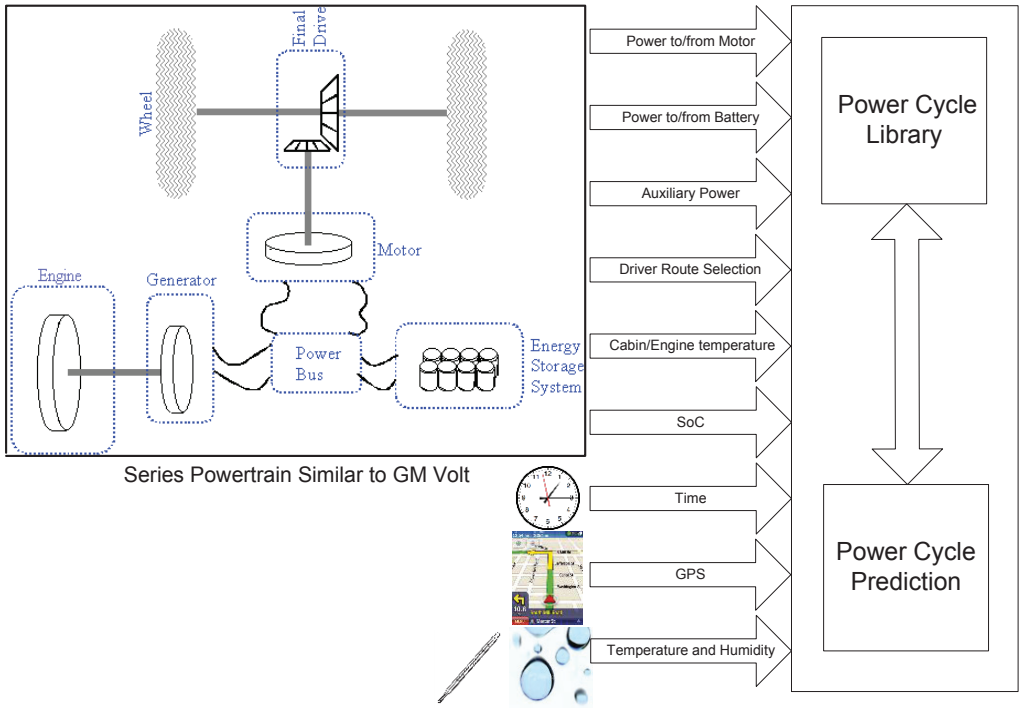

Figure 4.1. Required inputs for developing the power-cycle library

PHEVs employ an in-built control strategy defined by OEM, normally an AER-CS similar to what has been designed for GM Volt. However, for the known power-cycles, which would be defined later on by each vehicle owner, a more sophisticated energy management strategy would be implemented. The power demand information can be repeatedly stored in the low cost memory devices and updated whenever necessary to account for stochastic factors over time. The logged power-cycle based on the real commute history can be used to reasonably predict many stochastic factors. Still, good understanding of the noise factors is essential to predict a realistic power-cycle based on the vehicle power-cycle library and update it on-line even during the journey.

4.2.2 Noise factors

The noise factors can potentially modify the power demand and alter the performance of a PHEV. The proposed power-cycle library method that could help in the prediction of the noise factors is explained in the following.

Effect of traffic diversity and aggressiveness factor on velocity

According to Eq. 3-2, vehicle velocity is the most important factor for prediction of different traction power components. One of the major advantages of power-cycle library over the drive-cycle prediction methods is that the prediction of velocity is more accurate considering driver behaviour and various road traffic conditions in a specific journey. In particular, for daily commutes such as home-work which mostly occur during the rush hours, the drive-cycle modelling based on maximum speed limits, employed in references [49, 91], would be far from reality. The chance of stopping when the vehicle reaches traffic lights also alters the power-cycle during deceleration and acceleration or by the accessories' power demand during stop time.

The power-cycle library inherently considers the aggressiveness factor of different drivers that affect the power demand during accelerating or braking. This means that the power-cycle library could save driver's name and define an aggressiveness factor for each driver. The term $MV(dV/dt)$ in Eq. 3-2 is the power required for acceleration or braking.

Road grade

The road grade considerably alters the power demand of the vehicle. In reciprocal journeys, any downhill part would be uphill in return. Correct allocation of electric energy for downhill or uphill parts of the journey would improve the efficiency and the battery health in mountainous areas. By means of using a GPS which provides elevation information, it is possible to predict road grade power for a journey in advance.

Wind

The crosswind speed against the vehicle movement raises the power demand of the vehicle especially in high speed driving at highways; hence, the drag force increases with the square of velocity. For instance, the drag force at 100 km/hr is around 30% higher with 20 km/hr crosswind.

Eq. 4-1 represents the drag force which is a function of both vehicle and wind speeds, V, V_w, vehicle frontal area, A_f, drag coefficient,C_D, and air density, ρ.

$$F_d = \frac{1}{2}\rho A_f C_D (V + V_w)^2 \qquad \textit{Eq. 4-1}$$

Based on the daily wind speed and direction forecasts and the journey speed and direction saved in the power-cycle library, *Eq. 4-1* can predict the effect of daily wind velocity on vehicle power demand.

Temperature and change in aerodynamic force

Even change in air density can cause discrepancy for the power demand prediction as it changes around 25% between temperatures -25 ℃ and 35 ℃. This change is proportional to the same drag force change according to *Eq. 4-1* .

Temperature and engine and catalyst converter operation

It is well known that cold engine operation increases fuel consumption and pollution of the vehicle [92, 93]. For instance, the hydrocarbon and carbon monoxide emissions increases by 650% and 800% respectively at -20 ℃, compared to the standard certification values at 25 ℃. The low ambient temperature raises lubricating oil viscosity and thus results in higher mechanical losses during engine cold start. In addition, combustion is affected due to lower ignitability of the fuel mixture. The low ambient temperature can also delay the three-way catalyst (TWC) activation, which is one of the most important reasons accounted for high emissions at cold start. The full operational temperature of TWC is around 400 ℃. The research on EURO4 emission compliant vehicle shows that for similar and even more aggressive than ECE 15 urban driving cycle, the lubricating oil temperature increases form the ambient temperature of $7\sim13$ ℃ to the full warmed up value ~80 ℃ in about 15 minutes, and it takes 100 seconds for upstream and 200 seconds for downstream of TWC to reach 400 ℃ [93]. The issue of cold start and warm-up period is even more significant for HEVs and PHEVs. When the vehicle is controlled by a blended mode charge management strategy, the engine on/off shifting occurs more frequently, and the

engine cools down when vehicle operates in the EV mode. The all electric range followed by the charge sustaining mode EMS for EREVs intrinsically solves this issue as the operation of EREV is similar to that of a HEV during the CS mode. Cold engine operation, however, should be investigated when dealing with the blended mode EMS. The cold engine fuel consumption penalty, cold-factor, is formulated in Section 3.6.2.

Temperature and battery performance

Battery thermal management is the current state of the art in battery designing. Temperature affects both performance and aging process of the battery. Battery have minimum operational temperature since their performance is degraded significantly in low temperatures. A plugged in battery is kept warm enough so that it can be used immediately. However, if the battery temperature goes below the minimum operational temperature, the engine should run until the battery warms up even if the battery is fully charged. On the other hand, high temperature significantly accelerates the aging and the degrading of battery, and the battery cooling system causes parasitic loads. From the energy management point of view, the effect of temperature on battery performance is significant when the operation is compared for summer or winter extreme temperatures. However, the power-cycle library based energy management provides the performance characteristics of battery in the specific time of the year. An important benefit of the library control approach is the flexibility to define effective energy management strategy regardless of different environmental and geographic condition.

Temperature and air-conditioning/cabin heating power demand

Unlike conventional vehicles in which the compressor of the air conditioning system is connected mechanically to the engine, a separate electric motor propels the compressor in PHEVs and most of HEVs. The AC can be considered as the most significant auxiliary load in a vehicle. As an example, the power demand of the AC compressor is equivalent to the vehicle when driving steadily at 56 kph [31]. The fuel economy of a vehicle drops substantially when the AC compressor load is added. This effect is even larger for high fuel economy vehicles. AER would be considerably reduced in PHEVs since the compressor is powered by the battery. A 3 kW accessory load will decrease AER on a repeated EPA Urban Dynamometer Driving Schedule (UDDS) by 38% [94]. During hot soaking which means parking in the open on a sunny and warm day, the interior temperature could easily exceeds 70°C. Through the initial surge cooling interval, the compressor of compact and mid-sized vehicles consumes around 2.9 kW to 3.4 kW respectively [95]. However, to avoid initial surge if the PHEV is connected to the grid, it is possible to use external electricity to start the AC or heater system in appropriate times before the journey starts. This opportunity simultaneously provides comfort and saves valuable battery energy.

The required power for the cabin heater and safety related demister is another issue in PHEVs when there is no hot water available from the engine coolant during the EV mode. It is necessary to devise a parallel electric heating system to warm up the cabin similar to electric vehicles. Using electric energy for heating is huge waste in comparison with engine coolant free energy. Heat pumps are not applicable for automotive heating applications because of the evaporator heat

exchanger limitations. Thus, resistive electric heaters should be employed. Assuming the absolute difference between the comfort and ambient temperatures is identical for both the AC and heater operations. The heater electric power demand is almost twice that of the AC because the electric power demand of the AC compressor is equal to the required cabin cooling power divided by the coefficient of performance (COP) of the refrigeration cycle.

With such a large AC and even more for heater power demands, any EMS neglecting the effect of AC and heater would not be accurate. Ambient temperature, humidity, soaking time and direction of sun shine, the colour of vehicle, clouds, amount of fresh air required for ventilation, metabolic heat load and clothing of passengers, and even the driver perception about comfort temperature are the effective factors in AC and heater power demand. To predict the power demand of the AC and heather, the lumped method for cabin mass, m_{cabin}, and specific heat capacity, C_{cabin}, is considered in energy balance *Eq. 4-2* and *Eq. 4-4* for the cabin control volume. Positive direction of heat transfer is selected towards the cabin.

$$m_{cabin}C_{p-cabin}\frac{dT_{cabin}}{dt} = \dot{Q}_{metabolic} + \dot{Q}_{radiation} + \dot{Q}_{convection} + \dot{Q}_{ventilation} + \dot{Q}_{dehumidification} - \dot{Q}_{evaporator} \qquad \textit{Eq. 4-2}$$

where

$$\dot{Q}_{metabolic} = metabolic\ heat\ load$$

$$\dot{Q}_{radiation} = \dot{I}S$$

$$\dot{Q}_{convection} = hA(T_{ambient} - T_{cabin})$$

$$\dot{Q}_{ventilation} = \dot{m}_{air}C_{air}(T_{ambient} - T_{cabin})$$

$$\dot{Q}_{dehumidification} = \dot{m}_{water}C_v + \dot{m}_{water}C_{water}(T_{ambient} - T_{evaporator})$$

$$\dot{Q}_{evaporator} = rate\ of\ heat\ absorption\ by\ evaporator$$

and

$$P_{compressor} = \dot{Q}_{evaportor}/COP \qquad Eq.\ 4\text{-}3$$

where the passengers' metabolic heat load, $\dot{Q}_{metabolic}$, is affected by the number of passengers. Solar radiation load, $\dot{Q}_{radiation}$, is related to sun radiation heat flux, $\dot{I}$, and the incidence surface, S. For convectional heat transfer, $\dot{Q}_{convection}$, heat transfer coefficient, h, behaviour is very complex and varying regarding vehicle and wind speed. A is effective area of convection heat transfer. Fresh air mass flow rate, $\dot{m}_{air}$, causes ventilation heat load, $\dot{Q}_{ventilation}$, which is related to the air specific heat capacity, C_{air}, consisting both air and its water content [96, 97]. If dehumidification is necessary, the dehumidification load, $\dot{Q}_{dehumidification}$, is related to condensed water mass rate, $\dot{m}_{water}$, water latent heat vaporization, C_v, and water specific heat capacity, C_{water}. COP is coefficient of performance of

the AC. *Eq. 4-2* can be simplified to *Eq. 4-4* when a warming function is required.

$$m_{cabin}C_{cabin}\frac{dT_{cabin}}{dt} = \dot{Q}_{metabolic} + \dot{Q}_{radiation} - \dot{Q}_{convection} - \dot{Q}_{ventilation} + \dot{Q}_{heater} \qquad \textit{Eq. 4-4}$$

Prediction of all the parameters that can affect the AC power demand in a drive-cycle is complex, particularly when the passenger perception plays an important role. The power-cycle library could capture the general trend of the AC or heater operation requirements of a specific driver for a specific commute. Having access to a library of AC power demand for a routine commute, the AC power demand would be easier to derive based on lookup tables and simpler but more accurate equations.

For a routine commute, we can assume that for *Eq. 4-2* and *Eq. 4-4*, $\dot{Q}_{metabolic}$ and $\dot{m}_{air}$ remain unchanged, as we can assume that the driver perception about the comfort temperature is unchanged. Although S, A, h change with the vehicle speed and the direction of route against the sun, but we can assume these parameters change in a repeatable manner for a specific journey. For a desired cabin temperature, to predict the everyday AC power demand, the only remaining variables are ambient temperature, humidity, and sun radiation heat flux for the specific day. With a developed library of AC or heater power demand by means of interpolation methods, the trend of required power demand of the AC or heater

are predictable with enough accuracy as required for the charge management of PHEVs.

Battery aging

State of health of the battery determines the amount of on-board available electric energy that PHEV could allocate for a specific power-cycle. The PHEV battery duty cycle is one of the most aggressive one that battery may encounter [98]. The battery life is dependent upon both storage and cycling. Capacity degradation and resistance growth have been shown to be dependent on a number of operational parameters. The following equation shows how the cycling, and the storage time affect resistance [99]:

$$R = a_1 t^{1/2} + a_{2,t} t + a_{2,Cyc} Cyc \qquad \textit{Eq. 4-5}$$

where t is storage time, and Cyc is number of cycles. Coefficients $a_1(\Delta SOC, T_b, v)$ and $a_2(\Delta SOC, T_b, v)$ are a function of the given state of charge swing, ΔSOC, battery cell temperature, T_b, and voltage exposure, v.

There are two mechanisms described for the capacity fade. Lithium loss is the dominant mechanism during storage, and isolation of the active sites is dominant during cycling [99]. Lithium capacity, C_{Li}, and active sites capacities, C_{sites}, are defined by the following equations. The minimum of them would be the actual capacity, C_{actual}. d_0, d_1, e_0, e_1 are constant values derived from experiments.

$$C_{Li} = d_0 + d_1 a_1 t^{1/2} \qquad \textit{Eq. 4-6}$$

$$C_{sites} = e_0 + e_1(a_{2,t} t + a_{2,Cyc} Cyc) \qquad \textit{Eq. 4-7}$$

$$C_{actual} = min(C_{Li}, C_{sites}) \qquad \textit{Eq. 4-8}$$

The impedance growth and the capacity fade due to the elevated voltage and temperature are inevitable. For instance, a battery stored in 35°C would have around 6% higher Lithium capacity loss in comparison to the same battery stored at 20°C after 5 years [99]. Since a PHEV may be used under different geographical locations with various climates, and depending on the aggressiveness of the driving pattern, the state of health of each battery would be different during the effective life of a PHEV. The EV mode followed by the CS mode EMS would not be affected by this noise factor. The only difference that the driver would notice is that the shift from the EV to CS modes occurs earlier compared to an ordinary vehicle for identical journeys. However, for the blended mode EMS, the real available battery energy is one of the initial input data for the controller. The power-cycle library could save the available energy of battery each time it is used. As a result, the slow dynamics of the battery aging is intrinsically considered inside the controller based on the power-cycle libraries.

4.3 CONCLUSION

The blended mode energy management strategies are efficient choices for energy management of plug-in hybrid electric vehicles (PHEVs). Development of

an optimal energy management strategy including an appropriate battery charge management requires the knowledge of the vehicle power demand trajectory in advance. Other than the speed-time profile, i.e. drive-cycle, there are many noise factors which affect both the drivetrain power demand and the vehicle performance. Therefore, the term power-cycle was defined in this chapter. In addition, the noise factors that could potentially alter the power demand of the vehicle even in identical journeys were discussed. These noise factors consist of driver aggressiveness factor, traffic, road grade and environmental conditions like temperature, humidity, wind, and sun radiation heat flux.

Due to the nature of noise factors, power-cycle prediction and their interaction with the performance of the vehicle, the effect of these factors for each PHEV should be investigated individually. The power-cycle library concept proposed in this chapter helps achieve more accurate power-cycle prediction for repetitive commutes of PHEVs owners. The library of power-cycles provides a basic knowledge of power trajectory in both time and spatial domains. This helps prediction of the velocity and grade trajectory of any selected route with acceptable precision. Then, it is necessary to update the power-cycle before each journey for changes accounted for environmental disturbances like temperature, humidity, sun radiation, and wind.

CHAPTER 5

ENERGY MANAGEMENT OF PHEVS: A RULE-BASED APPROACH

5.1 INTRODUCTION

It has been demonstrated that the blended mode or the controlled charge management strategies are efficient choices for energy management of plug-in hybrid electric vehicles [13, 36-39]. In this chapter, a rule-based EMS is introduced to demonstrate the benefits of having access to the proposed power-cycle library described in Chapter 4. The EMS also considers the effect of the temperature noise factor on engine cold-factor penalty. The model of a series EREV capable of 64 km AER, described in Chapter 3, is employed to investigate

the developed EMS. Simulations are carried out to compare the performance and efficiency of the vehicle controlled by an AER-CS EMS against the rule-based blended mode EMS.

5.2 AER-CS ENERGY MANAGEMENT

As explained in Section 2.2.1, the easiest operation mode of PHEVs is the EV mode followed by the charge sustaining mode, when there is no information available about the future driving pattern.

Here, the controller in the EV mode utilizes the battery energy up to the minimum applicable battery SOC, and during the CS mode a rule based power follower strategy is defined to sustain the battery SOC. The vehicle modelling and component sizing of the PHEV was described in Chapter 3. The rules for the power follower strategy are listed below and the Figure 5.1. gives a graphical representation of the rules.

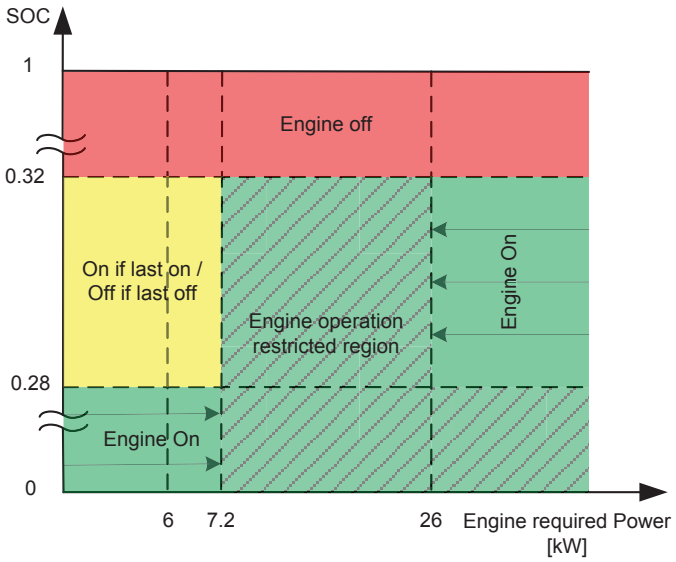

Figure 5.1. Schematic representation of power follower rules

The rules employed for this controller are:

- Engine is kept off until the battery charge reaches minimum applicable SOC (AER rule).
- Engine may be turned off if the battery SOC reaches the defined high limit (here 32%).
- Engine may be turned on again if the power required by the vehicle gets high enough (here 7.2 kW).
- Engine may be turned off again if the power required by the vehicle gets low enough (here 6 kW).
- Engine may be turned on if the battery SOC gets to a defined low limit (here 28%).
- When the engine is on, its power output tends to follow the power required by the vehicle, accounting for the losses in the generator so that the generator power output matches the vehicle power requirement. As the wheel and engine speeds are independent, the engine torque and speed are selected based on the designed curve or confined optimal operation line (see Section 5.2.1).
- The engine output power may be adjusted by the SOC bringing the SOC back to the centre of its operating range.
- The engine output power may be kept above a minimum value (here 6 kW).
- The engine output power may be kept below a maximum value (which is enforced unless the SOC gets too low) (here 26 kW).

- The engine output power may be allowed to change no faster than a prescribed rate (+2 and -3 kW/s).
- If engine turns on, it is kept on for at least a prescribed time, min_eng_on (here 60 s).

During engine-on, the battery only provides the power shortage required by the vehicle when the engine inertia or the power follower rate limiter rules cause a difference between the powertrain required power and the engine available power. Also, when very high power demand (more than 26 kW) is required, the battery compensates the power deficit. The battery SOC range between 0.28 to 0.32, defined in the Figure 5.1, are adequate for the vehicle operation like a conventional HEV when the battery is depleted to minimum SOC of 0.3. The engine power output range between 6 kW to 26 kW is defined as if the engine efficiency is constrained into the 0.3 contour depicted in the engine efficiency map of Figure 3.4. The 1.2 kW difference between, 6 kW and 7.2 kW, vehicle power demand thresholds to switch the engine on/off, engine power change rate limiter, and minimum engine on time are defined to prevent unsteady and transient operation of the engine.

5.2.1 Confined optimal operation line

The engine-generator operation is independent of the vehicle speed in the series architecture. Therefore, the engine-generator can operate over its optimal operation point for any required power. The combination of these optimal operation points defines a line in the engine-generator brake specific fuel consumption (BSFC) map called confined optimal operation line (COOL). (see

Figure 5.2). Therefore, a bijective function can be defined between the engine power demand, P_{Eng} and fuel consumption. That is, for each engine power demand only one fuel consumption rate could be defined as the engine torque and speed are restricted to COOL.

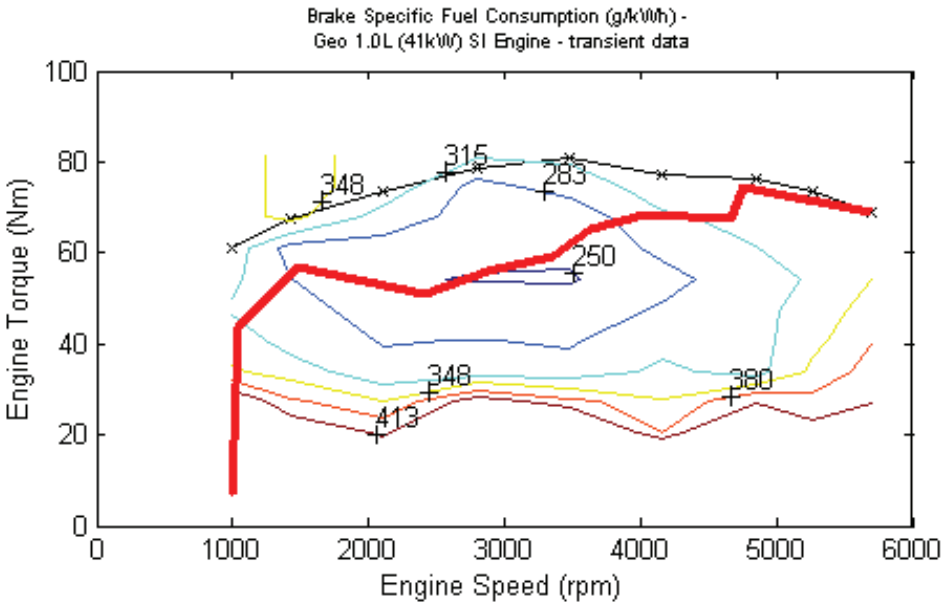

Figure 5.2. Confined optimal operation line [ADVISOR database]

When the limits of minimum 6 kW and maximum 26 kW are enforced by the rule-based vehicle controller, most of the engine operation points are located into the contour with lower than 283 g/kWh BSFC in Figure 5.2 .

5.2.2 Driving scenario

To compare an AER-CS energy management with the suggested EMS, a typical work-home commute which is longer than AER is simulated. This journey starts with a UDDS, then continues with a HWFET and ends with another UDDS. The return journey is the mirror of the drive-cycle. This drive-cycle is based on

the idea that the driver starts the car in a suburban area and after driving on a highway arrives to a downtown urban area where the destination elevation is around 400 meters higher than the start point. Then, the vehicle returns back to complete the 80 km journey. Figure 5.6 (a) shows the speed and elevation of the vehicle in the defined cycle. The power-cycle in Figure 5.6 (b) consists of both traction and accessories such as air conditioner power demand.

5.3 PROPOSED RULE BASED BLENDED MODE EMS

The difference between the total energy demand in the power-cycle and the available battery energy is equal to the required energy from the engine/generator or the energy share provided by fuel. The series drivetrain has the advantage of blending both the battery and the engine power independent of the powertrain required load and the vehicle speed. It is possible to use the engine as a power source anywhere in a journey to provide its share in total energy demand of a power-cycle. However, the amount of engine energy share should be anticipated in advance by means of the power-cycle prediction method described in Chapter 4. Fuel consumption in the series PHEV architecture with an AER-CS strategy only depends on the engine/generator performance during the end of power-cycle when the vehicle operates in the CS mode. With the knowledge of the power-cycle, it is possible to find efficient sections to get the engine energy share. These sections should be long enough to prevent complications associated with the transient operation. In the following, a three-step procedure to define a controlled charge management strategy is described. This procedure considers the engine temperature as one of the most important noise factors on the engine performance.

Intentionally, to have a fair comparison between the AER-CS and the proposed blended mode energy management, the power follower strategy for the vehicle controller, and also the regenerative braking rules are kept unchanged. The only difference is more efficient charge management that is defined with the proposed EMS compared to the AER-CS.

The suggested EMS is developed in a three steps (i) step 1: Hot engine efficiency cycle, CD1 strategy, (ii) step 2: Engine warmth conservation, CD2 strategy and (iii) step 3: Engine cold start investigation, CD3 strategy (see Figure 5.3). Since a deterministic approach is chosen for the rule-based EMS, the first perquisite to implement the method is the knowledge of the power-cycle and available charge in the battery. In the first step, it is assumed that temperature noise factor does not affect the performance of the vehicle. As a result, the hot engine efficiency map is used to develop the charge management strategy. In the second step, however, the engine thermal model is employed to explore the effect of the temperature noise factor. Finally, the last step investigates the possibility of elimination of excessive cold start-warm up in the reciprocal commutes if it secures more efficient operation of the vehicle.

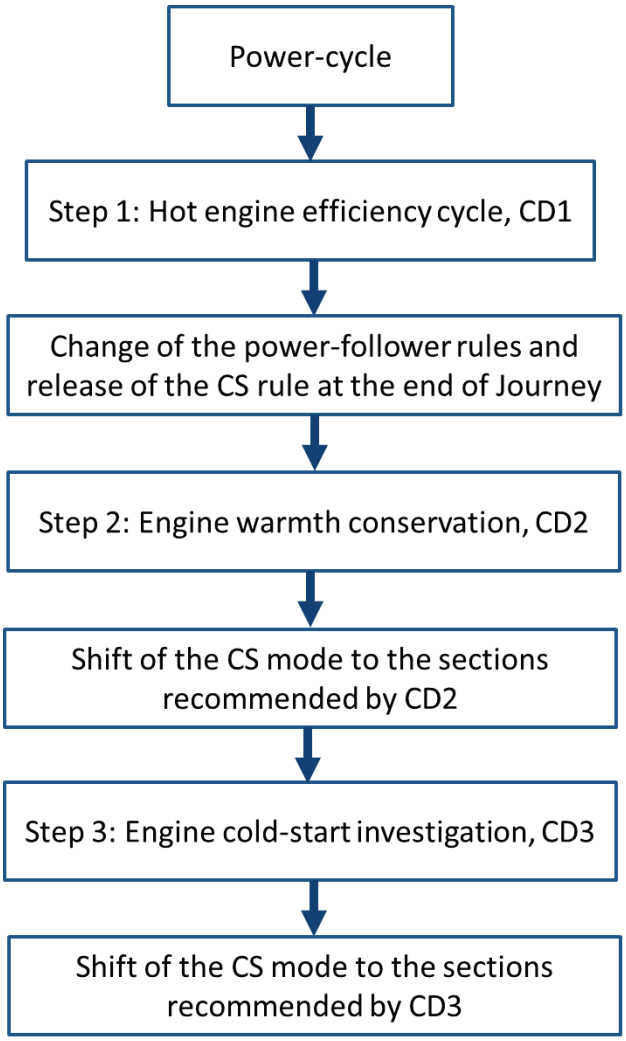

Figure 5.3. Three-step rule-based blended mode EMS

5.3.1 Step 1: Hot engine efficiency cycle, CD1 strategy

With the knowledge of the power-cycle, efficiency cycle can be derived assuming that the engine is on, hot, and controlled by the power follower strategy rules over the power-cycle. Since frequent engine on/off is not pleasant, the smoothed power-cycle with averaging span of 60 seconds equal to the minimum engine-on-time, $\min\_eng\_on = 60$ [s], in power follower strategy is used for developing the efficiency cycle. For the required powers higher than maximum efficiency point, here 15.3 kW, the efficiency cycle is manipulated to the fixed

maximum efficiency (see Figure 5.6 (b)). The corresponding efficiency of each power demand could be found from COOL.

The reason to smooth the power-cycle is that the accurate power-cycle prediction is practically impossible. However, with the approach described in Chapter 4, a power-cycle with enough accuracy could be predicted to define the trend of required power in a journey. In addition, an accurate trend prediction is more appealing for energy management purposes as it deals with slow dynamic parameters like a large battery SOC and temperature.

Efficiency line

A known efficiency cycle is explored for sections with steadier, longer, and higher efficiency during the journey to acquire the engine energy share from. Codes have been developed to find the horizontal efficiency line shown by the dash-dot red in Figure 5.6 (b). The position of the efficiency line over the efficiency cycle is defined such that the amount of energy delivered by the engine in the shaded sections of the equivalent power-cycle in Figure 5.6 (b) becomes equal to the required engine energy share to complete the journey with a minimum applicable battery SOC. A minimum 60 seconds engine-on mode is considered in this procedure. Generally, high efficiency sections coincide with high power demand in power-cycle. Although power higher than the maximum efficiency point of the engine reduces the engine efficiency, it is worth to select them for the engine-on mode to reduce the load over the battery. In other words, when the required power from the engine is between the most efficient point at 15.7 kW, and the maximum allowed power defined by rules of the power follower

controller at 26 kW, logically these sections are acceptable for the engine operation. The shift of the engine operation from the end (CS mode) to the high power demand sections of the journey reduces the maximum power required from the battery that is beneficial for its state of health. The first step is named Charge Depleting 1 (CD1). The schematic illustration of the step one is depicted in Figure 5.4 and the flowchart of the finding the efficacy line is given in Figure 5.5.

The CD1 over the defined power-cycle mostly selects the first section of the journey for the engine operation while the drive-cycle is similar in both go and return journeys. The reason is the slope of the road which significantly increases the power demand of the vehicle (see Figure 5.6 (b)). Logically, the engine energy share is allocated in high speed sections of each side of the cycle. There is one section, around t=4900, where the efficiency is higher than the efficiency line but is not selected for the engine operation. The reason is that the section is shorter than minimum engine on time threshold, 60 sec.

When the engine-on sections are defined with CD1, to implement it in the vehicle controller, the rules of power follower are manipulated. The rule "Engine is kept off until the battery charge reaches minimum applicable SOC (AER rule) is eliminated, as this rule enforces the AER-CS EMS for the PHEV. The rules which enforce charge sustaining at minimum applicable SOC are also manipulated to keep the battery SOC constant during the engine-on sections ($t_1 \rightarrow t_2$, $t_3 \rightarrow t_4$, …) defined by CD1. Therefore, the vehicle operation in the CS mode moves to the engine-on sections instead of concentrating at the end of journey.

$$E_{Eng-share} = \int_0^{t_f} Power\_cycle - E_{Bat}$$

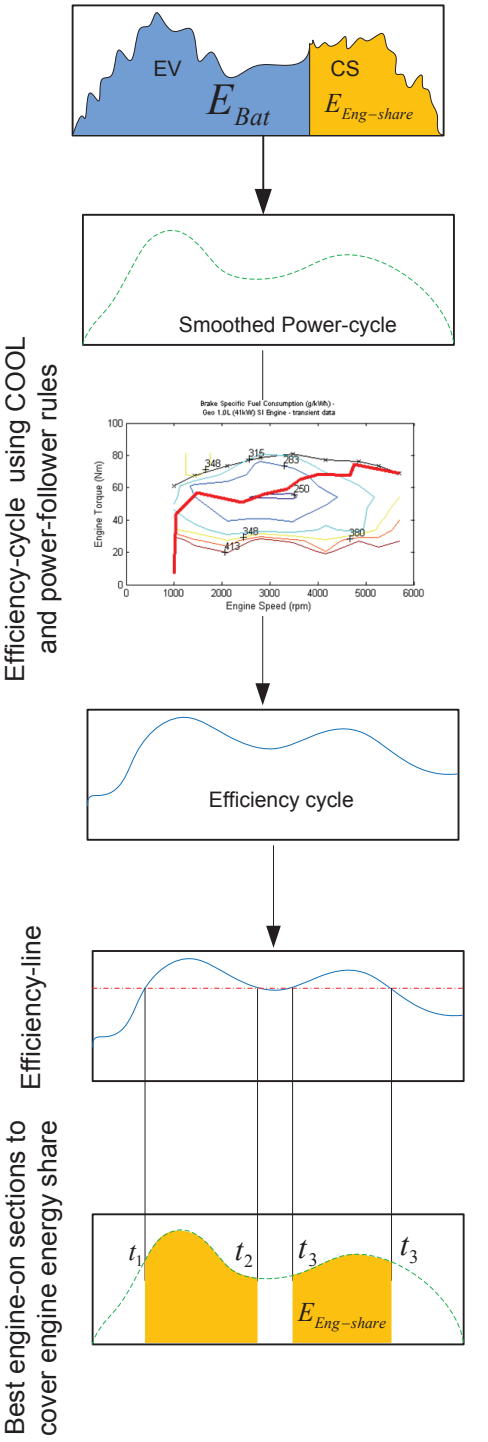

Figure 5.4. Schematic illustration of Step 1

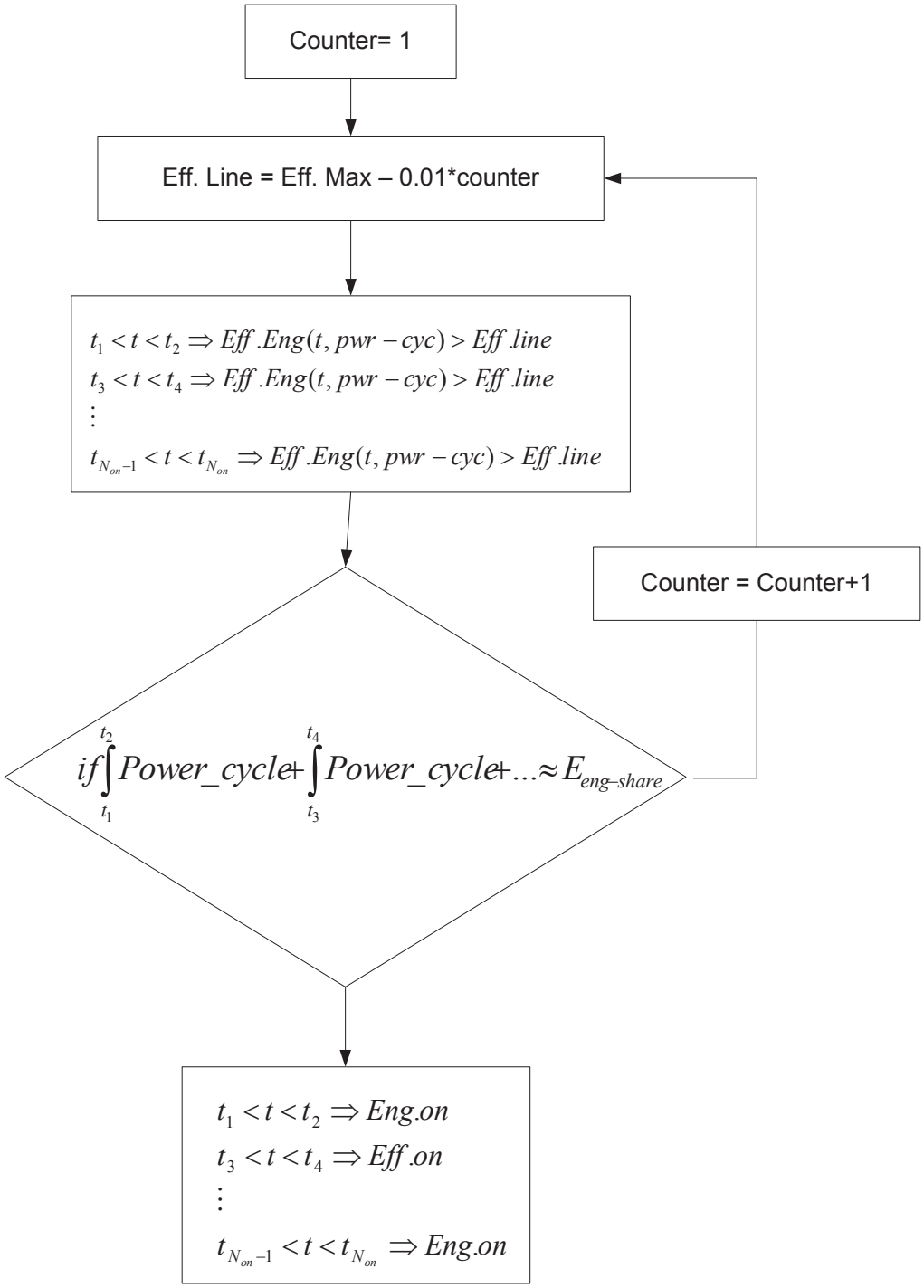

Figure 5.5. Flowchart of the process to find the position of the efficiency line in CD1

5.3.2 Step 2: Engine warmth conservation, CD2 strategy

Since the efficiency cycle in Step 1 is formulated based on the hot engine efficiency map, it does not consider the effect of temperature on the engine performance. Cold engine operation during the shifting between the EV and the engine-on modes at CD1 is a point of concern. The engine thermal model is a prerequisite to determine the effect of the cold engine operation. The engine thermal model, described in Section 3.6.2, is employed to investigate the effect of temperature on the engine performance.

The first question that needs to be answered when considering the effect of the engine temperature on the performance is to investigate whether it is more efficient to select the engine-on sections only based on the hot engine efficiency cycle, or to choose these sections more concentrated to conserve the engine warmth. To answer this question, the longest engine-on sections selected in CD1 are chosen in each side of the go and return journeys as there is a cool-down period at the middle of the journey. The nearby sections with less than 60 seconds engine-off interval are also added to the two longest sections at each side. It is obvious that these longest sections would be selected for engine operation even when the engine temperature noise factor comes to account. In other words, the engine-on sections might concentrate around the longest sections if it is more efficient to run the engine in lower efficiency cycle region (derived from hot engine assumption) but in higher temperatures. It is assumed that temperature is constant and equal to the thermostat set temperature during the chosen sections. That is, the cold-factor from Eq. 3-6 for the longest section of the engine-on is one. Applying the engine temperature code, coolant temperature and consequently

cold-factor penalty for fuel consumption would be calculated for both sides of the journey (see Figure 5.6 (c)). The engine temperature code should be run in both forward and backward directions to calculate the cold-factor in both sides of the longest engine-on sections. A new efficiency cycle is developed by dividing the hot engine efficiency cycle by the cold-factor derived for each point of the journey. The horizontal efficiency line approach described in CD1 and flowchart of Figure 5.5 is repeated on the newly developed efficiency cycle to find the new engine-on sections. As shown in Figure 5.6 (d), there is no significant change in the engine-on sections for the first part of the journey but for the return journey, the engine-on sections are closer to one another. Step 2 has an important role when the ambient temperature is low, thus, the engine thermal model predicts a higher cold-factor. The simulated journey is assumed to occur in 30˚C and 35˚C ambient temperature for a go and return journey, respectively, simulating a summer day morning and afternoon commute. The power demand of the AC is also added to the power cycle. The summer day simulation is intentionally selected to emphasize on the effect of the EMS on battery temperature which would be discussed in Section 5.4. The second step is named Charge Depleting 2 (CD2).

5.3.3 Step 3: Engine cold start investigation, CD3 strategy

Since CD1 and CD2 select engine-on sections in both go and return journeys, it is necessary to investigate the effect of the extra cold start engine operation. It may be more efficient to run the engine only in one side of the trip even in lower engine efficiency cycle sections and avoid the second engine cold start. First, the

side with the higher engine-on sections from CD2 is selected which logically provides larger share in the engine energy demand. Similar to the Step 1, the aforementioned efficiency line procedure is repeated to cover all the engine energy demand from only one side of the journey assuming that the vehicle operates in the EV mode for the return journey. The hot engine operation efficiency of the newly added sections, with darker colour in Figure 5.6 (e), is compared with the other side CD2 engine efficiency while the cold-factor penalty is considered. It is assumed that the efficiency of the newly added sections is equal to that of the hot engine because at least one cold start is inevitable. The engine thermal model code is again used to derive the cold-factor for the second part of the journey with extra cold start operation. If the hot efficiency of the newly added sections is higher than the cold start engine operation of the other side, the engine-on sections in CD3 will be set in the energy management strategy otherwise the CD2 sections remain unchanged. In the simulated power-cycle, CD3 is more efficient. The coolant temperatures of the engine in all three steps are depicted in Figure 5.6 (f). The summation of the shaded area in all three steps is equal to the engine energy share. That is, the charge management defined by each three steps, CD1, CD2, and CD3 only decides where to allocate the secondary energy source of EREV, battery energy. Here unlike the AER-CS, the battery energy is allocated for the return journey instead of the beginning of the journey.

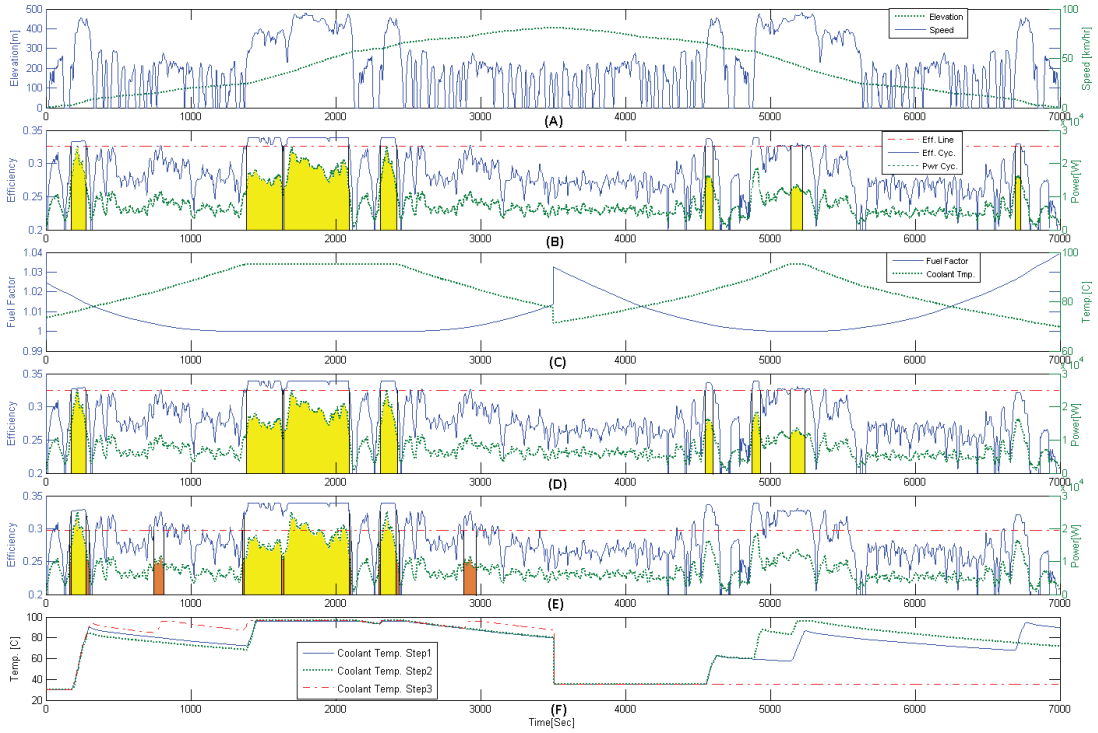

Figure 5.6. (a) Defined mirrored drive-cycle and elevation. (b) Power and equivalent efficiency cycle and efficiency line in CD1. (c) Engine coolant temperature and cold-factor for CD2. (d) Power and equivalent efficiency cycle modified by cold-factor and efficiency line in CD2. (e) Power and equivalent efficiency cycle and efficiency line in CD3. (f) Coolant temperature in CD1, CD2, and CD3

5.3.4 EMS for the cold weather

The power demand of the cabin heater in cold weather during AER is a significant electric load when there is no hot water available from the engine coolant. For a similar difference between the comfort and ambient temperatures, the heater power demand is even higher than that of the AC because the AC power demand in compressor is divided by the COP of the AC refrigeration cycle. In the AER-CS energy management strategy, the hot water is only available during the CS mode. However, with the knowledge of power-cycle and prediction of the heater power demand, it is possible to define an appropriate blended mode EMS that keeps the engine hot for much longer sections or even the whole journey. That is, it might be globally more efficient to run the engine more frequently in lower power, and consequently in lower efficiencies but use its coolant as the energy source for the cabin heater. As an illustration, for the minimum engine power, 6 kW, defined by power follower controller, the engine efficiency is 0.27. If the typical 2.5 kW required heater power is provided by coolant instead of battery, the engine efficiency increases up to 0.38 which is even higher than the maximum efficiency of the engine. With the knowledge of the power-cycle, the engine required energy, and the heater power demand during a specific cycle, it is possible to find an appropriate amount of power demand from the engine, and select the engine-on positions to reach maximum efficiency. To address this question, an optimization-based EMS is proposed in Chapter 6.

5.4 RESULTS

Table 5-1 compares the vehicle performance in three steps of the suggested blended mode EMS strategies against that of the AER-CS energy management strategy. The fuel consumption is reduced by around 4.7% in the specific defined power-cycle. The engine operation points are shown in Figure 5.7. It is clear that in the CD3 EMS, the engine operates more efficiently in higher loads without any manipulation in power management rules. The variations of engine performance and fuel economy in CD1, CD2, and CD3 show the significance of the engine temperature noise factor. This effect could be even more significant when the ambient temperature is low.

The other major benefit of the proposed blended mode approach is the 9.6% and 126% reduction in the amount of energy that flows from and to the battery, respectively. Reduction in power recirculation eliminates the battery charging/discharging losses and slows down the aging of the battery which is the most valuable part of the PHEVs. The power recirculation occurs in the low drivetrain power demand when the surplus of the minimum engine power (here 6 kW) is stored in the battery. The battery current and accordingly its temperature are declined when the engine propels the vehicle in the most vigorous part of a power-cycle. It has been proven that the temperature is one of the major parameters which deteriorates the battery state of health (see Section 4.2.2). The SOC history, the battery temperature, and the average current in both the AER-CS and CD3 EMSs are compared in Figure 5.8. When the performance of the battery in AER-CS and CD3 is compared, it can be observed that the waste of energy in the battery is reduced by 43%. This reduction is caused by the decrease in the

battery temperature and the elimination of the power recycling in the CS mode in a shallow SOC. Both the shallow SOC and the high temperature increase the internal resistance of the battery. The economic impact of the suggested EMS could be even more significant on the state of health of the battery when compared to the amount of saved fuel. An accurate state of health modelling and extensive physical tests are required to quantify the benefits of temperature and current reduction that is out of the scope of this research.

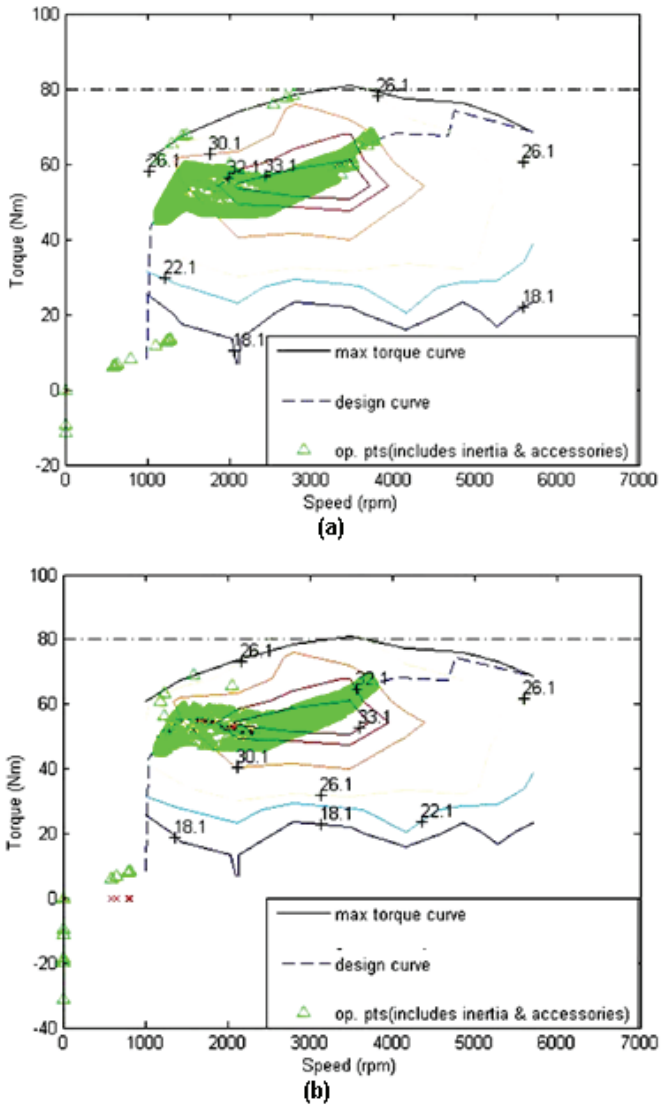

Figure 5.7. Engine operation points in the efficiency map. (a) AER/CS strategy. (b) CD3 strategy

As mentioned before, to have a fare comparison, the power-follower rules in both suggested EMS and AER-CS strategies are similar. That is, the fuel reduction recorded in Table 5-1 is only achieved by the charge management. The simplicity of the suggested approach makes it a completely applicable EMS for vehicles such as GM Volt, since the power management strategy is not changed by this approach. The only input to the vehicle is when to shift from the EV mode to the CS mode during a journey with a simple GPS feedback. Even the driver can make the decision of shifting from the EV mode to the CS mode like the input button designed for the GM Volt sister vehicle, Opel Ampera.

Table 5-1. Performance comparison of the AER-CS and the rule-based blended strategies

Parameter	AER-CS			CD1			CD2			CD3			Compare AER-CS with CD3 [%]		
	Go*	Return**	Sum***	Go	Return	Sum	Go	Return	Sum	Go	Return	Sum		Modified for final SOC=0.3	
Fuel consumption [Lit]	0	2.043	2.043	1.690	0.332	2.022	1.676	0.345	2.020	1.957	0.000	1.957	-4.39%	1.951	-4.70%
Engine Energy in [kJ]	0	65173	65173	53914	10584	64498	53465	10991	64456	62430	0	62430	-4.39%	N.A.	
Engine Energy out [kJ]	0	19763	19763	17098	3194	20292	16962	3344	20306	19773	0	19773	0.05%	19715	-0.25%
Engine Efficiency [%]	N.A.	30.32	30.32	31.71	30.18	31.47	31.73	30.42	31.51	31.67	N.A.	31.67	4.26%	N.A.	
Battery Energy in [kJ]	1135	6211	7346	1826	1232	3058	1761	1213	2974	2185	1068	3253	-126%	N.A.	
Battery Energy out [kJ]	35987	10826	46813	20438	21580	42018	20503	21419	41922	18256	24449	42705	-9.62%	N.A.	
Battery Loss [kJ]	394	195	589	178	218	396	178	214	392	161	253	414	-42.3%		
Final SOC (Initial 0.85)	0.3651	0.3041	0.3041	0.5938	0.3099	0.3099	0.592	0.3112	0.3112	0.6297	0.3049	0.3049	0.27%	0%	= 58.3kJ

*the go column presents the change of the investigated parameter in the first part of the commute, ** the return column presents the change of the investigated parameter in the second part of the commute after cool-down period, and *** the sum column presents the change of the investigated parameter during the whole journey

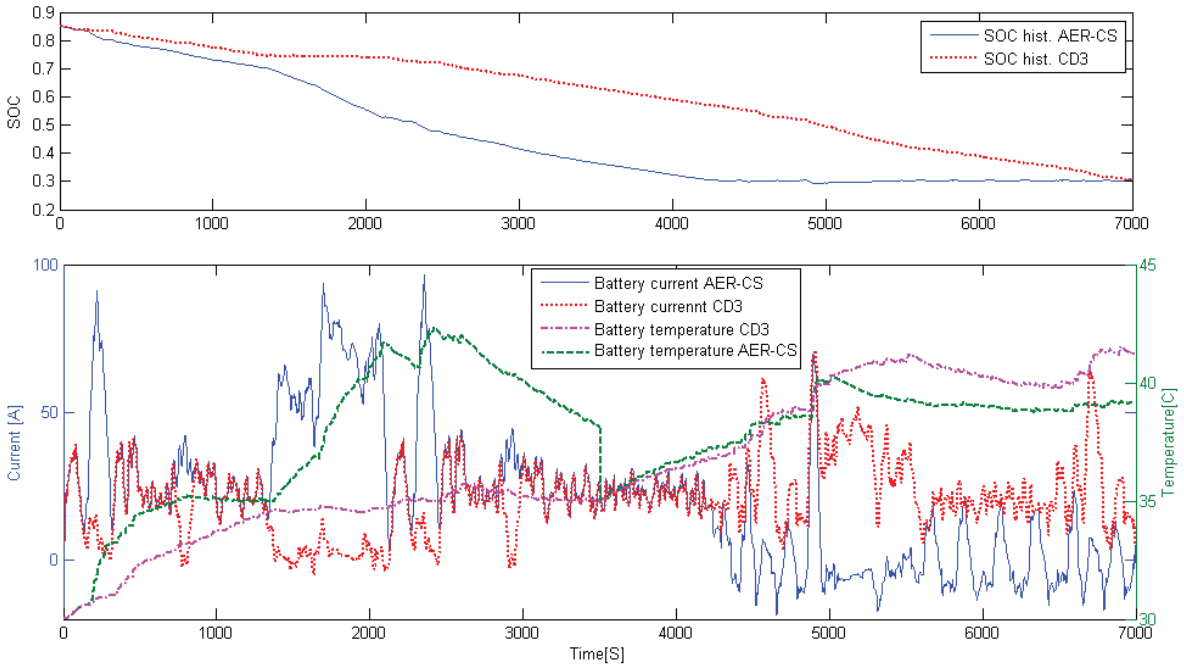

Figure 5.8. **Battery SOC history, current, and temperature in both the AER-CS and the CD3**

5.5 CONCLUSION

The blended mode energy management strategies are more efficient for the EMS of PHEVs. When the blended mode EMS is defined for a PHEV, shifting between the engine-on and off modes is frequent. Therefore, engine temperature plummets while the engine is turned off. When the engine is running at temperature lower than designated thermostatic temperature, its performance and efficiency deteriorates.

A power-follower rule-based EMS operates the vehicle in an AER-CS EMS for a simulated power-cycle. The same control rules also employed to operate the vehicle in the developed blended mode EMS to have a fair comparison. In other words, any reported improvement in the fuel economy of the vehicle is only the result of the more efficient charge management of the vehicle rather than the power management strategy. Based on the power-cycle of the simulated driving scenario, an efficiency cycle was developed by assuming that the vehicle operates based on the power follower rules, and the engine operates on confined optimal operation line (COOL). To define a blended mode EMS, the efficiency cycle was investigated in a three-step procedure to find the best sections to provide the required engine energy share. The cold-factor calculation by means of the engine thermal model was employed during the evolution of the efficiency cycle in the last two steps of the strategy, CD2 and CD3. The effect of the second cold-start of the vehicle for journeys with long cool-down periods was also investigated in the last step of the EMS, CD3.

The simulation results for the modelled series PHEV, which has similar specifications to GM Volt, show that the suggested CD energy management strategy improves both the vehicle fuel economy and the battery health by eliminating the significant power recirculation, reducing the battery load, and accordingly its temperature.

CHAPTER 6

OPTIMAL INTEGRATED THERMAL AND ENERGY MANAGEMENT OF PHEVS

6.1 INTRODUCTION

The rule-based controller for EREV that considers the cold-factor fuel consumption penalty and the cold start of the engine in the blended mode EMS was introduced in Chapter 5. The rule-based controllers are practical, simple to implement, and as explained in Section 5.4, the benefit of them is notable. In this chapter, a new EMS with the dynamic modelling approach based on the theory of dynamic programming (DP) is introduced to address three important aspects of EMS of PHEVs. First, the method, based on DP, establishes a mathematical

optimal solution of the modelled control problem. That is, if the modelling process is in accordance to the physical reality of the control problem, the result of the process could be accounted as the optimal benchmark for all other control approaches. In practice, it is impossible to reach the limit found by the optimal control theory; however, it is worth to access the benchmark solution. Second, the DP method is appealing because the result is a global rather than a local optimal solution. This is ideal for the charge management of PHEVs for known power-cycles. The last but not the least reason is by adding a temperature as a state variable into the optimal control problem formulation, it is possible to address the optimal solution for the engine thermal management, and the battery charge management, synchronously. This solution finds the best engine thermal management to maximise the engine hot operation as well as the availability of hot water from the engine coolant for the cabin heating propose.

In this chapter, first an introduction to the basics of the theory of dynamic programing is given. Then, the formulation of the control problem and the required cost function for the optimization process are discussed. Finally, the results of a warm and a chilly day simulation, employing the suggested blended mode EMS, are compared with those the conventional AER-CS strategy.

6.2 OPTIMAL CONTROL AND DYNAMIC PROGRAMMING

The objective of optimal control is to determine the control signals that satisfy the physical constraints and also minimise (or maximise) a performance criterion [100].

6.2.1 Mathematical modelling for dynamic approach

The basic part of any control problem is to mathematically model the process. The main objective of modelling is to find the simplest mathematical description of the process which sufficiently describes dynamics of the system to all possible inputs. A system is described by ordinary differential equations in state variable form, where:

$x_1(t), x_2(t), \dots, x_n(t)$

are state variables and

$u_1(t), u_2(t), \dots, u_n(t)$

are control inputs, and the system could be described with n first order differential equations:

$\dot{x}_1(t) = a_1(x_1(t), x_2(t), \dots, x_n(t), u_1(t), u_2(t), \dots, u_m(t), t)$

$\dot{x}_2(t) = a_2(x_1(t), x_2(t), \dots, x_n(t), u_1(t), u_2(t), \dots, u_m(t), t)$

$\vdots$

$\dot{x}_n(t) = a_n(x_1(t), x_2(t), \dots, x_n(t), u_1(t), u_2(t), \dots, u_m(t), t)$

By defining the state vector $x(t)$ and input control vector $u(t)$, the state equation can be written [100]:

$$\dot{x}(t) = a(x(t), u(t), t) \qquad \textit{Eq. 6-1}$$

6.2.2 The performance measure or the cost function

In order to evaluate the performance of a control system quantitatively, it is necessary to define a performance measure or a cost function that the optimal control method tries to minimize. Therefore, the aim of the control problem is to find an admissible control u^* to follow, and admissible x^* to minimise the cost function:

$$J = h\big(x(t_f), t_f\big) + \int_{t_0}^{t_f} g(x(t), u(t), t)dt \qquad \textit{Eq. 6-2}$$

$u^*$is called an optimal control and x^*an optimal trajectory.

6.2.3 The principle of optimality

Dynamic Programming is based on Bellman's principle of optimality:

"An optimal policy has the property that no matter what the previous decision (i.e., controls) have been, the remaining decisions must constitute an optimal policy with regard to the state resulting from those previous decisions"[100, 101]

In the discrete time format:

$$x_{k+1} = f(x_k, u_k) \qquad \textit{Eq. 6-3}$$

where x_k is the state vector, u_k is the vector of control variables, and k is the time index.

The performance index or cost function in discrete time format is:

$$J = h(x(N), N) + \sum_{k=0}^{N-1} L[x(k), u(k)] \qquad \textit{Eq. 6-4}$$

where L is an instantaneous cost which is a function of the state and control input at each intermediate time k. Based on the principle of optimality, discretization of states and time, and by finding the minimum instantaneous cost for all admissible input variables, the optimal input variable could be found for each time step with recursive loops. For more information please refer to references [100, 101].

6.3 EMS OF PHEVS AND DYNAMIC PROGRAMMING

As explained in Chapter 1, an intelligent charge management as a part of the EMS is required to get the maximum benefits out of the energy stored in the PHEV ESS. Dynamic programing (DP) is a global optimal approach which can find the best charge depleting profile, also can act as the benchmark solution for PHEVs' online EMSs. It represents the best possible solution of the control problem with respect to the used discretization of time, state space, and inputs. Its main disadvantage is the high computational effort which opposes a real-time implementation for the online control of a vehicle. With an acceptable estimate of power-cycle described in Chapter 3, however, DP can help find the optimal charge depleting trajectory for a known driving pattern. That is, DP could be run off-line before the journey starts to find the best SOC and engine temperature trajectories, and also to calibrate the real-time EMS of PHEVs. Using external sources via cloud-computing could be a feasible solution to overcome this computational burden. The online approaches like equivalent consumption

minimization strategies (ECMS), model predictive control, stochastic dynamic programming, and heuristic strategies are locally optimal approaches which cannot predict the optimal charge depleting strategy and engine thermal management, accordingly.

6.3.1 Vehicle model

An inverse powertrain model analogous to the PHEV model described in Chapter 3 is formulated as an optimal control problem in dynamic programming to find the optimal charge depleting trajectory and EMS of the PHEV. Based on the principle of optimality suggested by Bellman, the optimal path from any of its intermediate steps to the final states corresponds to the terminal part of the entire optimal solution [2, 49, 100, 102, 103]. For the series powertrain architecture, the states are the battery charge, Ch, and the engine internal temperature, T_i, and duration of engine operation since last start, $t_{eng_{on}}$, and the control vector is the engine power, P_{Eng}. In the discrete time format and using *Eq. 6-3* :

$$Ch(k+1) = f_1\left(Ch(k), T_i(k), t_{eng_{on}}(k), P_{Eng}(k)\right) \qquad \textit{Eq. 6-5}$$

$$T_i(k+1) = f_2\left(Ch(k), T_i(k), t_{eng_{on}}(k), P_{Eng}(k)\right) \qquad \textit{Eq. 6-6}$$

$$t_{eng_{on}}(k+1) = f_3\left(Ch(k), T_i(k), t_{eng_{on}}(k), P_{Eng}(k)\right) \qquad \textit{Eq. 6-7}$$

Electric power equilibrium at the power bus, depicted in Figure 3.2, could be expressed in the form of Eq. 6-8. Power-cycle, the right side of Eq. 6-8, consists

of the electric motor power, P_M, and accessories loads, $P_{Acc_{nohtr}}$, and the heater power demand, $\dot{Q}_{htr}$. When the engine is warm enough, $T_i \geq T_{htr}$, the heater power demand, $\dot{Q}_{htr}$, could be supplied by the engine waste heat. As a prerequisite of DP modelling, it is assumed that the power-cycle is predicted based on the approach described in Chapter 3.

$$P_{ESS} + \eta_{Gen}.P_{Eng} = P_M + P_{Acc_{nohtr}} + \begin{cases} \dot{Q}_{htr} & T_i < T_{htr} \\ 0 & T_i \geq T_{htr} \end{cases} \qquad Eq.\ 6\text{-}8$$

where P_{ESS}, η_{Gen}, P_{Eng} are ESS power, generator efficiency, and engine power respectively.

There are some simplification assumptions for the battery subsystem of the DP model of the vehicle compared to the model discussed in Chapter 3. First, it is assumed that the resistance of the battery is independent of the SOC of the battery. Moreover, the effect of temperature on the battery resistance is neglected. Therefore, the battery thermal model is not considered. Dynamic programming suffers from the curse of dimensionality. That is, adding each state variable increases the computational load exponentially. Therefore, clever simplification could limit the required computational effort to make the process reasonably accurate and implementable in practice. Assuming that the ESS model is a perfect open circuit voltage source in series with an internal resistance, and using Eq. 6-8 and Eq. 3-34 the relation between the state, Ch, and the input variable, P_{Eng}, is described by Eq. 6-9. The motor power demand, P_M, the accessories excluding cabin heater power demand, $P_{Acc_{nohtr}}$, and the cabin heater power demand, P_{htr}, are fed into the DP model from the simulation results of the quasi-static model

over the same power-cycle. In a series drivetrain, as the electric motor is the sole vehicle traction provider, the control strategy does not affect the motor power demand of the vehicle. Therefore, the results could be used in a dynamic approach as well. The battery nominal voltage, U_0, and resistance, R, are kept similar to quasi-static simulation.

$$I = \frac{U_0}{2R} - \sqrt{\left(\frac{U_0}{2R}\right)^2 - \frac{P_M + P_{Acc_{nohtr}} + \begin{cases}\dot{Q}_{htr} & T_i < T_{htr} \\ 0 & T_i \geq T_{htr}\end{cases} - \eta_{Gen}.P_{Eng}}{R}} \quad \textit{Eq. 6-9}$$

$$\Delta Ch = \Delta t \times I$$

Using Eq. 6-5 and Eq. 6-9, the relation between the state, Ch, and the input variable, P_{Eng}, in discrete format is:

$$Ch(k+1) = Ch(k) + \Delta t * \left(\frac{U_0}{2R} - \sqrt{\left(\frac{U_0}{2R}\right)^2 - \frac{P_M(k) + P_{Acc_{nohtr}}(k) + \begin{cases}\dot{Q}_{htr}(k) & T_i(k) < T_{htr} \\ 0 & T_i(k) \geq T_{htr}\end{cases} - \eta_{Gen}.P_{Eng}(k)}{R}} \right)$$

Eq. 6-10

In this modelling, the simulation time step, Δt, is assumed to be 1 second.

The internal engine temperature state, T_i(k), is dependent on the input variable, P_{Eng}, with the heat transfer equations described in the engine thermal model.

Similar equations that were described in Section 3.6.2., in discrete time format are employed in the coding environment of Matlab instead of Simulink. Therefore, temperatures at each nodes of the engine thermal model of Figure 3.5 can be represented by following equations:

$$T_c(k+1) = T_c(k) + \frac{Q_{Eng}(k) - Q_{c2i,c}(k)}{m_{Eng,c} * C_{p,Eng} * \Delta t} \qquad \textit{Eq. 6-11}$$

$$T_i(k+1) = T_i(k) + \frac{Q_{c2i,c}(k) - Q_{Radiator}(k) - Q_{Htr}(k) - Q_{i2x,c}(k)}{m_{Eng,i} * C_{p,Eng} * \Delta t} \qquad \textit{Eq. 6-12}$$

$$T_x(k+1) = T_x(k) + \frac{Q_{i2x,c}(k) - Q_{x2h,r}(k) - Q_{x2h,v}(k) - Q_{x2h,c}(k) - Q_{x2a,r}(k) - Q_{x2a,v}(k)}{m_{Eng,x} * C_{p,Eng} * \Delta t} \qquad \textit{Eq. 6-13}$$

$$T_h(k+1) = T_h(k) + \frac{Q_{x2h,r}(k) + Q_{x2h,v}(k) + Q_{x2h,c}(k) - Q_{h2a,r}(k) - Q_{h2a,v}(k)}{m_{Eng,x} * C_{p,Eng} * \Delta t} \qquad \textit{Eq. 6-14}$$

The last state variable, $t_{eng_{on}}$, which is the duration of the engine operation before the last start is defined to prevent the frequent transitions between the engine on and off modes. There is a threshold designed for minimum duration, t_eng_on, that engine is kept operating. A lock inside the code prevents

the engine to turn off before the minimum engine on time threshold. In this study, the threshold is defined as 10 second.

$$t_{eng_{on}}(k+1) = \begin{cases} t_{eng_{on}}(k) + \Delta t & if\ P_{Eng}(k) > 0 \\ 0 & if\ P_{Eng}(k) = 0 \end{cases} \qquad \textit{Eq. 6-15}$$

The optimization problem in discrete format is to find the control input, u_k, to minimize a cost function which represents the fuel consumption from the initial time, t_0, and states, $Ch(t_0)$, $T_i(t_0)$, to the final time, t_f, and states, $Ch(t_f), T_i(t_f)$.

From *Eq. 6-4* in which the $\mathrm{h(x(N), N)} = 0$, the fuel cost function can be defined as:

$$J = \sum_{k=0}^{t_f-1} L[x(k), u(k)] = \sum_{k=0}^{t_f-1} fuel(T_i(k), P_{Eng}(k)) \qquad \textit{Eq. 6-16}$$

$x \in X$

$u \in U$

where L is an instantaneous cost which is hereby defined as fuel consumption. It is possible to add emission and its correspondent weighting factor to the cost function. X and U are admissible PHEV states and control inputs, respectively, which are defined based on the operational restrictions of the battery and the engine-generator. $\mathrm{h(x(N), N)}$ could be defined as non-zero when the final SOC is a soft constraint. The soft constraint means that the final SOC is acceptable in a range rather than a fixed predefined SOC. Hence, a penalty to compensate the

charge deviation should be considered. For HEVs with smaller battery, and for short drive-cycle simulation, this might be useful which is not the case here.

6.3.2 Initialization of DP approach

As described in Section 5.2.1, the engine-generator operation is independent of the vehicle speed in the series HEVs' architecture. Therefore, the engine-generator could operate over confined optimal operation line (COOL). (see Figure 5.2). Therefore, a bijective function can be defined between any engine power demand, P_{Eng} and fuel consumption.

In the dynamic programming initialization phase, the heater power demand can be supplied by either the engine waste heat or electricity. Accordingly, two corresponding change of charge against fuel consumption, $\Delta Fuel_{htr}(k, \Delta Ch)$, $\Delta Fuel_{nohtr}(k, \Delta Ch)$, are calculated for each time step by using COOL, Eq. 6-10, and power-cycle. $\Delta Fuel_{htr}(k, \Delta Ch)$ and $\Delta Fuel_{nohtr}(k, \Delta Ch)$ define instantaneous cost for any possible change in the state variable, Ch(k), regardless of second state variable, T_i(k). In other words, $\Delta Fuel_{htr}(k, \Delta Ch)$ and $\Delta Fuel_{nohtr}(k, \Delta Ch)$ define a one-to-one correspondence function between fuel consumption and change of charge for each point of power-cycle for two cases of heater power demand provided electrically or from engine waste heat respectively. Obviously, for implementation purposes in Matlab, coding environment $\overrightarrow{\Delta Fuel_{htr}}(k, \Delta Ch)$ and $\overrightarrow{\Delta Fuel_{nohtr}}(k, \Delta Ch)$ are saved in vector format for each time-step.

6.3.3 Cost-to-go matrix

By implementing a forward DP approach, a cost-to-go matrix, J, is defined recursively from the initial time-step via discretising the charge of battery and time defined by the duration of drive-cycle. Any node on the cost-to-go matrix represents the minimum cost to reach that specific charge and time from the beginning of the journey. The time discretisation is $\Delta t = 1\ [s]$, and the charge discretisation in this simulation is $\Delta ch = 1\ [A.s]$. With the selected sizing of the battery, the total charge capacity is:

$$
\begin{aligned}
&battery\ capacity\ [A.s] \\
&= battery\ capacity\ [A.hr] * 3600\ \left[\frac{s}{hr}\right] \\
&* numer\ of\ modules = 7 * 3600 * 10 \\
&= 252000\ [A.s]
\end{aligned}
\qquad \textit{Eq. 6-17}
$$

$$
\begin{aligned}
&J\ matrix\ number\ of\ rows \\
&= (SOC_{max} - SOC_{min}) *\ battery\ capacity \frac{[A.s]}{\Delta ch} \\
&= (0.9 - .35) * 252000 =\ 138\,600
\end{aligned}
\qquad \textit{Eq. 6-18}
$$

$$
J\ matrix\ number\ of\ columns = Drive\_cycle\ duration/\Delta t \qquad \textit{Eq. 6-19}
$$

The initial and final charges, as well as the maximum and minimum change of charge in each time-step are used to determine the possible maximum and

minimum charges of each time-step. This reduces dimensions of the recursive loops for calculation of the cost-to-go matrix to the irregular hexagon shown in schematic cost-to-go matrix in Figure 6.1. When the initial and final charges are known, there are limited possible paths available in the cost-to-go matrix which connects them. Indeed, maximum and minimum applicable charges of the battery define the extremum horizontal boundaries. Two forward and backward calculations are required to find the other four inclined boundaries. In forward calculation, both maximum and minimum charge start from initial predefined charge for the first column. For the next step, maximum and minimum possible charge correspond to the charge of the battery if the engine operates at maximum power or turns off, respectively. On the other hand, in the backward approach, both maximum and minimum charge starts from final predefined charge for the last column. For the next step backward, maximum and minimum possible charge correspond to the charge of battery if engine turns off or operates at maximum power, respectively. Eq. 6-20 and Eq. 6-21 represent forward and backward calculation of the maximum and minimum charges in each step. The boundaries of the possible charges in irregular hexagon in Figure 6.1. are defined by Eq. 6-22.

$$Ch_{Max_{fwd}}(K+1) = Ch_{Max_{fwd}}(K) + \Delta Ch_{max}(k)$$

$$Ch_{Min_{fwd}}(K+1) = Ch_{Min_{fwd}}(K) + \Delta Ch_{min}(k) \qquad \textit{Eq. 6-20}$$

$$K=0:1:N-1$$

$$Ch_{Max_{bwd}}(K-1) = Ch_{Max_{bwd}}(K) - \Delta Ch_{min}(k)$$

$$Ch_{Min_{bwd}}(K-1) = Ch_{Min_{bwd}}(K) - \Delta Ch_{max}(k) \qquad \textit{Eq. 6-21}$$

K=N:-1:1

$$Ch_{Max}(k) = min\begin{cases} Ch_{Max_{fwd}}(k) \\ Ch_{Max_{bwd}}(k) \\ Ch_{Max-SOC} \end{cases}$$

Eq. 6-22

$$Ch_{min}(k) = max\begin{cases} Ch_{Min_{fwd}}(k) \\ Ch_{Min_{bwd}}(k) \\ Ch_{Min-SOC} \end{cases}$$

In summary, only all possible paths from the initial to the final SOC are investigated instead of finding the cost-to-go matrix for all the discretised charges and times. This could significantly reduce the calculation time for large battery and for drive-cycles longer than the AER of PHEVs.

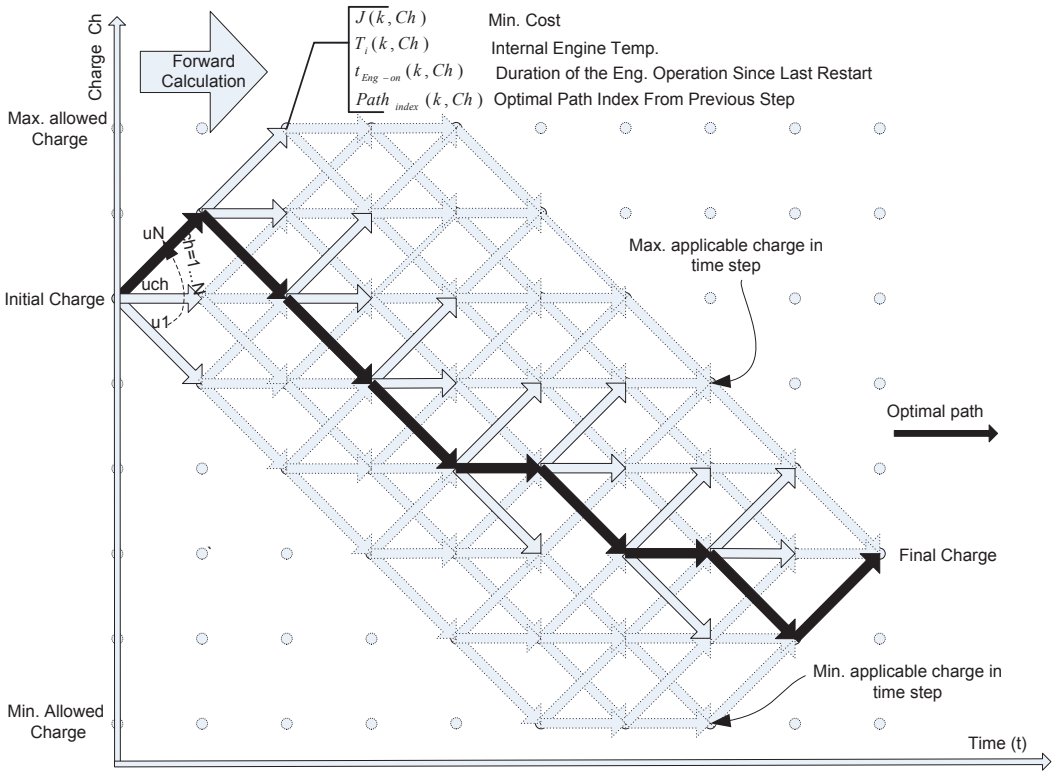

Figure 6.1. Graphical representation of cost-to-go matrix

Based on the Bellman's recursive equation approach, the cost function, *Eq. 6-23* is solved by an interpolation method to find the minimum cost to reach a specific node from all possible charges of the previous time step considering both minimum engine-on-time and cold-factor. Cold-factor relates the cost function to the second state variable, T_i(k), using Eq. 6-25. Also, minimum engine-on-time defines the minimum duration that the engine is permitted to turn off again after it starts. This prevents excessive transient operation of the engine which is generally associated with low efficiency and high emission. All possible charges, $\overrightarrow{\text{ch}}$, costs, $\vec{\text{J}}$, and fuel consumptions, $\overrightarrow{\Delta fuel_{htr}}$ and $\overrightarrow{\Delta fuel_{nohtr}}$, are shown in vector format in *Eq. 6-23*. The engine on-time, $t_{eng_{on}}$, defining duration of the engine

operation, and the engine internal temperature, T_i, derived from the thermal model of the engine, are also calculated and saved for each node. Two inequality functions in *Eq. 6-23* define the condition for supplying the heater power demand by the engine waste heat and prevent the engine to turn off before a minimum engine-on-time threshold. For each node of the cost-to-go matrix, the index of the ascendant node defining the optimal path to the specific node is also saved. This is required to identify the initial conditions for cost, $\vec{J}\left(k\text{-}1, \overrightarrow{ch}\right)$, thermal model, $T_i(k-1)$, engine on time, $t_{eng_{on}}(k-1)$ for forward cost-to-go calculations and also to find the SOC trajectory in the backward phase of DP. The schematic calculation of cost-to-go for each node is depicted in Figure 6.2.

$$J\,(k, Ch)$$

$$= \begin{cases} \min\left(\vec{J}\,(k-1,\overrightarrow{ch}\,) + \text{Cold\_factor}(k-1,\overrightarrow{ch}\,)\cdot\overrightarrow{\Delta fuel_{\text{htr}}}(\text{k}-1,\overrightarrow{ch}\,)\cdot\Delta\, t\cdot\begin{Bmatrix} inf & ch=1\ and\ t_{eng_{on}}(k-1) < \min\_eng\_on \\ 1 & ch\neq 1\ \ or\ t_{eng_{on}}(k-1)\geq \min\_eng\_on \end{Bmatrix}\right) & T_i(k-1) < T_{htr} \\ \min\left(\vec{J}\,(k-1,\overrightarrow{ch}\,) + \text{Cold\_factor}(k-1,\overrightarrow{ch}\,)\cdot\overrightarrow{\Delta fuel_{\text{nohtr}}}(\text{k}-1,\overrightarrow{ch}\,)\cdot\Delta\, t\cdot\begin{Bmatrix} inf & ch=1\ and\ t_{eng_{on}}(k-1) < \min\_eng\_on \\ 1 & ch\neq 1\ \ or\ t_{eng_{on}}(k-1)\geq \min\_eng\_on \end{Bmatrix}\right) & T_i(k-1) \geq T_{htr} \end{cases}$$

Eq. 6-23

Based on the thermostat engine temperature set point, $T_{Eng_{tstat}}$, and the coolant temperature, $T_{coolant}$, which is assumed equal to the engine internal temperature,T_i, from Eq. 6-12 where temperature is in centigrade degrees. :

$$\gamma(k) = \frac{T_{Eng_{tstat}} - T_{coolant}(k-1)}{T_{Eng_{tstat}} - 20} \qquad \textit{Eq. 6-24}$$

$$Cold\ Use = Hot\ Use * Cold\_factor$$

$$where \quad Cold\_factor(k) = (1 + (\gamma(k))^{3.1}) \qquad \textit{Eq. 6-25}$$

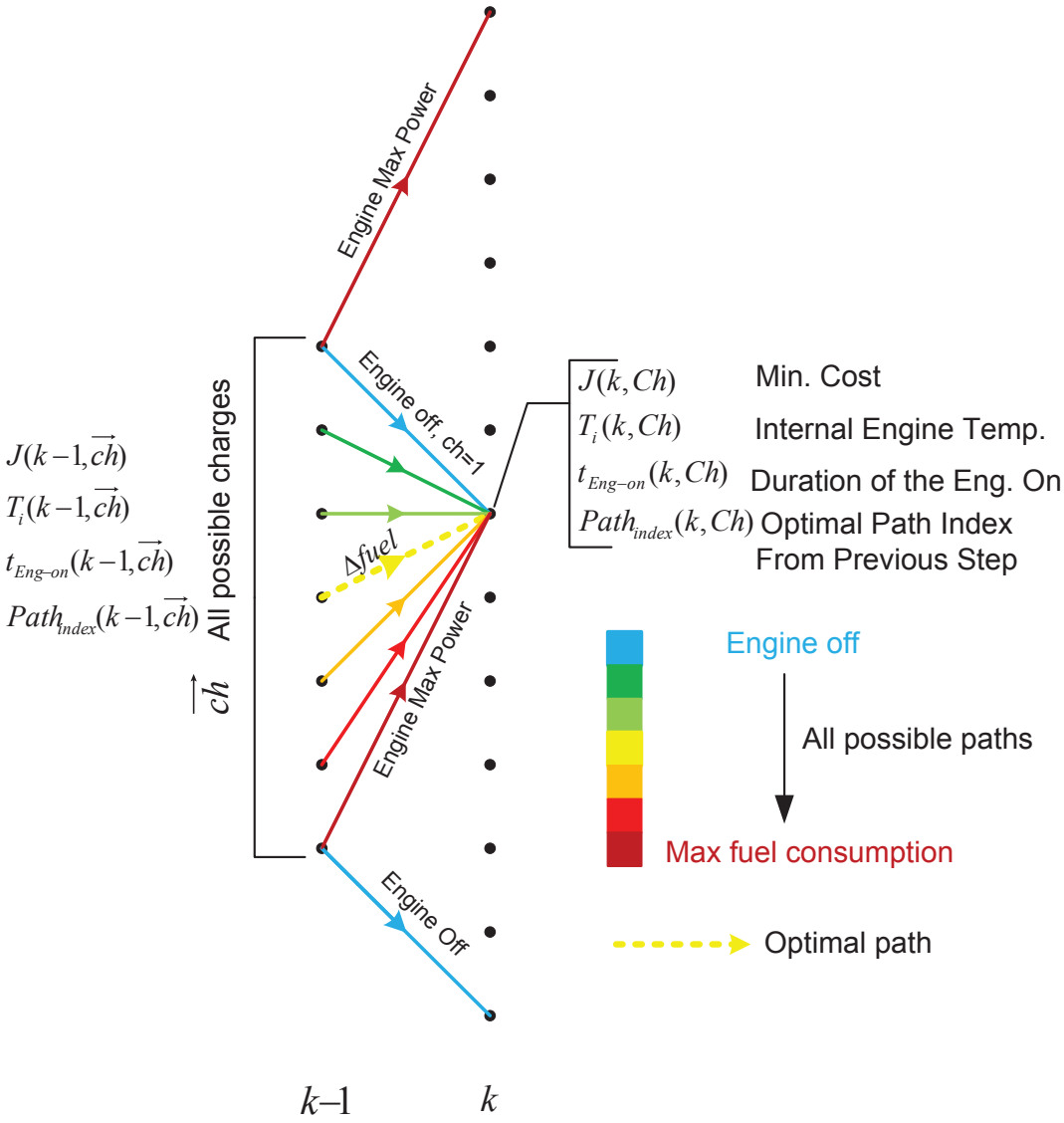

Figure 6.2. Schematic calculation of cost-to-go for each node

After completion of the cost-to-go calculation, in the backward calculation stage, optimal charge, temperature, fuel consumption, and engine power trajectories are calculated. The flowchart of the DP code is shown in Figure 6.3. The calculation of each time step charge limits and vectorization of the algorithm have improved the performance of the code and the simulation time for the PHEV battery size and the long drive-cycles.

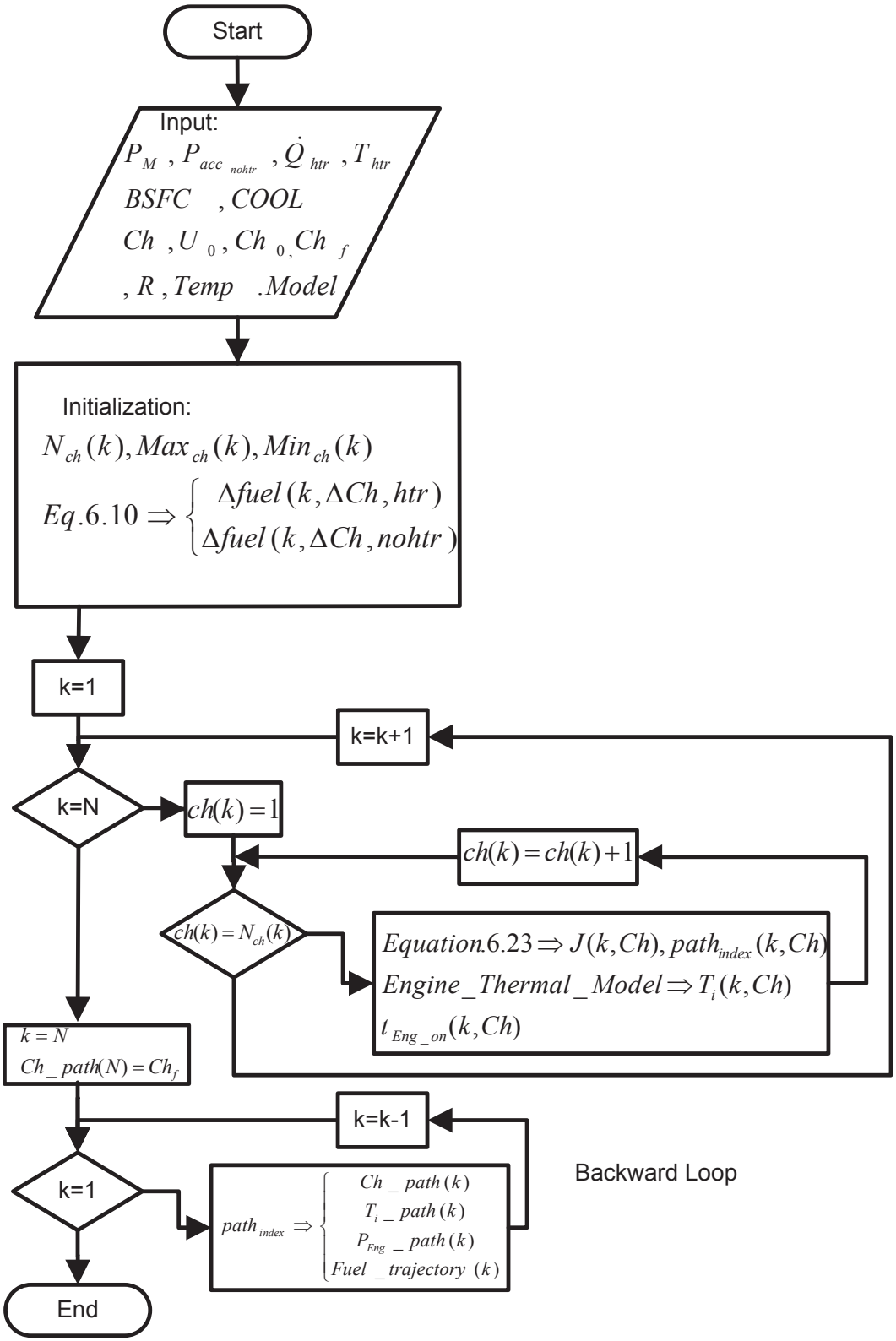

Figure 6.3. Flowchart of the developed dynamic programming code

6.3.4 Forward DP instead of backward DP

Generally, dynamic programming is known as a backward approach. That is, in case of energy management strategy of HEVs and PHEVs, the calculation of cost-to-go matrix starts from the end of journey back to the initial point. There are two main reasons that make it necessary to use forward instead of backward DP. First, the initial conditions at the end of the journey are unknown, thus the thermal model equations cannot be solved in a backward manner. In the engine thermal model, the engine mass is lumped to four temperatures, cylinder, T_{cyl}, engine interior, T_i, engine exterior, T_x, and hood temperature, T_h. If a backward approach is selected, the initial conditions of the heat transfer equations are unknown at the end of the journey. In addition, when the coolant reaches the thermostat temperature, the radiator heat transfer rate, $\dot{Q}_{Radiator}$, as an extra unknown, is added if the thermal model is to be solved backward. Therefore, it is impossible to form the cost-to-go matrix with backward approach if the temperature as a state variable is considered.

6.4 SIMULATION RESULTS

To prove the significance of temperature on the optimal EMS of PHEVs, two 80 km driving scenarios simulating warm and chilly days are defined. Simulations conducted to find the optimal battery charge and engine power trajectories using the developed DP code. The results are compared against those of the AER-CS and DP EMS methods which neglect the cold-factor, engine cold start, and heater/AC power demands. The name “DP with cold-factor” is selected for the developed dynamic programming-based method proposed in Section 6.3. The

formulation of "DP without cold-factor" is similar, but does not consider the engine temperature as a state variable in the control problem. Therefore, for the "DP without cold-factor", the cost function in *Eq. 6-23* is defined without considering the cold-factor and the heater power demand inequality function. To show the real fuel consumption, the cold-factor multiplied by the cost. The cold-factor is not considered in the minimization function (see Eq. 6-26) of "DP without cold-factor".

$$J^*(k, Ch^*) = min\left(\vec{J}\left(k-1, \overrightarrow{ch}\right) + \overrightarrow{\Delta fuel_{htr}}\left(k-1, \overrightarrow{ch}\right) \cdot \Delta t_{k-1,k} \cdot \begin{cases} inf & ch = 1 \; and \; t_{eng_{on}}(k) < min\_eng\_on \\ 1 & ch \neq 1 \;\; or \; t_{eng_{on}}(k) \geq min\_eng\_on \end{cases}\right) \qquad Eq.\ 6\text{-}26$$

$$J(k, Ch) = \begin{cases} \left(J(k-1, Ch^*) + Cold\_factor(k-1, Ch^*) \cdot \Delta fuel_{htr}(k-1, Ch^*) \cdot \Delta t\right) & T_i(k-1) < T_{htr} \\ \left(J(k-1, Ch^*) + Cold\_factor(k-1, Ch^*) \cdot \Delta fuel_{nohtr}(k-1, Ch^*) \cdot \Delta t\right) & T_i(k-1) \geq T_{htr} \end{cases}$$

6.4.1 Driving scenario

The drive-cycle represents a typical work-home commute which starts in a suburban area, characterized by UDDS, then continues on a highway, simulated by HWFET, and finally arrives to downtown urban area, UDDS. Destination elevation is around 400 meters higher than the starting point. For the warm day driving scenario, vehicle stops during working hours and the engine cools down to the ambient temperature. The return journey is the mirror of the defined driving

scenario but the acceleration and deceleration are kept identical. The reason is that by simple mathematical mirroring of the cycle all accelerations are replaced to braking and vice versa. To keep the power required for acceleration similar to initial journey, acceleration and deceleration should be kept similar. The drive-cycle of both chilly and warm days is similar, yet to show the significance of the heater power demand regardless of the effect of cool-down period in the middle of the journey, a continuous 80 km journey without a cool-down period is simulated. 1.5 kW power demand and COP of 2 for AC refrigeration cycle are assumed for the warm day; therefore, for a similar 10 K difference between cabin comfort, 20˚C, and ambient temperatures, the heater power demands is defined as 3 kW for the chilly day. The initial power surge and fluctuations during journey are neglected. The simulation results for the warm and chilly days are depicted in Figure 6.4 and Figure 6.5, respectively. The fuel consumption information is given in Table 6-1 and Table 6-2.

Figure 6.4 demonstrates the simulation results of three EMSs for the warm day commute over the drive-cycle, and the elevation profile depicted in Figure 6.4 (A). “AER-CS”, blended mode “DP without cold-factor”, and blended mode “DP with cold-factor” are three different EMSs which are compared in this simulation. The corresponding power-cycle of the journey is shown in Figure 6.4 (B). The engine power trajectory for the AER-CS simulation is illustrated in Figure 6.4 (C). During AER, the engine is maintained off until the charge sustaining time, t_{CS}, when the battery charge reaches the minimum applicable SOC. To have a fair comparison with other blended mode EMSs, the DP without cold-factor is used to find the engine power trajectory during the CS mode only for the period of t_{CS} to

t_f. Therefore, while the result is optimal for only the CS duration, it would not be a global optimal solution for the whole journey.

The restriction of having the AER at the beginning of the journey is relaxed to develop a blended mode EMS. The DP without cold-factor is employed for the whole journey; hence, the engine power trajectory follows the profile illustrated in Figure 6.4 (D). The DP without cold-factor finds the global optimal solution for the control problem if it is assumed that the hot engine efficiency map is acceptable for whole journey. Due to the elevation profile, the vehicle power demand is generally lower in return section of the journey. The DP without cold-factor, unlike the AER-CS, allocates most of the battery energy to the return journey and selects the engine-on sections where the wheel power demand is generally higher. Therefore, power recirculation is prevented by supplying the wheel power demand directly from the engine instead of recharging the battery when power surplus is available. Although similar code is used for both the CS section and the DP without cold-factor EMS simulations, the fuel consumption is reduced by around 2% via the global optimal charge management. That is, the blended mode EMS allocates battery electric energy more efficiently than the AER-CS which consumes all of the battery energy during AER.

The engine coolant temperature trajectories shown in Figure 6.4 (G) prove that the hot engine operation is not an accurate assumption for EREVs in which the battery supplies significant share of the vehicle required energy. This requires modification in the DP formulation to consider the effect of temperature as a state variable as explained in Section 6.3. Employing the DP with cold-factor, the EV mode completely shifts to return journey and all engine-on sections are

concentrated before the cool-down period. This eliminates the second cold start warm-up procedure which leads to cold engine operation and consequently the cold-factor penalty. The DP with cold-factor selects the first section of the commute for the blended mode operation, as the battery energy is adequate to run the downhill return journey in the EV mode. The overall engine efficiency for the whole journey is higher when one extra engine warm-up is eliminated. That is, the effect of warmer engine operation overcompensate the reduction of the vehicle efficiency because of the engine operation in the lower power demand when compared with the DP without cold-factor. Our proposed "DP with cold-factor" approach improves the fuel economy of the vehicle by 3.2% compared with the AER-CS EMS. Therefore, it improves the performance of the DP without cold-factor by 1.2%. This result simulates inaccuracy of relying on the DP without cold-factor for PHEVs with large battery as the optimal EMS benchmark. In addition, as described in the introduction section, the cold operation of the engine and catalyst converter has a major role in the emission of the vehicle. Therefore, the environmental impact of the emission reduction by elimination of the second cold-start may outweigh the amount of fuel saved. According to the simulation conducted in ADVISOR, the HC, CO, and NOx emissions are reduced by almost 27%, 11%, and 17% respectively compared to the AER-CS simulation (see Table 6-1).

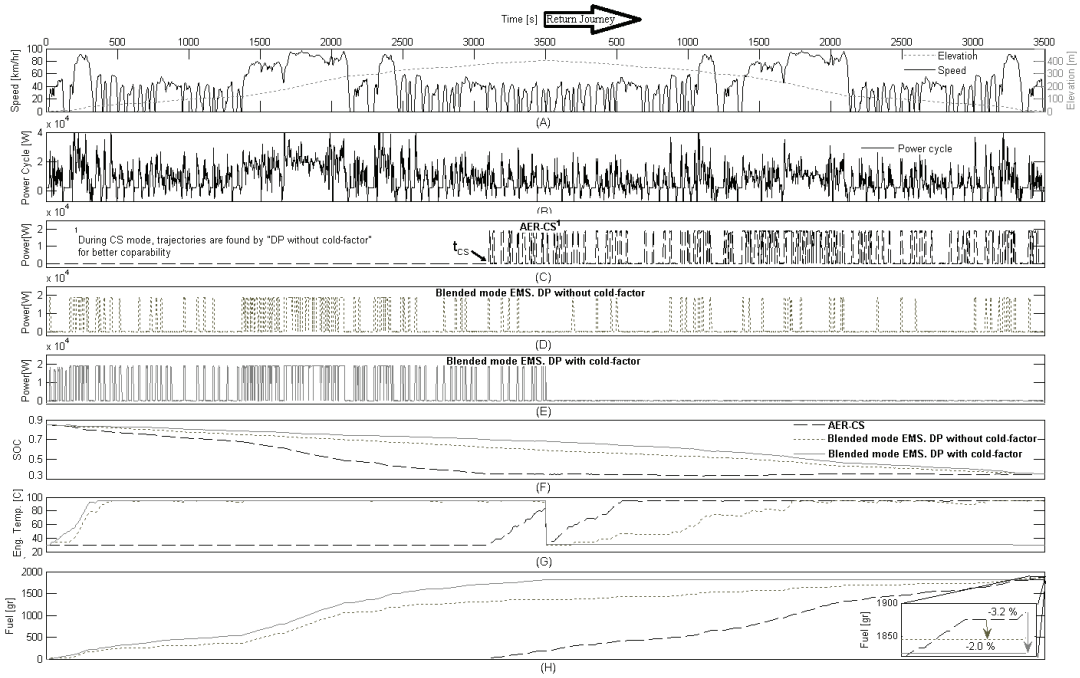

Figure 6.4. Simulation results for a warm day with 1.5 kW constant AC power demand and cool-down period at t=3500 (A) drive-cycle and elevation profile, (B) power-cycle, (C) engine power trajectory of AER-CS EMS, (D) engine power trajectory of blended mode EMS by DP without cold-factor, (E) engine power trajectory of blended mode EMS by DP with cold-factor, (F) battery SOC trajectories, (G) engine coolant temperature trajectories, and (H) fuel consumption trajectories

Table 6-1. DP and ADVISOR simulation results for warm day

		Fuel Consumption	HC [gr/km]	CO [gr/km]	NOx [gr/km]	Engine Efficiency	Final SOC
DP Simulation warm day	AER-CS	1885.4 [gr]	N.A.	N.A.	N.A.	N.A.	0.35
	1) DP without clod-factor	1847.3 [gr]	N.A.	N.A.	N.A.	N.A.	0.35
	2) DP with cold-factor	1824.5 [gr]	N.A.	N.A.	N.A.	N.A.	0.35
	Improvement (case 1 compared to AER-CS)	-2.0 * [%]	N.A.	N.A.	N.A.	N.A.	0
	Improvement (case 2 compared to AER-CS)	-3.2 [%]	N.A.	N.A.	N.A.	N.A.	0
ADVISOR Simulation warm day	AER-CS	2137.8 [gr]	0.100	0.379	0.179	0.301	0.346
	Blended EMS, following DP with cold-factor charge trajectory	2010.0 [gr]	0.073	0.336	0.148	0.309	0.349
	Improvement/change [%]	-6.0 [%]	-27 [%]	-11.4 [%]	-17.3 [%]	2.5 [%]	0.9 [%]

The engine operation trajectories of the AER-CS EMS of a full electric cabin heater vehicle and a vehicle in which the heater power is supplied by both the battery and the engine waste heat are compared in Figure 6.5 (B-C). The significant 34% improvement in the fuel economy could be realised by employing the waste heat of the engine like conventional vehicles. Based on the author's knowledge gained at 2011 Frankfurt motor show, the GM Volt cabin heater is an all-electric, while Opel has solved the issue for the Ampera models. The engine power path shown in Figure 6.5 (D) is derived based on the DP EMS with cold-factor for a vehicle with both engine coolant and electric heater. Figure 6.5 (F) illustrates how the optimal EMS found by the DP with cold-factor tends to keep the engine warm for longer duration to provide the cabin heater power demand free of cost. Indeed, holding the temperature not exactly at the thermostat temperature comes at a cost of a reduction in engine efficiency defined by the cold-factor. The optimal EMS based on DP compromises between maximum availability of the hot water from the engine by distributing engine-on sections during the journey and the effect of cold-factor on the engine efficiency. Referring to Table 6-2, for ADVISOR simulation, 14% improvement in the fuel economy is achieved, while the engine efficiency is reduced by 3% because of the operation at temperatures below thermostat set-point. That is, the amount of fuel saved by keeping the engine warm outweighs the drawback of its operation at not exactly the thermostat temperature set-point. When heater operation is required for cold weather, the DP with cold-factor method finds the optimal trajectory of state variables, ESS charge and accordingly the engine internal temperature, to minimise the fuel consumption cost function. It is interesting how the optimal

method still selects a short EV mode at the end of the journey. Since the energy demand of the heater is directly related to the duration of the journey, as well as the ambient temperature, its influence on the optimal EMS of PHEVs is more significant for cold weather, long journeys, and especially for low power demand city drive-cycles. Although the wheel power demand of the vehicle in both simulations of warm and chilly days is similar, the final optimal charge depleting and EMS for different temperatures and AC/heater power demands are significantly different. The warm day simulation shows how a cold-factor might affect the optimal EMS to concentrate engine operation before the cool down period for the defined driving scenario. On the other hand, the combination of the effect of cold-factor and the desirability of keeping the engine warm for the cabin heater purpose distributes the engine operation sections throughout the journey for the chilly day simulation. While for warm weather operation keeping the engine temperature close to thermostat temperature is the dominant parameter to achieve optimal overall efficiency, for the chilly day simulation, the availability of hot water for the cabin heater dominates, thus avoiding the electric heater operation.

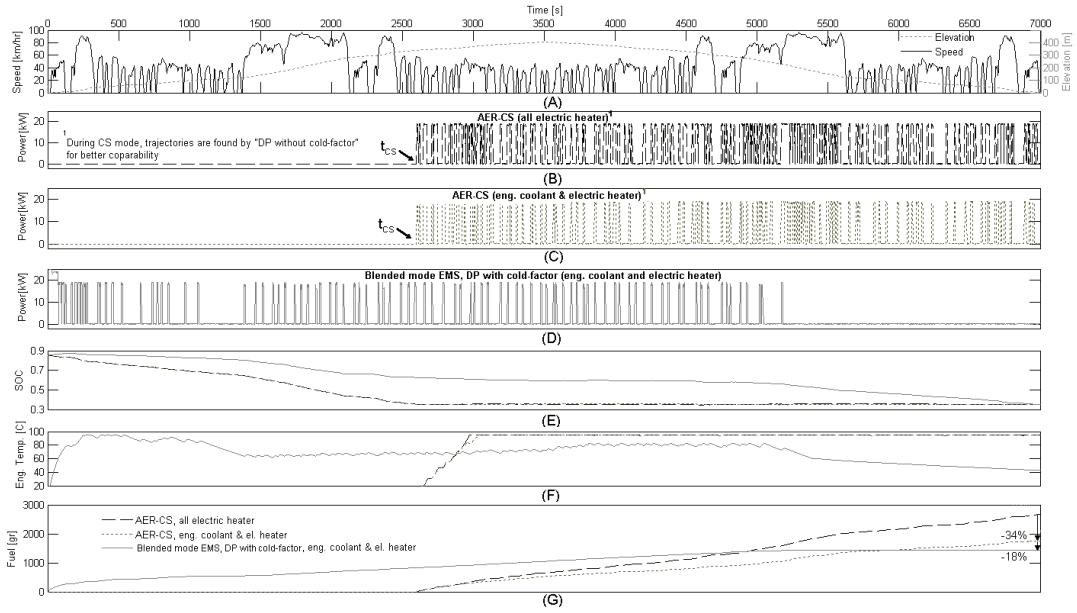

Figure 6.5. Simulation results for a chilly day with 3 kW constant heater power demand without a cool-down period (A) drive-cycle and elevation profile, (B) engine power of AER-CS EMS of a vehicle with all electric heater (C) engine power of AER-CS EMS, heater power demand is supplied by engine waste heat if $T_i > 60^{\circ}C$ (D) engine power of CD EMS with cold-factor and heater power demand, heater power demand is supplied by engine waste heat if $T_i > 60^{\circ}C$ (F) coolant temperature trajectories (G) fuel consumption trajectories

Table 6-2. DP and ADVISOR simulation results for chilly day

		Fuel Consumption	HC [gr/km]	CO [gr/km]	NOx [gr/km]	Engine Efficiency	Final SOC
DP Simulation chilly day	1) AER-CS All electric heater	2667.2 [gr]	N.A.	N.A.	N.A.	N.A.	0.35
	2) AER-CS both engine coolant and electric heater	1754.7 [gr]	N.A.	N.A.	N.A.	N.A.	0.35
	DP with cold-factor	1434.4 [gr]	N.A.	N.A.	N.A.	N.A.	0.35
	Improvement (DP compared to case 1)	-34.2 [%]	N.A.	N.A.	N.A.	N.A.	0
	Improvement (DP compared to case 2)	-18.3 [%]	N.A.	N.A.	N.A.	N.A.	0
ADVISOR Simulation chilly day	1) AER-CS All electric heater	2784.8 [gr]	0.162	0519	0.194	0.307	0.349
	2) AER-CS both engine coolant and electric heater	1892.6 [gr]	0.139	0.440	0.142	0.298	0.350
	Blended EMS, following DP with cold-factor charge trajectory	1628.4 [gr]	0.136	0.415	0.132	0.289	0.354
	Improvement/change (Blended EMS compared to case 1)	-41.5 [%]	-16.1[%]	-20.0[%]	-32.0[%]	-5.9 [%]	1.4 [%]
	Improvement/change (Blended EMS compared to case 2)	-13.9 [%]	-2.2 [%]	-5.7 [%]	-7.0 [%]	-3.0 [%]	1.1 [%]

Simulations also show another interesting result that is the engine power has limited fluctuations around the most efficient engine operation point regardless of the changes in the power demand (see Figure 6.6). This implies that the optimal operation of the vehicle dominantly depends on the engine efficient operation. Since the large PHEV ESS benefits from parallel modules, its internal resistance compared to the conventional HEVs is significantly lower. Therefore, the electrical waste in PHEV ESS is reduced accordingly.

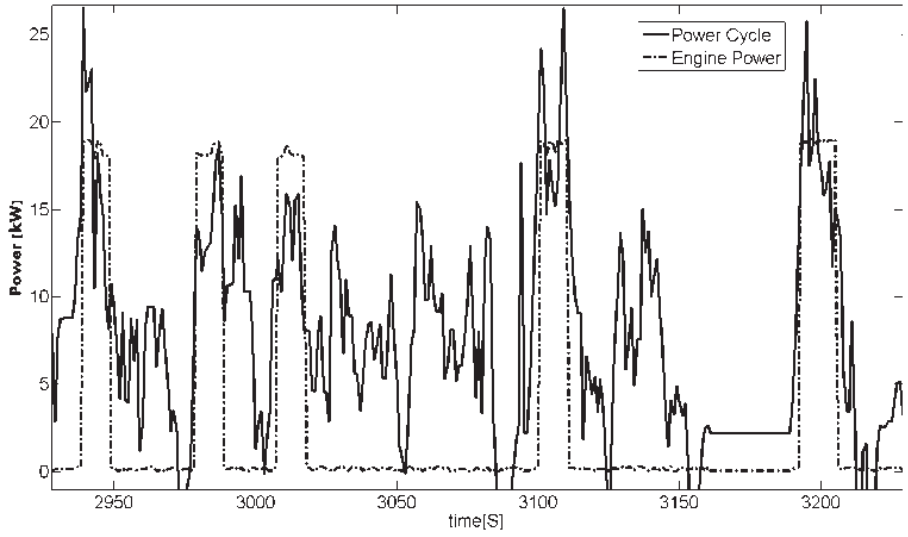

Figure 6.6. A superimposed selected section of Figure 6.4(B) and (D)

6.5 REAL-TIME IMPLEMENTATION

Although the DP approach could not be implemented in a real-time control of a vehicle, the optimal charge depleting trajectory for a known driving scenario could help calibrate the EMS in an online fashion. That is, the real-time EMS tries to implement the same optimal charge management by following the charge trajectory found by the DP approach. Particularly, the DP approach can suggest the best sections of the journey to run on the pure EV mode for EREV. The

charge trajectory should be followed based on a position feedback from the vehicle in a journey instead of the time domain using a GPS. In the following, it is described how effectively only the knowledge of optimal charge trajectory regardless of the type of real-time EMS could significantly improve the performance of PHEV.

The rule based power follower described in Section 5.3 controls the vehicle in ADVISOR simulation tool for the same driving scenario explained in the previous section. The ADVISOR model is manipulated to simulate the heater and AC loads and the effect of heater cool-down on engine thermal model. Also, the vehicle control unit is redesigned to sustain the ESS SOC around charge depleting trajectory derived from the DP approach by using a feedback control. The results are shown in Figure 6.7, Table 6-1, and Table 6-2. By following the charge trajectory found by DP with cold-factor, however, the battery to engine energy ratio during the journey is remained similar to the DP optimal trend. This results in almost a similar engine temperature trajectory. The slight deviation between the temperature trajectories of DP with cold-factor and the simulations is a result of the difference between the engine operation trajectories and the difference between the heater cooling effect on engine thermal model of the DP and ADVISOR. Due to discretization, the heater power demand is defined step-wise for the DP model which shifts at a defined threshold. Yet, the heater cooling effect on engine thermal model of ADVISOR is defined by a linear equation so the cooling effect continues for all temperatures.

The amount of fuel saved for the chilly day simulation proves the significant drawback of using only electric heater. Improvement in fuel efficiency of vehicle

could be even considerably increased for extreme low temperatures. Besides, the emission reduction is another positive aspect of an EMS considering temperature noise factor; particularly, when an unnecessary cold-start/warm-up of the engine and catalytic converter is eliminated.

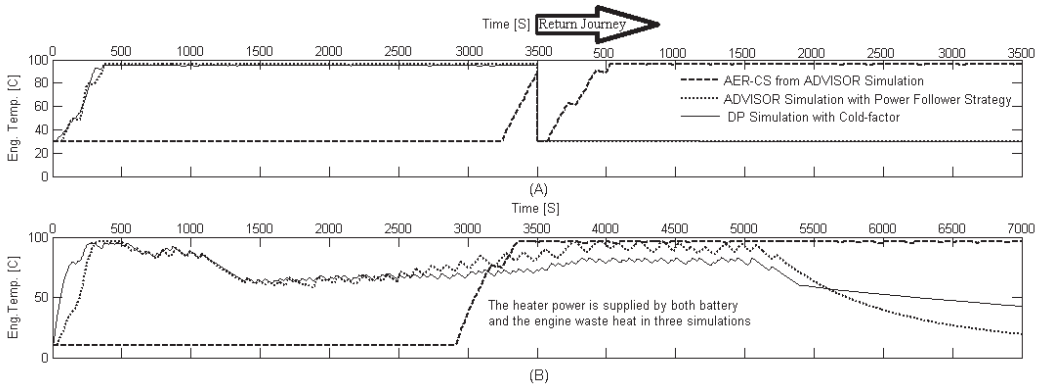

Figure 6.7. (A) Comparison of the coolant temperature trajectories in ADVISOR and DP with cold-factor simulations for (A) Warm day (B) Chilly day

6.6 CONCLUSION

The influence of the temperature noise factor on the optimal energy management strategy of PHEVs was demonstrated in this Chapter via developing a Dynamic Programming-based approach. DP based on Bellman's principle of optimality derives the optimal charge depleting trajectory of the battery. This coincides with the optimal thermal management of the engine for minimum fuel consumption, while maximizing employing engine waste heat for cabin warming instead of the battery electricity. The simulation results prove that temperature considerably changes the optimal EMS and accordingly fuel consumption and emission of PHEVs even for identical drive-cycles. A practical approach to

implement the result of the optimal EMS for calibrating a real-time EMS that addresses the realistic disturbances of real world driving was also proposed.

CHAPTER 7

CONCLUSION AND FUTURE WORK

7.1 CONCLUSION

This thesis focused on optimisation of energy management strategy for plug-in hybrid electric vehicles. The energy management strategy tries to control the energy flow in the powertrain components of PHEVs to find the most efficient energy path to provide the vehicle power demand. Unlike HEVs in which the engine is the sole source of energy, grid charged battery alongside the engine adds an extra energy path to provide vehicle power demand in PHEVs. Therefore, a

battery charge management strategy is incorporated into the EMS of PHEVs to fully harness the benefits of the extra energy source.

All available approaches, implementable for the EMS of PHEVs, were categorised in Chapter 2. Among them, two different methods: (i) a rule-based/deterministic, and (ii) an optimization-based/deterministic were selected to be investigated in this research. The deterministic methods tackle the control problem globally (i.e. for the whole journey). Hence, they are suitable choices for addressing the optimal battery charge management. The rule-based approaches are easily implementable while the optimization-based approaches can be used as optimal solutions.

Different modelling and simulation methods available in the literature were introduced in Chapter 3. The method selected for this research was also outlined and different vehicle components models were discussed. The vehicle components were sized to simulate an EREV with 64 km AER capability similar to GM Volt. The battery energy source reduces the engine load and during the EV mode engine is turned off for long periods. Therefore, the engine is more likely to operate cold compared with conventional HEVs. This leads to lower engine efficiency and higher emission. In addition, while the engine is cold, the power demand of the cabin heater needs to be supplied by battery. An engine thermal model and a cold-factor fuel consumption penalty were incorporated into the vehicle model to investigate these phenomena. Existing studies on the EMS of PHEVs mostly focus on the improvement of fuel efficiency based on hot engine characteristics neglecting the effect of temperature on the engine performance and vehicle power demand.

The implementation of globally optimal energy management strategies based on the deterministic approaches is only feasible when an accurate prediction of power-cycle is available. Many noise factors affect both drivetrain power demand and vehicle performance even in identical drive-cycles. In Chapter 4, the effect of each noise factor was investigated and the power-cycle library was proposed to improve the accuracy of the power-cycle prediction. A library of power-cycles provides the required information about the journey in both time and spatial domains, which helps to predict the power-cycle affected by the environmental noise-factors before a journey starts. PHEVs employ an in-built control strategy defined by OEM, normally an AER-CS similar to what has been designed for GM Volt or Toyota Prius PHEV. However, for known power-cycles, defined later by each vehicle owner, a more sophisticated energy management strategy would be implemented.

Chapter 5 introduced a blended mode rule-based EMS for the modelled vehicle. A driving scenario was simulated and fuel economy of the vehicle with a conventional AER-CS EMS was compared against that of the suggested rule-based EMS. Based on the power-cycle of the simulated driving scenario, an efficiency cycle was developed. The efficiency cycle was investigated in a three-step procedure to find the best sections to provide the required engine energy share. One of the characteristics of the blended mode EMS is frequent shifting between the engine-on and off modes. Therefore, the effect of the engine cooler operation on its performance should be investigated. The cold-factor calculation by means of the engine thermal model was employed to modify the efficiency cycle in the last two steps of the EMS. Moreover, the effect of the second cold-

start of the vehicle for journeys with long cool-down periods was also investigated. The result of the EMS was a sub-optimal solution that defines the best section of the journey to shift from the EV to CS mode. The rule-based approach is a practical and easily implementable approach due to the limited computational effort required.

In Chapter 6, optimal EMS control problem was formulated by using the dynamic programming method. One input variable, engine power, and three state variables, battery charge, engine internal temperature, and engine operation time were employed for formulating of the control problem. The cost function of the dynamic programming method correlates fuel economy of the vehicle to all these three state variables. The optimal battery charge depleting and the engine temperature trajectories secure globally optimal fuel economy for a prescribed journey with specific environmental conditions. The proposed approach also maximises the usage of the engine waste heat for cabin warming instead of the battery electricity in cold weather conditions. The simulation results proved that temperature considerably changes the optimal EMS, and accordingly the fuel consumption and emissions of PHEVs even for identical drive-cycles. A practical approach to implement the result of the optimal EMS for calibrating a real-time EMS was also proposed.

The simulations show significant improvement in the fuel efficiency of PHEVs with integration of the engine thermal management and EMS. Around 4.7% improvement in the fuel economy is achieved by the rule-based EMS, described in Chapter 5, according to the simulation of a warm day commute. The power recirculation, one of the major reasons for the battery degradation, is also reduced

significantly so that the amount of battery charging energy is declined by 126% during the commute simulation. Since the suggested EMS forces the engine to provide the required power of the drivetrain in the most vigorous part of the journey, the battery energy is consumed during a longer period and logically at lower power. Therefore, the maximum current and battery temperature, one the major reasons for battery degradation, are also declined accordingly. The deterministic optimal method, described in Chapter 6, provides even better results compared to the rule-based EMS. 6% and 13.9% improvement in the fuel economy of the vehicle in warm and chilly day simulations are recorded respectively.

7.2 FUTURE WORK

Some potential future directions that merit further study are listed as follows:

- As described in Section 3.6.2, the cold-factor fuel consumption is formulated mathematically based on the internal combustion engine coolant temperature. Sensibility of the engine efficiency to its internal temperature is not uniform at all speeds and torques. Therefore, the best way to formulate the engine efficiency at each specific speed, torque, and temperature is via engine dynamometry tests. In other words, it is more accurate to rely on the efficiency maps of the engine at different temperatures rather than using a single variable cold-factor function. This helps avoid specific torque-speed operation points that are more sensitive to cold engine operation during the transitional warm-up procedure.

- Prediction procedure of power-cycle with the aim of the power-cycle library was described in Chapter 4. As discussed, power-cycle can be predicted individually for each vehicle. In case of availability of a PHEV, it is possible to equip it with required sensors, schematically shown in Figure 4.1. As control by wire is completely dominant in PHEVs, there is not any expensive equipment required for this purpose. This helps evaluate sensitivity and accuracy of the power-cycle prediction process in real-world operation condition.
- In case of availability of a PHEV like GM Volt, Opel Ampera, or Prius PHEV, the performance of the suggested rule-based EMS can be evaluated easily. As explained in Chapter 5, the rule-based EMS defines the best sections to operate in the EV or CS modes for a journey. Since a manual EV mode selection is available in these vehicles, it is possible to manually select the EV mode sections based on the rule-based EMS suggestions.
- Here the optimization procedure cost function is only defined based on fuel consumption. However the cost function could be defined based on both fuel economy and emission. Since fuel consumption and emission do not follow similar dynamic, reduction of fuel consumption could result in an increase in emission and vice versa. The thermal dynamic of the catalytic converter is also should be modelled in optimisation process. The appropriate weighting factors should be defined to compromise between emission and fuel consumption.

BIBLIOGRAPHY

[1] *M. Ehsani, Y. Gao, S. E. Gay, and A. Emadi, Modern electric, hybrid electric, and fuel cell vehicles : fundamentals, theory, and design: CRC, 2005.*

[2] *L. Guzzella and A. Sciarretta, Vehicle propulsion systems: introduction to modeling and optimization, Second ed.: Springer, 2007.*

[3] *C. Mi, M. Abul Masrur, and D. W. Gao, Hybrid electric vehicles: principles and applications with practical perspectives: John Wiley & Sons, 2011.*

[4] *I. Husain, Electric and Hybrid Vehicles: Design Fundamentals, Second ed.: CRC Press 2010.*

[5] *J. Barnes, M. v. Walwijk, and C. Saricks, Hybrid and electric vehicles: The electric drive gains momentum : Progress towards sustainable transportation: International Energy Agency, 2007.*

[6] *J. Tollefson, "Charging up the future," Nature, vol. 456, pp. 436–440, Nov. 2008.*

[7] *M. Yamamoto, "Development of a Toyota plug-in hybrid vehicle," in SAE World Congress & Exhibition, Detroit, MI, USA, 2010.*

[8] *R. Zito, "EVs and Travel Behavior change," Institute for Sustainable Systems and Technologies -Transport Systems, Adelaide 2010.*

[9] *IEEE-USA Board of Directors. Position Statement: Plug-in Electric Hybrid Vehicle [Online]. Available: http://www.ieeeusa.org/policy/positions/PHEV0607.pdf*

[10] *X. Yu, "Impacts assessment of PHEV charge profiles on generation expansion using national energy modeling system," in IEEE Power and Energy Society General Meeting - Conversion and Delivery of Electrical Energy in the 21st Century, 2008, pp. 1-5.*

[11] *IEEE-USA Policy Position Statement. National Energy Policy Recommendation [Online]. Available: http://www.ieeeusa.org/policy/energyplan/files/2009.pdf*

[12] *S. G. Wirasingha, N. Schofield, and A. Emadi, "Plug-in hybrid electric vehicle developments in the US: Trends, barriers, and economic feasibility," in IEEE Vehicle Power and Propulsion Conference 2008, pp. 1-8.*

[13] *Y. Gao and M. Ehsani, "Design and control methodology of plug-in hybrid electric vehicles," presented at the IEEE Vehicle Power and Propulsion Conference, 2008.*

[14] *IEEE-USA Board of Directors. (15 June 2007, 15/09/2009). Position statement: plug-in hybrid electric vehicle Available: http://www.ieeeusa.org/policy/positions/PHEV0607.pdf*

[15] *IEEE-USA Policy Position Statement. National energy policy recommendation [Online]. Available: http://www.ieeeusa.org/policy/energyplan/files/2009.pdf*

[16] *Y. Li, "Scenario-based analysis on the impacts of plug-in hybrid electric vehicles' (PHEV) penetration into the transportation sector," in IEEE International Symposium onTechnology and Society, 2007, pp. 1-6.*

[17] *M. Miller, A. Holmes, B. Conlon, and P. Savagian, "The GM "Voltec" 4ET50 multi-mode electric transaxle " presented at the SAE World Congress & Exhibition, Detroit, MI, USA, 2011.*

[18] *H. Ogawa, M. Matsuki, and T. Eguchi, "Development of a power train for the hybrid automobile - the Civic hybrid," presented at the SAE World Congress & Exhibition, Detroit, MI, USA, 2003.*

[19] *S. Sasaki, "Toyota's newly developed hybrid powertrain," in Proceedings of the 10th International Symposium on Power Semiconductor Devices and ICs 1998, pp. 17-22.*

[20] *D. Hermance, "Toyota hybrid system," presented at the SAE TOPTEC Conference, Albany, NY, USA, 1999.*

[21] *J. Liu, "Modelling, configuration and control optimization of power-split hybrid vehicles," Doctor of Philosophy Mechanical Engineering, University of Michigan, 2007.*

[22] *Toyota. (22/08/2012). Toyota hybrid synergy drive Available: http://www.toyota.com.au/hybrid-synergy-drive#how-hybrid-works*

[23] *Ford. (22/08/2012). Ford hybrid electric vehicle Available: http://www.ford.com/technology/electric/howevswork/?tab=HybridEV*

[24] *M. Shams-Zahraei, S. A. Jazayeri, M. Shahbakhti, and M. Sharifirad, "Look-forward longitudinal dynamic modelling for a series-parallel hybrid electric vehicle," International Journal of Electric and Hybrid Vehicles, vol. 1, pp. 342-363, 2008.*

[25] *M. Shams-Zahraei and A. Kouzani, "A study on plug-in hybrid electric vehicles " presented at the TENCON IEEE Conference, Singapore, 2009.*

[26] A. G. Holmes, Klemen, D., Schmidt, M. R., "Electrically variable transmission with selective input split, compound split, neutral and reverse Modes," US Patent 6,527,658 B2, issued Mar. 4, 2003.

[27] X. Li and S. S. Williamson, "Efficiency and suitability analyses of varied drive train architectures for plug-in hybrid electric vehicle (PHEV) applications," presented at the IEEE Vehicle Power and Propulsion Conference, Harbin, China, 2008.

[28] S. Jenkins and M. Ferdowsi, "HEV to PHEV conversion compatibility," in Vehicle Power and Propulsion Conference, 2008, pp. 1-4.

[29] J. Wu, A. Emadi, M. J. Duoba, and T. P. Bohn, "Plug-in hybrid electric vehicles: testing, simulations, and analysis," in Vehicle Power and Propulsion Conference, 2007. VPPC 2007. IEEE, 2007, pp. 469-476.

[30] V. Freyermuth, E. Fallas, and A. Rousseau, "Comparison of production powertrain configuration options for plug-in HEVs from fuel economy perspective," presented at the SAE World Congress & Exhibition, Detroit, MI, USA, 2008.

[31] V. H. Johnson, "Fuel used for vehicle air conditioning: A state-by-state thermal comfort-based approach," presented at the SAE World Congress & Exhibition, Detroit, MI, USA, 2002.

[32] J. Rugh, Howard, R., Farrington, R., Cuddy, M, "Innovative Techniques for Decreasing Advanced Vehicle Auxiliary Loads," in Future Car Congress, Crystal City, VA, USA, 2000.

[33] F. R. Salmasi, "Control Strategies for Hybrid Electric Vehicles: Evolution, Classification, Comparison, and Future Trends," IEEE Transactions on Vehicular Technology vol. 56, pp. 2393-2404, 2007.

[34] M. Shams-Zahraei, A. Z. Kouzani, and B. Ganji, " Effect of noise factors in energy management of series plug-in hybrid electric vehicles," International Review of Electrical Engineering, vol. 6, pp. 1715-1726, 2011.

[35] M. Shams-Zahraei, A. Z. Kouzani, S. Kutter, and B. Bäker, "Integrated thermal and energy management of Plug-in hybrid electric vehicles," Journal of Power Sources, vol. 216, pp. 237-248, 15 October 2012.

[36] Y. Gao and M. Ehsani, "Design and Control Methodology of Plug-in Hybrid Electric Vehicles," IEEE Transactions on Industrial Electronics, vol. 57, pp. 633-640, 2010.

[37] J. Gonder and T. Markel, "Energy management strategies for plug-in Hybrid Electric Vehicles," presented at the SAE World Congress & Exhibition, Detroit, MI, USA, 2007.

[38] P. B. Sharer, A. P. Rousseau, D. Karbowski, and S. Pagerit, "Plug-in hybrid electric vehicle control strategy: comparison between EV and charge depleting options," presented at the SAE World Congress & Exhibition, Detroit, MI, USA, 2008.

[39] Z. Bingzhan, C. C. Mi, and Z. Mengyang, "Charge-depleting control strategies and fuel optimization of blended-mode plug-in hybrid electric vehicles," IEEE Transactions on Vehicular Technology, vol. 60, pp. 1516-1525, 2011.

[40] P. Pisu and G. Rizzoni, "A comparative study of supervisory control strategies for hybrid electric vehicles," IEEE Transactions on Control Systems Technology, vol. 15, pp. 506-518, 2007.

[41] S. G. Wirasingha and A. Emadi, "Classification and review of control strategies for plug-In hybrid electric vehicles," IEEE Transactions on Vehicular Technology, vol. 60, pp. 111-122, 2011.

[42] S. G. Wirasingha and A. Emadi, "Classification and review of control strategies for plug-in hybrid electric vehicles," presented at the IEEE Vehicle Power and Propulsion Conference, 2009.

[43] H. Banvait, S. Anwar, and C. Yaobin, "A Rule-based energy management strategy for plug-in hybrid electric vehicle (PHEV)," in American Control Conference, 2009, pp. 3938-3943.

[44] H.-D. Lee and S.-K. Sul, "Fuzzy-logic-based torque control strategy for parallel-type hybrid electric vehicle," IEEE Transactions on Industrial Electronics, vol. 45, pp. 625-632, 1998.

[45] N. J. Schouten, M. A. Salman, and N. A. Kheir, "Fuzzy logic control for parallel hybrid vehicles," IEEE Transactions on Control Systems Technology vol. 10, pp. 460-468, 2002.

[46] B. M. Baumann, G. Washington, B. C. Glenn, and G. Rizzoni, "Mechatronic design and control of hybrid electric vehicles," Transactions on Mechatronics, IEEE/ASME vol. 5, pp. 58-72, 2000.

[47] R. Langari and J.-S. Won, "Intelligent energy management agent for a parallel hybrid vehicle-part I: system architecture and design of the driving situation identification process," IEEE Transactions on Vehicular Technology, vol. 54, pp. 925-934, 2005.

[48] J.-S. Won and R. Langari, "Intelligent energy management agent for a parallel hybrid vehicle-part II: torque distribution, charge sustenance strategies, and performance results," IEEE Transactions on Vehicular Technology, vol. 54, pp. 935-953, 2005.

[49] Q. Gong, Y. Li, and Z.-R. Peng, "Trip-based optimal power management of plug-in hybrid electric vehicles," IEEE Transactions on Vehicular Technology, vol. 57, pp. 3393-3401, 2008.

[50] M. Shams-Zahraei and A. Z. Kouzani, "Power-cycle-library-based Control Strategy for plug-in hybrid electric vehicles," presented at the IEEE Vehicle Power and Propulsion Conference Lille, France 2010.

[51] Q. Gong, Y. Li, and Z.-R. Peng, "Optimal power management of plug-in HEV with intelligent transportation system," presented at the IEEE/ASME International Conference on Advanced Intelligent Mechatronics 2007.

[52] Q. Gong, Y. Li, and Z.-R. Peng, "Trip based optimal power management of plug-in hybrid electric vehicles using gas-kinetic traffic flow model," presented at the American Control Conference, 2008.

[53] A. Brahma, Y. Guezennec, and G. Rizzoni, "Optimal energy management in series hybrid electric vehicles," presented at the American Control Conference, 2000.

[54] C.-C. Lin, H. Peng, J. W. Grizzle, and J.-M. Kang, "Power management strategy for a parallel hybrid electric truck," IEEE Transactions on Control Systems Technology vol. 11, pp. 839-849, 2003.

[55] S. Kutter and B. Baker, "Predictive online control for hybrids: Resolving the conflict between global optimality, robustness and real-time capability," presented at the IEEE Vehicle Power and Propulsion Conference 2010.

[56] U. Zoelch and D. Schroeder, "Dynamic optimization method for design and rating of the components of a hybrid vehicle," International Journal of Vehicle Design, vol. 19, pp. 1–13, 1998.

[57] L. V. Perez, G. R. Bossio, D. Moitre, and G. O. Garcia, "Optimization of power management in an hybrid electric vehicle using dynamic programming," Mathematics and Computers in Simulation, vol. 73, pp. 244–254, 2006.

[58] L. Johannesson and B. Egardt, "A novel algorithm for predictive control of parallel hybrid powertrains based on dynamic programming," in Fifth IFAC Symposium on Advances in Automotive Control, Monterey, USA, 2007.

[59] L. Johannesson and B. Egardt, "Approximate dynamic programming applied to parallel hybrid powertrains," in Proceedings of the 17th IFAC World Congress, Seul, Korea, 2008.

[60] S. Kutter and B. Baker, "An iterative algorithm for the global optimal predictive control of hybrid electric vehicles," in Vehicle Power and Propulsion Conference (VPPC), 2011 IEEE, 2011, pp. 1-6.

[61] G. Paganelli, S. Delprat, T. M. Guerra, J. Rimaux, and J. J. Santin, "Equivalent consumption minimization strategy for parallel hybrid powertrains," in IEEE 55th Vehicular Technology Conference, 2002, pp. 2076-2081 vol.4.

[62] A. Sciarretta, M. Back, and L. Guzzella, "Optimal control of parallel hybrid electric vehicles," IEEE Transactions on Control Systems Technology, vol. 12, pp. 352-363, 2004.

[63] C. Musardo, G. Rizzoni, and B. Staccia, "A-ECMS: an adaptive agorithm for hybrid electric vehicle energy management," in 44th IEEE Conference on Decision and Control and 2005 European Control Conference. CDC-ECC '05., 2005, pp. 1816-1823.

[64] M. Koot, J. T. B. A. Kessels, B. de Jager, W. P. M. H. Heemels, P. P. J. van den Bosch, and M. Steinbuch, "Energy management strategies for vehicular electric power systems," IEEE Transactions on Vehicular Technology, vol. 54, pp. 771-782, 2005.

[65] L. S. Pontryagin, The mathematical theory of optimal processes: Wiley 1962.

[66] L. Serrao, S. Onori, and G. Rizzoni, "ECMS as a realization of Pontryagin's minimum principle for HEV control," in American Control Conference, 2009, pp. 3964-3969.

[67] C. Musardo, G. Rizzoni, and B. Staccia, "A-ECMS: An Adaptive Algorithm for Hybrid Electric Vehicle Energy Management," in IEEE Conference on Decision and Control, Seville, Spain, 2005.

[68] S. J. Moura, H. K. Fathy, D. S. Callaway, and J. L. Stein, "A stochastic optimal control approach for power management in plug-In hybrid electric vehicles," in Proceedings of the 2008 ASME Dynamic Systems and Control Conference, 2008.

[69] S. J. Moura, H. K. Fathy, D. S. Callaway, and J. L. Stein, "A stochastic optimal control approach for power management in plug-in hybrid electric vehicles," IEEE Transactions on Control Systems Technology, vol. 19, pp. 1-11, 2010.

[70] I. Kolmanovsky, I. Siverguina, and B. Lygoe, "Optimization of powertrain operating policy for feasibility assessment and calibration: stochastic

dynamic programming approach," in Proceedings of the American Control Conference, 2002, pp. 1425-1430 vol.2.

[71] J. Liu and H. Peng, "Modeling and control of a power-split hybrid vehicle," IEEE Transactions on Control Systems Technology, vol. 16, pp. 1242-1251, 2008.

[72] C.-C. Lin, H. Peng, and G. J. W. , "A stochastic control strategy for hybrid electric vehicles," in American Control Conference, 2004, pp. 4710-4715 vol.5.

[73] L. Johannesson, "Predictive control of hybrid electric vehicles on prescribed routes," Doctor of Philosophy Department of Signals and Systems, CHALMERS UNIVERSITY OF TECHNOLOGY, 2009.

[74] L. Johannesson, M. Asbogard, and B. Egardt, "Assessing the potential of predictive control for hybrid vehicle powertrains using stochastic dynamic programming," IEEE Transactions on Intelligent Transportation Systems, vol. 8, pp. 71-83, 2007.

[75] P. Struss and C. Price. (2003) model-based systems in the automotive industry. AI Magazine. 17-34.

[76] M. Tiller, Introduction to Physical Modeling with Modelica: Springer, 2001.

[77] Modelica Association. (2000, 1/08/2012). Modelica - A unified object-oriented language for physical systems modeling. Available: https://modelica.org/documents/ModelicaTutorial14.pdf

[78] L. Glielmo, O. R. Natale, and S. Santini, "Integrated simulations of vehicle dynamics and control tasks execution by Modelica," in IEEE/ASME International Conference on Advanced Intelligent Mechatronics 2003, pp. 395-400 vol.1.

[79] T. Markel, A. Brooker, T. Hendricks, V. Johnson, K. Kelly, B. Kramer, M. O'Keefe, S. Sprik, and K. Wipke, "ADVISOR: a systems analysis tool for advanced vehicle modeling," Journal of Power Sources, vol. 110, pp. 255-266, 2002.

[80] *Argonne National Laboratory. PSAT. Available: http://www.transportation.anl.gov/modeling_simulation/PSAT/*

[81] *W. Gao, S. Neema, J. Gray, J. Picone, S. Porandla, S. Musunuri, and J. Mathews, "Hybrid powertrain design using a domain-specific modeling environment," in Vehicle Power and Propulsion Conference 2005, pp. 423-429.*

[82] *B. K. Powell, K. E. Bailey, and S. R. Cikanek, "Dynamic modeling and control of hybrid electric vehicle powertrain systems," IEEE Control Systems, vol. 18, pp. 17-33, 1998.*

[83] *K. L. Butler, M. Ehsani, and P. Kamath, "A Matlab-based modeling and simulation package for electric and hybrid electric vehicle design," IEEE Transactions on Vehicular Technology, vol. 48, pp. 1770-1778, 1999.*

[84] *G. Rizzoni, L. Guzzella, and B. M. Baumann, "Unified modeling of hybrid electric vehicle drivetrains," IEEE/ASME Transactions on Mechatronics, vol. 4, pp. 246-257, 1999.*

[85] *NREL. Transferring NREL's advanced vehicle simulator to industry. Available: http://www.nrel.gov/vehiclesandfuels/success_advisor.html*

[86] *J. D. Murrell, "Emission simulations: GM Lumina, Ford Taurus, GM Impact, and Chrysler TEVan," J. Dill Murrell and Associates, LLC., Saline, MI1996.*

[87] *A. F. Mills, Basic heat and mass transfer: Irwin, 1995.*

[88] *E. Finkeldei and M. Back, "Implementing a mpc algorithm in a vehicle with a hybrid powertrain using telematics as a sensor for powertrain control," in IFAC Symposium on Advances in Automotive Control, University of Salerno, Italy, 2004.*

[89] *M. Back, S. Terwen, and V. Krebs, "Predictive powertrain control for hybrid electric vehicles," in IFAC Symposium on Advances in Automotive Control, University of Salerno, Italy, 2004.*

[90] *Y. Deguchi, K. Kuroda, M. Shouji, and T. Kawabe, "HEV charge/discharge control system based on car navigation information," in JSAE Spring Conference, Yokohama, Japan, 2003.*

[91] *Y. Bin, Y. Li, Q. Gong, and Z.-R. Peng, "Multi-information integrated trip specific optimal power management for plug-in hybrid electric vehicles," presented at the American Control Conference, 2009.*

[92] *G. W. Taylor and S. Stewart, "Cold start impact on vehicle energy use," presented at the SAE World Congress & Exhibition, Detroit, MI, USA, 2001.*

[93] *H. Li, G. E. Andrews, D. Savvidis, B. Daham, K. Ropkins, M. Bell, and J. Tate, "Study of thermal characteristics and emissions during cold start using an on-board measuring method for modern SI car real world urban driving," SAE International Journal of Engines, vol. 1, pp. 804-819, 2008.*

[94] *R. Farrington and J. Rugh, "Impact of vehicle air-conditioning on fuel economy, tailpipe emissions, and electric vehicle range," presented at the Earth Technologies Forum, Washington, D.C., 2000.*

[95] *M. A. Lambert and B. J. Jones, "Automotive adsorption air conditioner powered by exhaust heat. Part 1: conceptual and embodiment design," Proceedings of the Institution of Mechanical Engineers, Part D: Journal of Automobile Engineering, vol. 220, pp. 959-972, 2006.*

[96] *H. Khayyam, A. Z. Kouzani, and E. J. Hu, "Reducing energy consumption of vehicle air conditioning system by an energy management system," presented at the IEEE Intelligent Vehicles Symposium, 2009.*

[97] *H. Khayyam, A. Z. Kouzani, E. J. Hu, and S. Nahavandi, "Coordinated energy management of vehicle air conditioning system," Applied Thermal Engineering, vol. 31, pp. 750-764, 2010.*

[98] *T. Markel, K. Smith, and A. Pesaran, "Improving petroleum displacement potential of PHEVs using enhanced charging scenarios," presented at the EVS-24 International Battery, Hybrid and Fuel Cell Electric Vehicle Symposium, Stavanger, Norway, 2009.*

[99] K. Smith, T. Markel, and A. Pesaran, "PHEV battery trade-off study and standby thermal control," presented at the 26th International Battery Seminar & Exhibit, Fort Lauderdale, FL, 2009.

[100] D. Kirk, Optimal Control Theory An Introduction Mineola, New York: Dover Publications, 2004.

[101] F. L. Lewis, D. Vrabie, and V. L. Syrmos, Optimal Control, 3 ed.: Wiley, 2012.

[102] L. Serrao, "A comperative analyses of energy management strategies for hybrid electric vehicles," Doctor of Philosophy The Ohio State University, 2009.

[103] S. Bradley , A. Hax , and T. Magnanti, Applied mathematical programming: Addison-Wesley Pub. Co., 1977

APPENDIX A.

NOMENCLATURE

A	Effective area of convection heat transfer
A_f	Vehicle frontal area
AC	Air condition
AER	All electric range
BSFC	Brake specific fuel consumption
Ch	Battery charge
COOL	Confined optimal operation line
COP	Coefficient of performance
CD	Charge depleting

CS	Charge sustaining mode
Cyc	Number of battery cycles
C_{actual}	Battery actual capacity
C_{air}	Air specific heat capacity
C_{cabin}	Lumped cabin specific heat capacity
C_D	Coefficient of drag
C_{Li}	Battery defined lithium capacity
C_p	Thermal heat capacity
C_{sites}	Battery active sites capacities
C_v	Water latent heat vaporization
C_{water}	Water specific heat capacity
DP	Dynamic programming
d_0, d_1	Experimental constant values for battery aging formulation
ECMS	Equivalent consumption minimization strategies
Eng	Engine
EMS	Energy management strategy
EREV	Extended range electric vehicle
ESS	Energy storage system
EV	Electric vehicle
e_0, e_1	Experimental constant values for battery aging formulation
fuel	Fuel
Flw	Flow rate

F_d	Drag force resistance
F_g	Grading resistance
F_r	Rolling resistance
f_r	Coefficient of rolling resistance
F_t	Traction force of vehicle
Fc_{tstat}	Fuel converter (engine) cooling system thermostat set point
GIS	Geographical information system
GPS	Global positioning system
h	Heat transfer coefficient
HEV	Hybrid Electric Vehicle
HWFET	Highway fuel economy test
I	Battery current
İ	Sun radiation heat flux
inf	Infinity
J	Cost function
k	Index for time discretization
L	Instantaneous cost
lhv	Fuel lower heating value
m	Mass
M	Vehicle mass
$\dot{m}$	Mass flow rate
min _eng_on	Minimum engine on time

m_{cabin}	Lumped cabin mass
$\dot{m}_{air}$	Fresh air mass flow rate
$\dot{m}_{water}$	Condensed water mass rate
N	Number of possible change of charge in each time-step
N_f	Normal load on front wheels
N_r	normal load on rear wheels
Nu_l	Nusselt number
PHEV	Plug in hybrid electric vehicle
P	Engine power
Pr	Prandtl number
P_0	Ambient pressure
$P_{compressor}$	Air-conditioning compressor power demand
P_t	Traction power of vehicle
$\dot{Q}$	Rate of thermal energy
$\dot{Q}_{convection}$	Air-conditioning convection heat load
$\dot{Q}_{dehumidification}$	Air-conditioning dehumidification heat load
$\dot{Q}_{evaporator}$	Rate of heat absorption by evaporator
$\dot{Q}_{heater}$	Cabin heater heat rate
$\dot{Q}_{metabolic}$	Air-conditioning metabolic heat load
$\dot{Q}_{radiation}$	Air-conditioning radiation heat load
$\dot{Q}_{ventilation}$	Air-conditioning ventilation heat load
R	Battery internal resistance

Ra_l	Rayleigh number
Re	Raynods number
S	Incident surface for radiation heat transfer
sarea	Surface area
SOC	State of charge
t	Time
T	Temperature
$T_{ambient}$	Ambient temperature
T_b	Battery cell temperature
T_{cabin}	Vehicle cabin temperature
$T_{coolant}$	Engine coolant temperature
T_{htr}	Temperature threshold for using engine coolant waste heat for cabin heater
u	Input variable
U	Admissible input variables
U_0	Battery nominal voltage
UDDS	Urban dynamometer driving schedule
V	Velocity
V_w	wind velocity
x	State variable
X	Admissible State variables
$\propto$	Angle of road slope
γ	Normalised engine temperature factor

ΔSOC	Given state of charge swing
γ	Normalized engine temperature
ω	Engine angular velocity
σ	Stefan–Boltzmann constant
η	Efficiency
ρ	Air density
v	Battery voltage exposure

Subscripts

air	Air
acc	Accessories
amb	Ambient
c	Conduction
coolant	Engine coolant
cyl	Cylinder
emisv	Emissivity factor
Eng	Engine
exh	Exhaust gas
f	Final time
fuel	Fuel
Gen	Generator
h	Hood

Htr	Cabin heater
i	Engine interior
k	Index for time discretization
M	Electric traction motor
nohtr	Heater is not using electric power
traction	Traction
r	Thermal radiation
Radiator	Radiator
th_c	Thermal conduction coefficient
tstat	Thermostat set point
x	Engine exterior
0	Initial time